SUBCELLULAR LOCALIZATION AND ROLE OF

POTATO VIRUS X (PVX) TGBp2

IN VIRUS CELL-TO-CELL

MOVEMENT

By

RUCHIRA MITRA

Master of Science

Ranchi University,

India

Submitted to the Faculty of the
Graduate College of the
Oklahoma State University
in partial fulfillment of
the requirements for
the Degree of
DOCTORATE OF PHILOSOPHY
May, 2005

SUBCELLULAR LOCALIZATION AND ROLE OF

POTATO VIRUS X (PVX) TGBp2

IN VIRUS CELL-TO-CELL

MOVEMENT

Thesis approved:

Dr Jeanmarie Verchot-Lubicz
Thesis Advisor

Dr Jacqueline Fletcher

Dr Richard S Nelson

Dr Yinghua Huang

Dr A Gordon Emslie
Dean of Graduate College

ACKNOWLEDGEMENTS

I would like to especially thank my advisor, Dr. Jeanmarie Verchot-Lubicz, for the opportunity to develop research skills and experimental design. I acknowledge the help and guidance I received from Drs. Mark Payton, Ellison Blancaflor and Richard Nelson for their instruction and provision of materials. I would like to thank my Drs. Jacqueline Fletcher and Ulrich Melcher, for their mentoring and guidance. I would take this opportunity to thank my committee member Dr. Y. Huang for his helpful suggestions and guidance. I would like to give a special thanks to Dr. Krishnamurthy Konduru who generated constructs for this study. I wish to thank Dr. Charlotte Ownby, Terry Coburn and Phoebe Doss of the Electron microscopy laboratory for their support, and understanding. I owe to my laboratory mates, Amanda Howard, Jeannie Te, Barbara Driskel, HoJong Ju, Teferra Mekuria, and Tim Samuels a special thanks for their unwavering friendship and support. I would also like to thank my friends Anamika Ray, Aswathy Sreedharan, Mohini Patil and Mohua Bardhan for their encouragement and companionship. Finally, I would like to thank my father, mother and uncle (Mr Dilip Mitra) for their encouragement. I dedicate this thesis to my father (Dr. Pranab Mitra) who is a constant inspiration.

TABLE OF CONTENTS

LIST OF TABLES

Table Page

CHAPTER II

CHAPTER III

CHAPTER IV

LIST OF FIGURES

Figure Page

CHAPTER I

CHAPTER II

CHAPTER III

CHAPTER IV

ABBREVIATIONS

BFA....................Brefeldin A

CFP....................Cyan fluorescent protein

CLSM....................Confocal laser scanning microscope

CP....................Coat Protein

EM....................Electron microscope

ER....................Endoplasmic reticulum

GFP....................Green fluorescent protein

G....................Golgi

M....................Mitochondria

MP....................Movement protein

ORF....................Open reading frame

PD....................Plasmodesmata

PVX....................Potato virus X

TGB....................Triple gene block

TMV....................Tobacco mosaic virus

CHAPTER I

Introduction and Literature Review

An RNA Highway in Plants

There is a pathway for local and systemic transport of proteins and nucleic acids in plants that has been named an "RNA-based information highway" (Jorgensen et al., 1998). For local movement within the leaf, there are symplastic connections between cells, referred to as plasmodesmata, which promote the transport of proteins, nucleic acids, and low molecular weight molecules between neighboring cells. For long distance movement between leaves, molecules typically utilize the phloem (Jorgensen et al., 1998). This "information highway" is a pathway used by invading viral pathogens, and is essential for local and systemic control of plant gene expression and gene silencing (Jorgensen et al., 1998). For example, the maize knotted-1 (Kn-1) homeobox gene mRNA is expressed in the shoot apical meristem and is important for cell differentiation (Hake et al., 1992; Kim et al., 2002). While the Kn-1 transcription factor acts mainly in the cell nucleus, it also moves into neighboring cells providing local control of gene expression within the meristem (Hake et al., 1992; Kim et al., 2002). For systemic gene silencing, there is a signal that is broadcast throughout the plant, triggering suppression of gene expression. This signal is part of an "RNA surveillance" mechanism that recognizes transcripts expressed at high levels and triggers their degradation (Voinnet et al., 2000; Waterhouse *etal.,*1999). Plant viruses have been valuable tools to study cellular transport mechanisms, and they have also helped reveal important information about the structure of plasmodesmata (Ding et al., 1992). The study of plant virus movement has revealed that plasmodesmata can expand for active and selective transport of proteins and nucleic acids between cells (Fig. 1). The plasma membrane and the endoplasmic reticulum (ER) are continuous between adjacent cells through the plasmodesmata. The desmotubule is central to the plasmodesmata and consists of an appressed ER membrane surrounded by globular proteins. Actin filaments, radiate from the cell wall to the desmotubule like spokes on a wheel. Microchannels run between the actin filaments and are likely to act as molecular sieves controlling movement of molecules between cells (Fig. 1).

Plasmodesmata typically have a size exclusion limit (SEL) below 1 kDa, allowing passage of only small molecules between adjacent cells (Robards and Lucas, 1990). There are plant and viral factors that increase plasmodesmal SEL for movement of macromolecules such as plant proteins or plant viruses (Ding et al., 1992; Fujiwara et al., 1993; Oparka et al., 1997; Waigmann et al., 1994; Wolf et al., 1989). Components of the cellular machinery, which control dynamic changes within plasmodesmata, have not yet been identified.

Plant viruses encode movement proteins (MPs), which are needed to transport virus between adjacent cells. Research within the last decade has determined that cell-to-cell movement of plant viruses involves four general steps:

1. Viral MPs form a complex with either the viral RNA or virion particle.
2. The movement complex is transported within the cell toward the plasmodesmata.
3. MPs increase plasmodesmal SEL for transport of the movement complex.
4. The movement complex is transported through the plasmodesmata into adjacent cells.

Phylogenetic analysis revealed that most characterized plant RNA viral MPs fall into four groups (Melcher, 2000). However, there are many plant viruses whose MPs have not been characterized and whose phylogenetic relationships are unknown (Melcher, 2000). Further research will expand our knowledge of each step in the movement process and will identify the structural and biochemical properties that define viral MPs.

Four mechanisms for plant virus cell-to-cell movement in plants

Figure 2 depicts four mechanisms for virus cell-to-cell movement. The first mechanism is based on studies of tobamo-, tobra-, diantho-, and cucumovirus (Fig. 2A) (Lazarowitz and Beachy, 1999). In this model the viral MPs bind viral nucleic acids and carry them through plasmodesmata into adjacent cells (Atsushi and Meshi 2001; Blackman et al., 1998; Canto et al., 1997; Waigmann et al., 1994; Citovsky and Zambryski., 1991.).

The second model describes movement of closteroviruses and is based on studies of *Beet yellow virus* (BYV) (Fig. 2B). BYV requires a single MP, named HSp70h, and two coat proteins (named CP and CPm) for virus movement (Alzhanova et al., 2001). Hsp70h has an ATPase active site and shares amino acid sequence homology with heat shock proteins from the HSP70 family (Alzhanova et al., 2001). Hsp70h proteins form dimers that attach to the end of the filamentous virion particle (Fig. 2B). The Hsp70h "tail assembly" anchors virion particles to microtubules and ATPase activity drives virion transport across plasmodesmata. At the plasmodesmata, the tail disassembles and the virion particle is destabilized revealing a short region of viral RNA. Ribosomes in the adjacent cell pull the RNA through the plasmodesmata to initiate translation (Alzhanova et al., 2001) (Fig. 2B).

The third mechanism is used by viruses belonging to the genera *Comovirus, Nepovirus,* and *Tospovirus* (Fig. 2C). These viruses move between adjacent cells as encapsidated particles (van Lent et al., 1991; Wellink et al., 1993; Wieczorek et al., 1993). Comoviruses and nepoviruses encode MPs and M proteins, which interact to form tubules that extend between adjacent cells (Kasteel et al., 1997). Tubules serve as conduits for movement of virion particles between adjacent cells (Fig. 2C). The tubule assembles inside the plasmodesmata modifying the plasmodesmata by destroying the desmotubule in the process (van der Wel et al., 2000).

A new model was recently proposed to describe cell-to-cell movement of TMV replication complexes (Kawakami et al., 2004) (Fig. 2D). TMV replication occurs in membrane vesicles that are derived from the ER. The TMV MP and CP associate with the vesicles containing TMV replication complexes. The accumulation of viral MPs in these vesicles is regulated by the TMV CP (Asurmendi et al., 2004).

Potato virus X

Potato virus X (PVX) is a member of the genus *Potexvirus* and is a positive RNA virus. The PVX genome is 6.4 kb in length (Baulcombe et al., 1995; Huisman et al., 1998), has a cap at the 5' terminus (Sonenberg et al.,1978), and is polyadenylated at the 3' end. The PVX genome contains five open reading frames (ORFs) (Huisman et al., 1988) (Fig. 3). The first ORF encodes a 166kDa viral replicase (Huisman et al., 1998). Next is the triple gene block (TGB) which is a genetic module of three overlapping ORFs that encode three viral MPs. The ORF closest to the 3' terminus encodes the viral CP (Fig. 3).

The TGB is conserved among potex-, hordei-, beny- carla-, and pecluviruses (Memelink et al.,1990; Morozov and Schiemann , 1999; Morozov et al., 1987; Skryabin et al., 1988). The TGB proteins are named TGBp1, TGBp2, and TGBp3 (Huisman , 1998; Konduru et al., 2002). The potexvirus TGBp1 is a multifunctional protein. The PVX TGBp1 has RNA helicase activity, unwinds PVX virions to promote translation of virion-derived RNA, suppresses gene silencing, and increases plasmodesmal SEL for virus transport (Atabekov et al., 2002; Baulcombe et al., 2000; Yang et al., 2000; Donald et al., 1997 Rouleau, 1994). Amino acid sequence analyses suggested that TGBp2 and TGBp3 are membrane-binding proteins (Morozov et al., 1987). The hordeivirus TGBp2 and TGBp3 proteins were reported to be associated with the ER (Solovyev et al., 2000).

A model describing potexvirus movement was proposed based on the studies of *White clover mosaic virus* (WClMV) (Lough et al., 1998; 2000). In this model the TGB and CP proteins form a complex with viral RNA (Fig. 3B). The movement complex moves along the ER or cytoskeletal network toward and through the plasmodesmata (Fig. 3B). This model was developed based on evidence that: a) TGBp1 increases plasmodesmal SEL; b) TGBp1 and CP bind viral RNA and carry it across plasmodesmata; and c) TGBp2 and TGBp3 strengthen the ability of TGBp1/CP/viral RNA complexes to move from cell to cell (Lough et al., 1998; 2000).

This model has several drawbacks. First, this model was proposed with little knowledge of how the TGBp1, TGBp2, TGBp3, and CP proteins interact with one another or with cellular components. The model also suggests that the TGBp1 and CP proteins equally bind viral RNA and carry it across the plasmodesmata. Since the TGBp1 and CP proteins have different biochemical properties, they likely contribute differently to plasmodesmata transport.

A PVX infectious clone containing GFP

Two plasmids, named pPVX.204e and PRP3.0 contain cDNA copies of the PVX genome adjacent to the *Cauliflower mosaic virus* (CaMV) 35S promoter and T7 promoter, respectively (Baulcombe et al.,1995)(Fig. 3A). The pPVX.204e plasmids containing the 35S promoter can be rub-inoculated to tobacco leaves to initiate virus infection.

Alternatively, plasmids can be delivered to tobacco leaves using the Helios Gene Gun (Biorad, Hercules, CA). Infectious transcripts can be synthesized *in vitro* from PRP3.0 plasmids and rub-inoculated to plants.

Both pPVX.204e and PRP3.0 infectious clones contain the green fluorescent protein (GFP) gene fused to a duplicated CP subgenomic RNA promoter inserted into the viral genome (Baulcombe et al.,1995). GFP gene has proved to be a powerful tool for studies of PVX cell-to-cell and systemic movement because it can be viewed in intact tissue using an ultraviolet light. Thus, GFP is used as to monitor virus cell-to-cell and systemic movement (Baulcombe et al., 1995).

OBJECTIVES

Research in our laboratory is being conducted to test the current model for PVX cell-to-cell movement. While amino acid sequence analyses (Morozov et al., 1988) suggest that the PVX TGBp2 and TGBp3 proteins are membrane-binding proteins, there is no experimental evidence to support this conclusion. Research described in this thesis focuses mainly on characterizing the subcellular targeting and functions of TGBp2. Similar studies characterizing the PVX TGBp3 has been conducted simultaneously by my colleague Dr. K. Konduru in this laboratory. This study has the following three objectives:

1) Characterize subcellular accumulation of TGBp2,

2) Determine if TGBp2 moves from cell to cell, and

3) *Potato virus X* TGBp2 causes reorganization of the ER network.

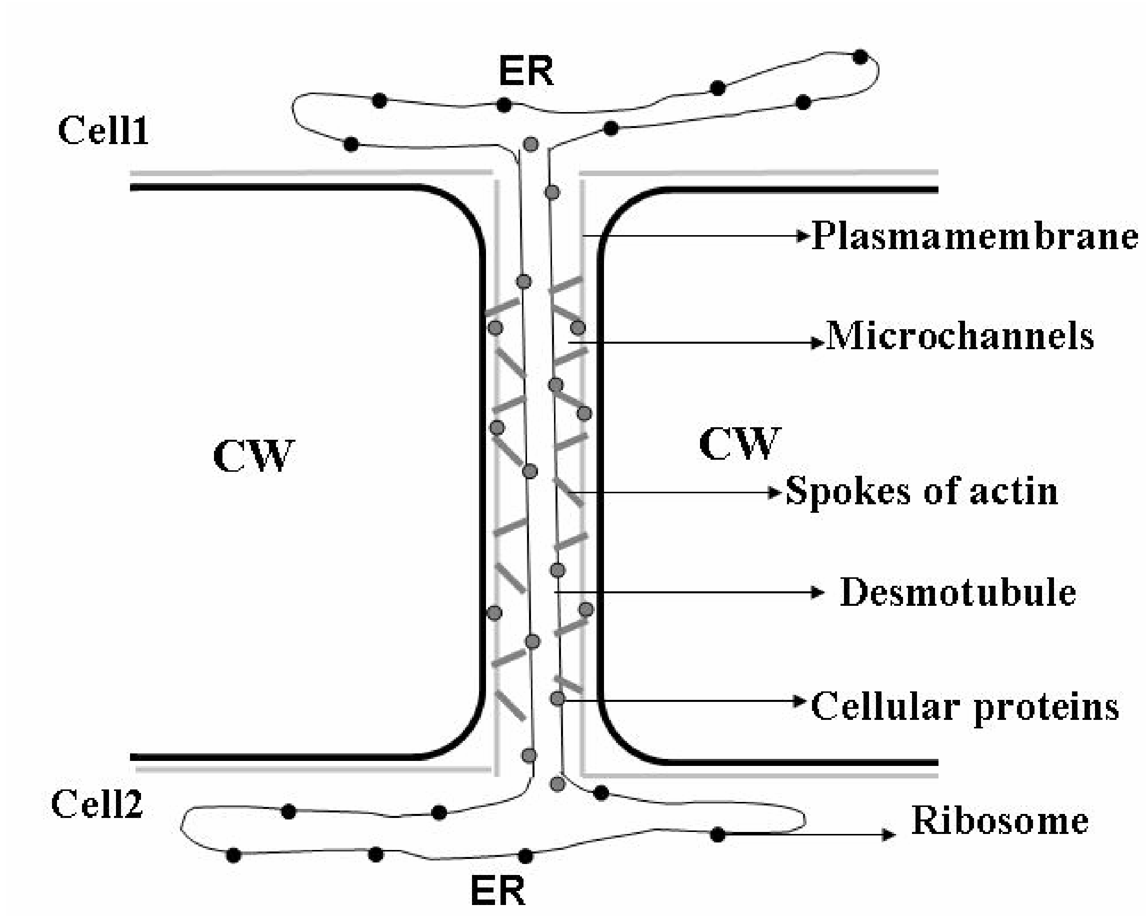

Fig.1. Diagrammatic representation of plasmodesmata. The wall of the pore is defined by the cell wall (CW) and plasma membrane as the continuous gray lines bordering the CW. The central part of the pore is occupied by the desmotubule, represented by the black hollow tube, which is comprised of ER and plant proteins which are represented by gray spheres. The ER is also seen on either ends of the plasmodesmatal pore in the form of black wavy lines, extending into the cells, dotted with black ribosomes. The light gray spheres along the plasma membrane and desmotubule indicate cellular proteins of unknown function. Spokes of actin filaments extend from the plasma membrane to the desmotubule are depicted with thick gray lines. In between the actin spokes are spaces called the microchannels.

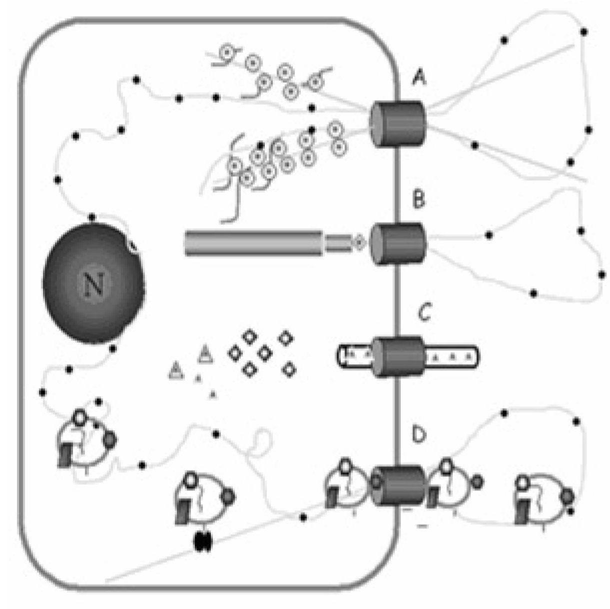

Fig. 2. Diagrams depicting four mechanisms used by different plant RNA viruses to move between adjacent cells. The black sphere with an N represents the nucleus, and the plasmodesmata are represented by dark gray cylinders along the cell wall. (A) Mechanism used by tobamo-, tobra-, diantho-, cucumoviruses. White balls with a black center represent viral MPs, which coat viral RNA and carry it along the ER (gray lines with black dots representing the ribosomes) or microtubule network (straight gray lines) toward the plasmodesmata (dark gray cylinders represent the plasmodesmatal pore). (B) A tail assembly, consisting of Cpm (gray triangle) and Hsp70h (diamond), transports the BYV virion (gray cylinder) to the plasmodesmata. (C) Como-, nepo-, and tospoviruses encode MPs that form tubules, indicated here as a black hollow cylinder inside the plasmodesmata. Gray diamonds represent free MPs which assemble into tubules which are represented by white hollow tubes. Gray triangles represent virion particles that move through the tubules into adjacent cells. (D) A recent model for movement of vesicles (gray circles) containing TMV replication complexes across plasmodesmata. These vesicles are represented by black circles that seem to mark from the center of the cell through the plasmodesmata into the adjacent cell. These vesicles contain viral RNA (gray wavy line), the viral replicase represented by the gray rectangles, CP by dark diamond shapes and MP by light gray diamond shapes (Kawakami et al., 2004). The VRC increase in size, and travels along the cytoskeleton to reach the plasmodesmata.

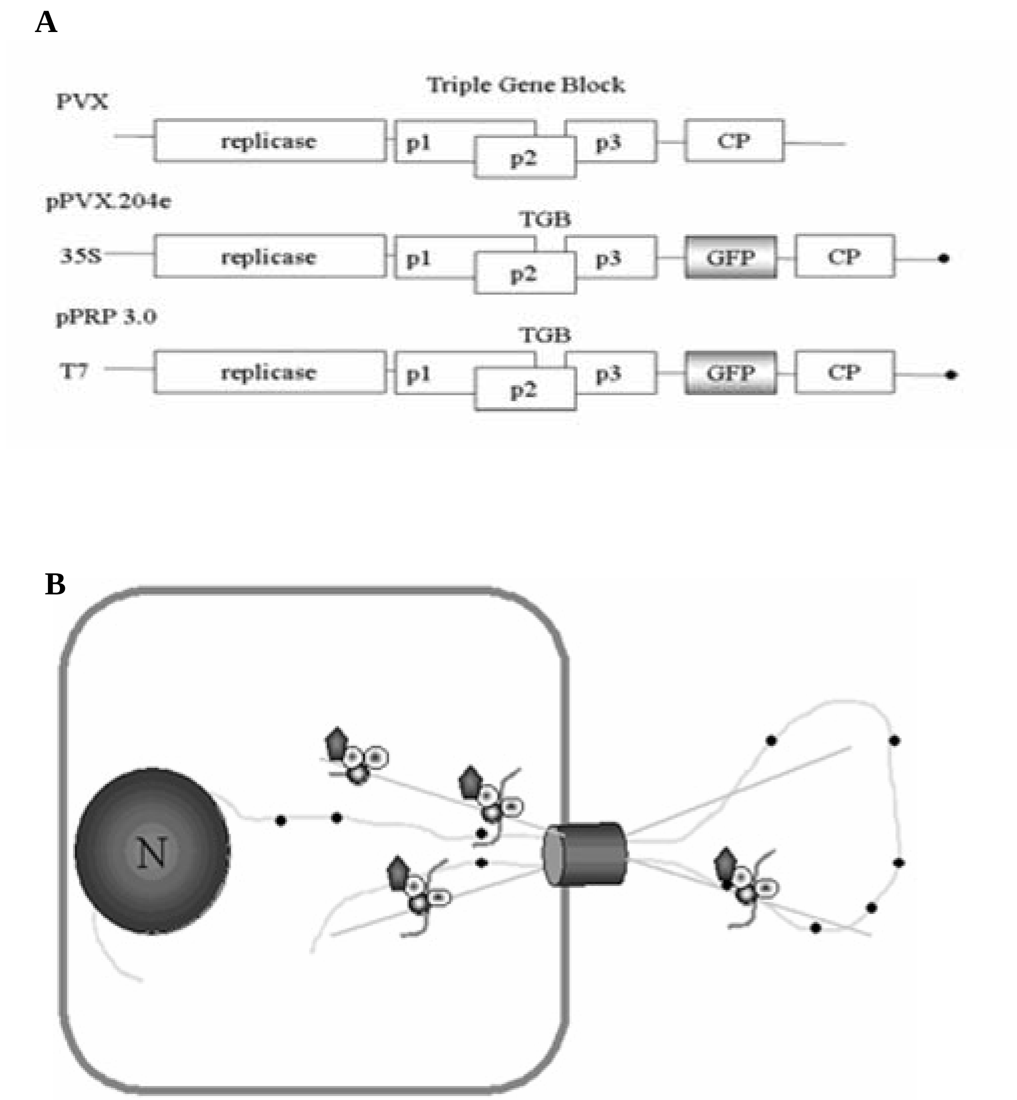

Fig. 3.A. A diagrammatic representation of the PVX genome. The black line represents the noncoding sequences. The gray boxes represent the replicase, triple gene block (TGB) and CP ORFs. The pPVX.204e and PRP3.0 are infectious clones contain the GFP gene, represented by the dark gray box. The pPVX.204e and PRP3.0 infectious clones contain the 35S promoter and the T7 promoter respectively (Baulcombe et al., 1995). The pPVX.204e infectious clone can either be rub-inoculated or biolistically delivered to leaves to initiate virus infection. Infectious RNA transcripts, synthesized in vitro from the PRP3.0 infectious clone, are rub inoculated to the leaves. **(B)** A model describing movement of potexviruses based on studies of WCIMV (Lough et al., 1998). Dark gray

spheres represent the TGBp1 MPs and the light gray spheres represent TGBp2 and TGBp3 MPs. The viral RNA is represented by a short dark gray wavy line. The ER and the cytoskeleton are represented by light gray wavy lines and light gray straight lines respectively. The ER is also dotted with black ribosomes. Nucleus is shown as a large black sphere on one side of the cell marked N and the plasmodesmata is represented by a dark gray cylinder on one side of the cell wall. The coat protein is represented by dark gray pentagon.

CHAPTER II

Cell-to-Cell Movement of the PVX TGBp2 Protein May Depend on the Host, Leaf Developmental Stage, and the PVX TGBp1 Protein.

ABSTRACT

To determine if the PVX TGBp2 moves through plasmodesmata, plasmids containing the green fluorescent protein (GFP) gene fused to the PVX TGBp2 were biolistically delivered to tobacco leaves. Similar experiments were conducted by Dr. K. Konduru in our laboratory to discover if PVX TGBp3 moves through plasmodesmata. The combined experiments showed that GFP:TGBp2 and GFP:TGBp3 moved from cell to cell in *N. benthamiana* but not *N. tabacum* leaves. When transgenic *N. tabacum* expressing TGBp1 were bombarded with plasmids expressing GFP:TGBp2 or GFP:TGBp3, both fusion proteins moved from cell to cell in source but not sink leaves. In *N. tabacum,* GFP:TGBp2 and GFP:TGBp3 intercellular movement requires TGBp1, and is regulated by the developmental stage of the leaf. Two different biolistic delivery methods were used to bombarded leaves and the results were similar, indicating that movement of GFP:TGBp2 or GFP:TGBp3 is independent of the delivery system. Mutations in GFP:TGBp2, GFP:TGBp3 genes within the PVX genome inhibited viral intercellular movement in both *Nicotiana* spp. Thus modification of the plasmodesmata for virus cell-to-cell movement is not an essential role of these proteins. These proteins likely provide other activities for virus cell-to-cell movement.

INTRODUCTION

Plant virus MPs promote trafficking of viral nucleic acids or virion particles through plasmodesmata. Plasmodesmata, that occur between epidermal cells in a tobacco leaf, have a SEL that is typically below 1-kDa (Robards and Lucas, 1990), but can be gated (i.e. dilated) by viral MPs to allow passage of large molecules between cells. This has been shown by microinjection studies in which the viral MPs have promoted plasmodesmata transport of 10-kDa FITC-conjugated dextrans (Ding et al., 1998; Lucas and Gilbertson, 1994; Wolf et al., 1989; Derrick et al., 1992; Fujiwara et al., 1993).

The potexvirus TGBp1 and CP have been reported to interact with plasmodesmata. The potexvirus TGBp1 increases plasmodesmal SEL and moves from cell-to-cell (Lough et al., 1998; Howard et al., 2004: Yang et al., 2000). The potexvirus CP also associates with plasmodesmata in virus-infected *N. benthamiana* leaves, but does not induce plasmodesmata gating (Oparka et al., 1996). A model was proposed suggesting the WClMV TGBp1 induces plasmodesmata gating for transport of a ribonucleoprotein complex containing TGBp1, CP, and viral RNA (Lough et al., 1998).

The roles of the PVX TGBp2 and TGBp3 proteins in viral cell-to-cell movement are not known. These two proteins likely do not induce plasmodesmata gating since cell-to-cell movement of 10-kDa dextrans was not viewed in transgenic *N. benthamiana* leaves expressing WClMV TGBp2 and TGBp3 (Lough et al., 1998). In another study, plasmids expressing either the PVX TGBp2 or TGBp3 ORFs were each co-bombarded with plasmids expressing the GFP gene into *N. benthamiana* leaves, and only PVX TGBp2 promoted cell-to-cell movement of GFP *in trans* (Tamai and Meshi, 2001). This report explores the ability of the PVX TGBp2 and TGBp3 to move through plasmodesmata.

Plasmids expressing GFP fused to the PVX TGBp2 or TGBp3 ORFs were biolistically delivered to *N. benthamiana* and *N. tabacum* leaves. Young sink and mature source leaves were used to determine if protein movement is dependent on the developmental stage of the leaf. Experiments were also conducted to find out if other PVX proteins affect cell-to-cell movement of GFP:TGBp2 and GFP:TGBp3.

RESULTS

Cell-to-cell movement of PVX TGBp2, TGBp3 in N. benthamiana but not N. tabacum leaves.

To determine if PVX TGBp2 and TGBp3 traffic between cells in *N. benthamiana* or *N. tabacum* leaves, the GFP gene was fused to the 5' end of each of these PVX ORFs and inserted into pRTL2 plasmids. The pRTL2-GFP:TGBp2 plasmids (Fig. 1A) were delivered to single tobacco leaf epidermal cells using the PDS1000/He biolistic delivery system. As a control, plasmids containing only GFP (pRTL2-GFP) (Fig. 1A) were also bombarded to tobacco leaves. GFP expression was monitored at 1 and 3 days post bombardment (dpb). Similar experiments were conducted concurrently by Dr. Konduru using the pRTL2-GFP:TGBp3 plasmids (Fig.1A).

Carboxyfluorescein (CF) dye was used to identify source and sink leaves. CF dye, when applied to the petiole of the most mature leaf, moves through the phloem in a source-to-sink direction, and unloads in sink leaves. A UV lamp is used to observe the dye and differentiate between source (which do not accumulate CF dye) and sink leaves which accumulate CF dye; data not shown)(Oparka et al., 1994; Roberts et al., 1997). Then leaves were taken from similar plants for biolistic bombardment experiments.

GFP accumulated mainly in single epidermal cells in *N. benthamiana* or *N. tabacum* leaves that were bombarded with pRTL2-GFP plasmids using the PDS1000/He system (Tables 1 and 2) (Itaya et al., 1997; Yang et al., 2000). On rare occasions GFP was detected in two adjacent cells. Similar background levels were reported in related studies, and might occur on occasions when plasmids were delivered to neighboring cells (Itaya et al., 1997; Yang et al., 2000).

GFP:TGBp2, and GFP:TGBp3 fusion proteins were detected in multiple cell clusters in *N. benthamiana* source leaves at 1 dpb (Table 1). For GFP:TGBp2 and GFP:TGBp3, 39% and 30% of the sites viewed, respectively, were multiple cell clusters. Both fusion proteins moved into clusters of three to four cells in *N. benthamiana* leaves but accumulated mainly in single cells in *N. tabacum* source or sink leaves (Tables 1 and 2; Fig. 2). *N. tabacum* leaves were studied at 1 and 3 dpb, and there was no evidence of protein movement beyond the first cells (Table 2). On rare occasions GFP:TGBp3 was detected in *N. tabacum* source leaves in clusters of three to four cells (Table 2). Statistical analyses were conducted to compare the proportions of cell clusters containing GFP:TGBp2 and GFP:TGBp3 in *N. benthamiana* leaves. The proportions of sites containing GFP:TGBp2 and GFP:TGBp3 in multiple cell clusters were each significantly greater than the proportion of sites that were cell clusters containing GFP ($P<0.05$)(Table 1). The proportions of cell clusters containing GFP, GFP:TGBp2, and GFP:TGBp3 in *N. tabacum* source or sink leaves were not significantly different ($P>0.05$) (Table 1). The values recorded for GFP, GFP:TGBp2, and GFP:TGBp3 in *N. tabacum* leaves suggest that these proteins rarely accumulate in two neighboring cells. While GFP:TGBp2, and GFP:TGBp3 could move from cell to cell in *N. benthamiana* leaves, the same proteins were restricted mainly to single cells in *N. tabacum* leaves.

Intercellular trafficking of GFP:TGBp2 and GFP:TGBp3 was also studied in transgenic tobacco expressing various PVX genes. Cell-to-cell movement of GFP:TGBp3 was studied by Dr. Konduru. Five transgenic N. tabacum lines, expressing the individual PVX TGBp1, TGBp2, or TGBp3 genes, or the combined TGBp2/ TGBp3 genes, were used (Fig 1B). Transgenic tobacco line TGB100 expresses the PVX TGBp1, TGB200 expresses the PVX TGBp2, TGB300 expresses the PVX TGBp3, TGB600 expresses the combined TGBp2/ TGBp3 (Fig. 1B). In a previous study, TGB100, TGB200, TGB300, and TGB600 plants restored intercellular movement to defective PVX viruses that had mutations in similar genes. Therefore, the transgenically expressed proteins are functional for virus cell-to-cell trafficking (Spillane et al., 1997; Verchot et al., 1998).

Cell-to-cell movement of GFP:TGBp2 or GFP:TGBp3 occurred in source but not sink leaves of TGBp1-transgenic *N. tabacum* (Tables 1 and 2; Fig 2). In TGB100 source leaves, 16% and 26% of the sites contained GFP:TGBp2 or GFP:TGBp3, respectively, in cell clusters that ranged to three or four cells (Tables 1 and 2). Leaves were viewed at 3 dpb and there was no change in protein movement between 1 and 3 dpb (Table 2). In TGB100 sink leaves, GFP:TGBp2 and GFP:TGBp3 accumulated mainly in single cells (Table 1). These data suggest that cell-to-cell movement of GFP:TGBp2 or GFP:TGBp3 depends on PVX TGBp1 and on leaf developmental stage.

GFP:TGBp2 and GFP:TGBp3 accumulated mainly in single cells in TGB200, and TGB300 leaves (Table 1). There was no evidence of protein movement in leaves analyzed at 3 dpb (data not shown). In all transgenic leaves bombarded with pRTL2-GFP plasmids, GFP was detected mainly in single epidermal cells (Table 1; Fig. 2). The transgenically expressed PVX proteins did not promote cell-to-cell movement of GFP.

Statistical comparisons were made between the nontransgenic and TGB100 source leaves bombarded with each plasmid. For GFP:TGBp2, and GFP:TGBp3, the proportion of fluorescent sites containing multiple cells in TGB100 leaves was higher than in nontransgenic leaves ($P<0.05$). Statistical comparisons were not conducted for TGB200, TGB300, or TGB600 leaves because there was no evidence of PVX protein cell-to-cell movement in these leaves.

Biolistic delivery of pRTL2-GFP:TGBp2 and –GFP:TGBp3 using the Helios gene gun.

Nonspecific movement of GFP between cells was reported in experiments using a handheld biolistic delivery system (Crawford and Zambryski, 2000; Imlau et al., 1999; Itaya et al., 2000; Oparka et al., 1999). Nonspecific movement of GFP results from diffusion of proteins across the plasmodesmata while targeted protein movement requires an active transport mechanism. Proteins move further by a nonspecific mechanism than by a targeted mechanism (Crawford and Zambryski, 2000; Imlau et al., 1999; Itaya et al., 2000; Oparka et al., 1999).

The Helios gene gun is a handheld biolistic delivery method, and is unlike the PDS1000/He system because it does not use a vacuum chamber for plasmid bombardment. In this study, experiments were conducted to determine if the pattern of PVX protein cell-to-cell movement would reflect nonspecific or targeted protein movement using different biolistic delivery methods. Nontransgenic and TGB100 *N. tabacum* leaves were bombarded with pRTL2-GFP and -GFP:TGBp2 plasmids using the Helios gene gun. Dr. Konduru also conducted similar experiments using pRTL2-GFP:TGBp3 plasmids (Tables 3 and 4).

GFP moved extensively between neighboring cells in nontransgenic or TGB100 *N. tabacum* leaves bombarded using the Helios gene gun (Fig. 3). Fluorescent sites in source or sink leaves expanded between 1 and 3 dpb to include more than 30 cells

(Tables 3 and 4). There were more multiple cell clusters in sink leaves than in source leaves. In nontransgenic or TGB100 sink leaves, GFP was detected in multiple cell clusters in 56 to 60% of the sites viewed at 3 dpb. In nontransgenic or TGB100 source leaves viewed at 3 dpb, GFP was in multiple cell clusters in 10 to 12% of the sites viewed (Tables 3 and 4).

The pattern of GFP:TGBp2 and GFP:TGBp3 protein accumulation in nontransgenic and TGB100 leaves following biolistic delivery using the Helios gene gun was similar to the pattern noted in leaves bombarded with plasmids using the PDS1000/He system. In TGB100 source leaves, 22 to 23% of the sites containing GFP:TGBp2, and 27 to 29% of the sites containing GFP:TGBp3, were multiple cell clusters (Table 3). Both GFP:TGBp2 and GFP:TGBp3 were more often detected in two adjacent cells than in clusters of three to four cells (Table 4). The proportions of cell clusters containing GFP:TGBp2 or GFP:TGBp3 in TGB100 source leaves did not increase between 1 and 3 dpb. In nontransgenic source or sink leaves and in TGB100 sink leaves, GFP:TGBp2 and GFP:TGBp3 were each observed mainly in single cells (Tables 3 and 4).

The pattern of GFP:TGBp2 or GFP:TGBp3 movement in TGB100 leaves resembles targeted protein movement. Using either the Helios gene gun or PDS1000/He system, GFP:TGBp2 or GFP:TGBp3 mostly accumulated in clusters of two to four cells in TGB100 source leaves.

Mutations in the PVX TGBp2, or TGBp3 genes effect viral cell-to-cell movement differently.

In previous studies, mutations in the PVX TGB within the PVX genome restricted virus cell-to-cell movement in *N. tabacum* leaves (Spillane et al., 1997; Verchot et al., 1998). Effects of these mutations on virus cell-to-cell movement in *N. benthamiana* have not been tested previously. Therefore, mutant PVX viruses were used to determine if mutations in the TGBp2 or TGBp3 ORFs would have different effects on virus movement in these two hosts.

The pPVX.GFP infectious clone contains the PVX genome plus the GFP gene (Fig. 4A). The pPVX.GFP-12D infectious clone encodes a deletion mutation within the TGBp2 gene in the PVX genome (Verchot et al., 1998). The pPVX.GFP-ΔCP infectious clone has most of the CP gene deleted (Spillane et al., 1997). The 12D and ΔCP mutations were shown previously to inhibit viral cell-to-cell movement in *N. tabacum* leaves. The pPVX-GFP-8FS infectious clone encodes a frame shift mutation within the TGBp3 gene that removes the 3' half of the TGBp3 gene. This TGBp3 mutation has not been tested in previous studies (Fig. 4A).

Infectious transcripts of PVX.GFP and PVX.GFP-12D were inoculated to the *N. tabacum* and *N. benthamiana* leaves to determine if these mutations have different effects on virus movement. GFP expression was used to monitor virus cell-to-cell movement for 14 days post inoculation (dpi). PVX.GFP moved systemically in *N. tabacum* and *N. benthamiana* plants within 7 to 10 dpi. PVX.GFP-12D viruses were restricted to single cells in *N. tabacum* and *N. benthamiana* leaves (Fig. 4A).

Dr. Konduru performed similar experiments using PVX.GFP, PVX.GFP-8 FS, -PVX.GFPΔCP infectious transcripts to inoculate *N. tabacum* and *N. benthamiana* leaves to determine if these mutations have different effects on virus movement. PVX.GFP-8FS virus moved slowly in *N. benthamiana* and *N. tabacum* leaves. PVX.GFP-8FS containing infection sites ranged from three to 20 cells by 4 dpi (Fig 4B). By 10 dpi, virus cell-to-cell movement was arrested (Fig. 4B). There was no secondary spread of virus out of the infection foci and no evidence of virus movement into the vasculature. Plants were maintained for a maximum of 21 days, and PVX.GFP-8FS viruses did not move systemically in either *Nicotiana* spp. These data suggest that the 5' half of the PVX TGBp3 gene is sufficient for cell-to-cell movement of the virus but the 3' half of the gene is required for successful vascular transport in either host.

DISCUSSION

The requirements for PVX protein plasmodesmata transport in *N. benthamiana* and *N. tabacum* leaves are different (Fig. 5). In *N. benthamiana* leaves, GFP:TGBp2 and GFP:TGBp3 independently moved through plasmodesmata. In *N. tabacum* leaves, PVX TGBp1 is required for cell-to-cell movement of TGBp2 or TGBp3. These data suggest that if cell-to-cell movement of TGBp2 and TGBp3 is required for PVX movement, then the virus has developed different mechanisms to achieve protein movement in different hosts.

In previous studies of the potexvirus WClMV, cell-to-cell movement of the WClMV TGBp1 was increased by the WClMV TGBp2 and TGBp3 in *N. benthamiana* leaves (Lough et al., 1998). Cell-to-cell movement of viral RNA also occurred in the presence of TGBp1 and CP. Thus a model was proposed for WClMV by Lough et al. (1998, 2000) suggests that in *N. benthamiana* leaves a ribonucleoprotein complex containing viral RNA, TGBp1, and CP moves through plasmodesmata. The TGBp2 and TGBp3 proteins associate with this complex for efficient plasmodesmata transport of viral RNAs. In support of the Lough et al. (1998) model, the results presented in this study suggest that PVX TGBp2 and TGBp3 each have the capacity to move through PD in *N. benthamiana* leaves and contribute to a complex transporting of viral RNAs between cells.

In *N. tabacum* leaves cell-to-cell movement of PVX proteins is more tightly regulated. Cell-to-cell movement of GFP:TGBp2 or GFP:TGBp3 was observed only in TGBp1-expressing TGB100 tobacco leaves. Moreover, cell-to-cell movement of GFP:TGBp2 or GFP:TGBp3 was observed only in TGB100 source but not sink leaves. Either protein movement is not important in sink leaves, or PVX uses an alternative (and as of yet undetermined) mechanism to achieve protein cell-to-cell transport in these leaves. Thus, the host and leaf developmental stage are important factors affecting cell-to-cell movement of PVX TGBp2 and TGBp3.

In a similar study, the PVX TGBp1 did not move cell-to-cell in CP-transgenic or TGB600 *N. tabacum* leaves (Fig.5; Yang et al., 2000). In contrast, we observed GFP:TGBp2 or GFP:TGBp3 cell-to-cell movement in TGBp1-expressing transgenic leaves. One explanation is that TGBp1/ TGBp2 or TGBp1/ TGBp3 but not TGBp1/ TGBp2/ TGBp3 complexes move between adjacent cells (Fig. 5). These data suggest that there are different interactions among the PVX proteins that regulate protein plasmodesmata transport. Further experiments are needed to characterize interactions occurring among the PVX proteins. Another possibility is that in TGB600 or CP transgenic leaves, TGBp2/ TGBp3 (but not the individual PVX TGBp2 or TGBp3) accumulate inside plasmodesmata and thereby block TGBp1 transport (Fig. 5).

PVX TGBp2 and CP are essential for viral cell-to-cell movement in both *Nicotiana* spp. Mutations deleting large segments of the TGBp2 or CP genes within the PVX genome restricted virus movement in *N. tabacum* and *N. benthamiana* leaves

(Verchot et al., 1998). Surprisingly, PVX.GFP-8FS virus moves between adjacent cells in *N. tabacum* and *N. benthamiana* leaves (Krishnamurthy et al., 2002). Cell-to-cell movement of PVX.GFP-8FS was slow and virus did not spread systemically in either *Nicotiana* spp. These data suggest that the C-terminal half of the TGBp3 protein may function to enhance virus cell-to-cell movement and to promote virus vascular transport.

In a previous report, a mutation was introduced into the TGBp3 gene within the PVX genome, which eliminated virus cell-to-cell movement (Verchot et al., 1998). That mutation was named TGBp3 $^{+6}$ and was a six-nucleotide insertion mutation introduced at a location in the genome that is approximately 20 nucleotides downstream of the 8 FS mutation. The TGBp3 $^{+6}$ mutation altered the translated sequence within the C-terminal region and likely caused either the entire protein to misfold or malfunction. In that way, changes due to the TGBp3 $^{+6}$ mutation may have also eliminated activities associated with the N' terminal half of the TGBp3 protein. The 8FS mutation, in this study was a 2 nt insertion mutation that introduced a translation stop codon and eliminated translation of the C' terminal half of the protein. The 8FS mutation also caused a frame shift in the sequence downstream of the stop codon. Thus, the 8FS mutation would eliminate only activities associated with the C' terminal half of the protein and likely had no effect on activities of the N-terminal region of the TGBp3 protein.

Evidence obtained using the Helios gene gun delivery method indicates that cell-to-cell movement of GFP:TGBp2 and GFP:TGBp3 is due to targeted movement and is not due to diffusion of the protein through plasmodesmata. As in experiments conducted using the PDS1000/He system, cell-to-cell movement of GFP:TGBp2 or GFP:TGBp3 was dependent on the PVX TGBp1 in *N. tabacum* but not in *N. benthamiana*. Neither

GFP:TGBp2 or GFP:TGBp3 moved cell-to-cell in nontransgenic leaves following Helios gene gun delivery. Cell-to-cell movement of GFP:TGBp2 and GFP:TGBp3 occurred only in TGB100 source leaves. Furthermore, the extent of GFP:TGBp2 and GFP:TGBp3 cell-to-cell movement in TGB100 source leaves following bombardment of plasmids using either the PDS1000/He system and Helios gene gun was similar. Thus the extent of protein movement between cells likely depends on intrinsic properties of the viral proteins and a specific transport mechanism. Using the PDS1000/He system or the Helios gene gun maximal cell-to-cell movement of GFP:TGBp2, and GFP:TGBp3 was seen at 1dpb. In Tables 2 and 4, GFP:TGBp2 and GFP:TGBp3 proteins were more often in two adjacent cells than in multiple cell clusters.

GFP moves extensively between cells in tobacco sink but not source leaves following biolistic bombardment of plasmids using the Helios gene gun (Fig. 3; Itaya et al., 2000). During a three-day period GFP moved through more than 30 cells in bombarded sink leaves. This is in contrast to targeted movement of GFP:TGBp2 or GFP:TGBp3 which required the TGBp1 to mediate transport through only a few adjacent cells. Movement of GFP in sink leaves may be due to the delivery system and to structural differences between plasmodesmata in source and sink leaves. In sink leaves the simple plasmodesmata are abundant and have a large basal SEL that may allow nonspecific trafficking of proteins between adjacent cells. In source leaves plasmodesmata structure is more often branched and may not permit nonspecific protein movement (Crawford and Zambryski, 2000; Itaya et al., 2000; Imlau et al., 1999; Oparka et al., 1999).

GFP has been frequently used as a visual marker to study viral protein movement. GFP has been fused to the PVX TGBp1, TMV P30, *Tomato mosaic virus* (ToMV) P30, or CMV 3a MP genes and inserted into plasmids that were biolistically delivered into single tobacco leaf epidermal cells (Atsushi and Meshi, 2001; Crawford et al., 2000; Yang et al., 2000; Itaya et al., 1997,1998). Typically, protein cell-to-cell movement was observed within the first 24 hours using this delivery method. The abilities of viral proteins to move GFP *in trans* have also been studied. Plasmids expressing individual PVX proteins were co-bombarded with plasmids expressing GFP (Tamai and Meshi, 2001). This experimental strategy does not directly measure viral protein cell-to-cell movement, but does indicate whether the PVX proteins can promote cell-to-cell movement of heterologous proteins. In *N. benthamiana* leaves, PVX TGBp2, but not TGBp1 or TGBp3, could promote GFP cell-to-cell movement *in trans*. Thus, based on data presented in this report and in the previous study by Tamai and Meshi (2001), the PVX TGB proteins are themselves capable of cell-to-cell movement in *N. benthamiana* leaves, but may differ in their ability to promote cell-to-cell movement of heterologous proteins.

In summary, it seems that an inherent ability of PVX TGBp2 or TGBp3 to move cell-to-cell in *N. benthamiana* leaves may be important for PVX movement. However, the inherent inability of these proteins to move cell-to-cell in *N. tabacum* leaves has no effect on PVX movement. That is not to say that cell-to-cell movement of PVX TGBp2 or TGBp3 is not important, because of the evidence indicating that PVX may utilize TGBp1to facilitate TGBp2 or TGBp3 movement in *N. tabacum* leaves. However, it does indicate that in *N. tabacum* leaves TGBp2 or TGBp3 do not function to induce PD gating or move themselves from cell-to-cell. Thus it is likely that these proteins provide other activities essential to virus cell-to-cell movement. In addition, cell-to-cell movement of the PVX.GFP- TGBp3 FS mutant virus suggests that the C-terminal half of the TGBp3 protein is not essential for viral cell-to-cell movement but is required for viral vascular transport.

MATERIALS AND METHODS

Bacterial strains and plasmids

All plasmids were constructed and used to transform *Escherichia coli* strain JM109 (Sambrook et al. 1989). In all constructs the GFP gene was the EGFP gene obtained from Clontech (Palo Alto, CA). Two constructs, pRTL2-GFP:TGBp2, -GFP:TGBp3 contain GFP fused to the 5' ends of the PVX TGBp2 or TGBp3 gene s. The pRTL2 plasmid (Carrington and Freed, 1990) contains the CaMV 35S promoter and the *Tobacco etch virus* (TEV) translational enhancer element. GFP:TGBp2, and GFP:TGBp3 translational fusions were prepared using a two-step PCR procedure, known as "overlap PCR". In the case of GFP:TGBp2, or GFP:TGBp3, GFP was PCR amplified, using a 5' primer (5'GFP) that contains an additional N*co*I restriction site. The 3' GFP primer contains an additional 15 nts overlapping the 5' end of either the PVX TGBp2, or TGBp3 gene s. Next, the TGBp2 and TGBp3 genes were each PCR amplified using 5' primers (TGBp2 5' and TGBp3 5'), which contain additional 15 nts overlapping the 3' end of GFP. Each 3' primer (TGBp2 3' and TGBp3 3') contains additional B*am*HI restriction sites. In the final step GFP and TGBp2, or GFP and TGBp3 PCR products were annealed to each other. The GFP5' primer and either the TGBp2 3', or TGBp3 3' primers were used to PCR amplify GFP:TGBp2 or GFP:TGBp3. The GFP:TGBp2, and

GFP:TGBp3 PCR products were digested with N*co*I and B*am*HI. The plasmid pRTL2 was similarly digested. Linearized vector and digested PCR products were ligated.

The pRTL2-GFP plasmid was provided by Dr. Biao Ding, (Ohio State University, Columbus, OH). The pPVX.GFP, pPVX.GFP-12D, pPVX.GFP-8FS were PVX infectious clones containing the T7 promoter and were obtained from Dr. David Baulcombe (Sainsbury Laboratory, Norwich, UK). The 12D mutation lacks the coding sequence for the entire TGBp2 ORF between nt position 5170 to 5423 (Verchot et al., 1998). The pPVX.GFP-8FS has two nts inserted at position 5520 within the viral genome. A TGT codon is changed to a TAA codon that is a translation termination signal. This mutation also causes a frame shift halfway through the TGBp3 ORF.

Plant material

N. benthamiana and *N. tabacum* (cv. Petit Havana) plants were used in this study. The transgenic *N. tabacum* lines TGB100, TGB200, TGB300, TGB600 and CP were described previously (Spillane et al., 1997; Verchot et al., 1998; Yang et al., 2000).

Biolistic bombardment of detached and intact tobacco leaves

To identify source and sink tobacco leaves, a mature leaf was excised above the petiole. CF dye (Sigma, St. Louis, MO, USA) was applied to the petiole and its direct movement through the plant was monitored by epifluorescence microscopy. Source leaves do not accumulate dye. Source and sink leaves of similar plants were bombarded.

Two methods of biolistic DNA delivery were used. First, tobacco leaves were detached and placed in a petri dish on wet filter paper and the lower epidermis was bombarded using the PDS1000/He system (Biorad, Hercules, California, USA) at a pressure of 1100 kPa with 23 Hg vacuum in the chamber. Ten micrograms of plasmid

DNA was combined with 1 mg of 1 μm gold particles, as described previously (Yang et al., 2000). Ten microliters of the DNA/gold mixture was used per bombardment of detached leaves. Second, the Helios gene gun (Biorad) was used to bombard intact leaves of tobacco plants at a pressure of 180 kPa. Each gene delivery cartridge was loaded with 2.5 μg plasmid DNA coated to 0.5 mg gold particles using a Tubing Prep Station (Biorad). Gold-coated tubing was cut into 0.5 inch pieces to make the gene delivery cartridges, and then used for bombardment. Leaves were detached from the plants at 1 and 3 dpb for observation.

In vitro transcription and plant inoculations

Transcripts were prepared from the pPVX.GFP, pPVX.GFP-12D, and pPVX.GFP-8FS plasmids as described previously (Baulcombe et al., 1995). Ten micro liters of transcripts and carborundum were used to rub inoculate two tobacco leaves (Baulcombe et al., 1995). GFP expression was monitored using a hand held UV lamp and using an epifluorescence microscope (Baulcombe et al., 1995).

Microscopy

A Nikon E600 epifluorescence microscope with a blue excitation filter (420-490 nm) (Nikon Corp. Tokyo, Japan) was used to visualize GFP expression in tobacco leaves. The Optronics Magnafire camera was used (Intelligent Imaging Innovations, Inc., Denver, CO). Images were processed using Image Pro (Intelligent Imaging Innovations, Inc.) and Adobe Photoshop (Adobe Systems Inc., San Jose, California, USA) software.

Statistical analyses

All data analysis was conducted by Mark Payton (Department of Statistics at Oklahoma State University) using procedures from SAS (Cary, North Carolina, USA) and a significance level of 0.05 was used for all mean comparisons. Statistical analysis

(Tables 1, and 3) comparing the effects of plasmids, dpb, and leaves were assessed by chi-square tests using PROC FREQ. Each factor's simple effects were analyzed by fixing the other factors.

Table1

Cell-to-cell movement of GFP, GFP:TGBp2, and GFP:TGBp3 in nontransgenic and transgenic tobacco leaves following PDS1000/He plasmid delivery

	Proportion of sites containing GFP activity in multiple cells[a]		
Plants	pRTL2-GFP	pRTL2-GFP:TGBp2	pRTL2-GFP:TGBp3
N. benthamiana			
Source	3.5(8/230)c	39(92/234)a	30(84/277)b
N. tabacum			
Nontransgenic			
Source	**5.7 (7/123)a**	**5.5 (19/344)a**	**7.1 (50/701)a**
Sink	3.8 (9/237)	5.3 (17/319)	7.0 (18/258)
TGB100			
Source	**2.5 (8/319)c**	16.0 (33/206)b	26.1 (84/322)a
Sink	2.1 (8/378)	3.3 (3/91)	5.4 (6/112)
TGB200			
Source	2.6 (8/310)	ND	2.3 (2/85)
Sink	2.2 (8/372)	ND	2.6 (2/78)
TGB300			
Source	2.5 (10/407)	6.7 (6/90)	ND
Sink	0.4 (2/472)	2.9 (2/68)	ND
TGB600			
Source	2.1 (4/193)	ND	ND
Sink	1.3 (3/227)	ND	ND

[a] The percent of fluorescent cell clusters observed 1dpb in *N.benthamiana* and transgenic or non transgenic *N.tabacum* leaves. The total numbers of cell clusters relative to the total number of fluorescent sites are in parentheses. Multiple comparisons were performed for transgenic and TGB100 leaves only using PROC FREQ of SAS at P>0.05.

The non transgenic and TGB100 source leaves were compared for each plasmid, and pairs of percentages in bold are significantly different ($p<0.05$).

Table 2

Total number of cells per cell clusters in nontransgenic and TGB100 source leaves following PDS1000/He plasmid delivery

	Number single, double, or multiple cells[a]								
	N. benthamiana			*N. tabacum*					
				Nontransgenic			TGB100		
Plasmid	**S**	**D**	**M**	**S**	**D**	**M**	**S**	**D**	**M**
pRTL2-GFP:TGBp2									
1dpb	193	57	27	325	19	0	173	30	3
3dpb	ND	ND	ND	298	15	0	159	31	3
pRTL2-GFP:TGBp3									
1dpb	142	64	28	651	46	4	238	64	20
3dpb	ND	ND	ND	508	41	2	234	61	19
pRTL2-GFP									
1dpb	222	6	2	116	7	0	311	8	0
3dpb	ND	ND	ND	106	4	0	283	7	0

[a] The total numbers of sites containing GFP expression at 1 and 3 dpb in single (S) double (D) or multiple cells (M) are indicated. The data presented here was obtained from the same experiments presented in Table 1.

Table 3

Cell-to-cell movement of GFP, GFP:TGBp2, or GFP:TGBp3 proteins in *N. tabacum* leaves following Helios gene gun plasmid delivery

	Proportion of sites containing GFP activity in multiple cells[a]		
Plants[b]	GFP	GFP:TGBp2	GFP:TGBp3
Source Leaves			
Nontransgenic			
1dpb	2.6 (2/77)a	1.8 (2/112)a	4.5 (5/111)a
3dpb	**10.3 (18/175)**a	**4.4 (5/113)**a	4.4 (4/91)a
TGB100			
1dpb	5.1 (6/118)b	22.4 (26/116)a	28.8 (38/132)a
3dpb	**11.7 (16/137)**b	**22.2 (24/108)**a	27.6 (40/145)a
Sink Leaves			
Nontransgenic			
1dpb	11.0 (33/300)a	3.9 (6/154)b	4.1 (5/121)b
3dbp	**60.4 (230/381)**a	**4.7 (7/150)**b	4.0 (3/75)b
TGB100			
1dpb	10.1 (37/365)a	4.9 (6/123)a	5.2 (6/115)a
3dpb	**56.8 (193/340)**a	**4.7 (6/127)**b	**1.1 (1/93)**b

[a] The percent of fluorescent cell clusters observed 1 and 3 dpb in sink and source leaves is indicated. Total numbers of cell clusters relative to total number of sites (single cells + cell clusters) containing GFP, GFP:TGBp2, or GFP:TGBp3 are in parentheses. Two to five source or sink leaves of each nontransgenic or transgenic tobacco line were bombarded with each plasmid to obtain the numbers indicated. Multiple comparisons were performed for nontransgenic and TGB100 leaves. The values for nontransgenic source or TGB100 source leaves were compared between plasmids at 1 or 3 dpb. Similarly, the values for nontransgenic sink or TGB100 sink leaves were compared between plasmids at 1 or at 3 dpb. The values followed by the same letter within each row are not significantly different ($P>0.05$). Values at 3dpb for nontransgenic source versus sink leaves, or TGB100 source versus sink leaves were compared and values indicated in bold were significantly different ($P>0.05$). When comparing nontransgenic with TGB100 source leaves bombarded with pRTL2-GFP:TGBp2 or -GFP:TGBp3, the differences were always significant ($P<0.05$).

Table 4

Total number of single, double, or multiple cell clusters in *N. tabacum* leaves following Helios gene gun plasmid delivery

	Number single, double, or multiple cells in nontransgenic and TGB100 leaves[a]					
	Nontransgenic			TGB100		
Plasmids	**S**	**D**	**M**	**S**	**D**	**M**
Source Leaves						
pRTL2-GFP:TGBp2						
1dpb	110	2	0	90	19	7
3dpb	108	5	0	84	15	9
pRTL2-GFP:TGBp3						
1dpb	106	5	0	94	24	14
3dpb	87	4	0	105	25	15
pRTL2-GFP						
1dpb	75	2	0	112	6	0
3dpb	157	0	18	121	0	16
Sink Leaves						
pRTL2-GFP:TGBp2						
1dpb	148	6	0	117	6	0
3dpb	143	7	0	121	6	0
pRTL2-GFP:TGBp3						
1dpb	116	5	0	109	6	0
3dpb	72	3	0	92	1	0
pRTL2-GFP						
1dpb	267	23	10	328	26	11
3dpb	151	0	230	147	0	193

[a] The total numbers of sites containing GFP expression at 1 and 3 dpb in single (S) double (D) or multiple cells (M) are indicated. The data presented here was obtained from the same experiments presented in Table 3.

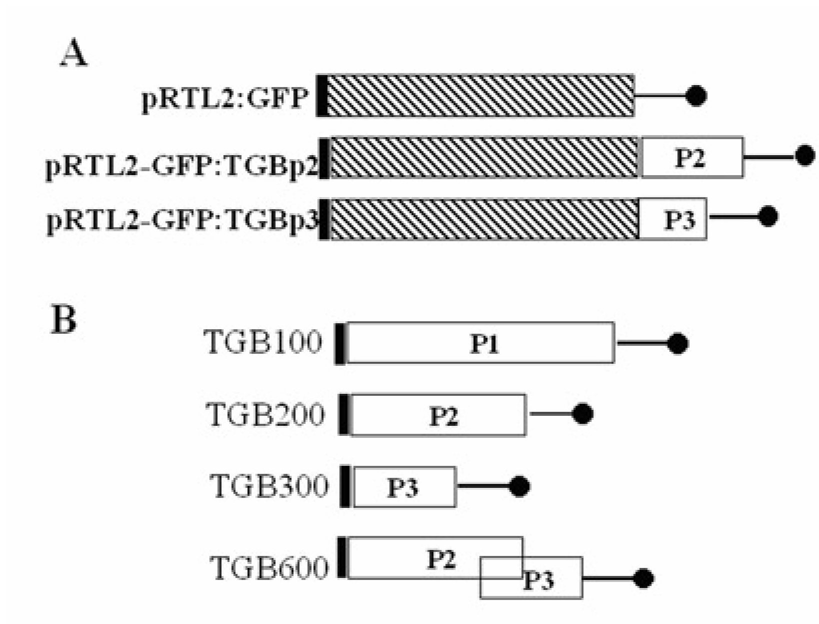

Fig. 1. Schematic representation of four plasmids and the five transgene s present in the transgenic plants used in this study. (A) The pRTL2-GFP, -GFP:TGBp2, and -GFP:TGBp3, plasmids contain the CaMV 35S promoter (black box) at the 5' end and a CaMV 35S transcription terminator (black circle) at the 3' end. The hatched boxes represent GFP and the open boxes represent each of the PVX genes. (B) Open boxes represent five PVX transgenes. The 35S promoter and transcription terminator is fused to each of the PVX ORFs.

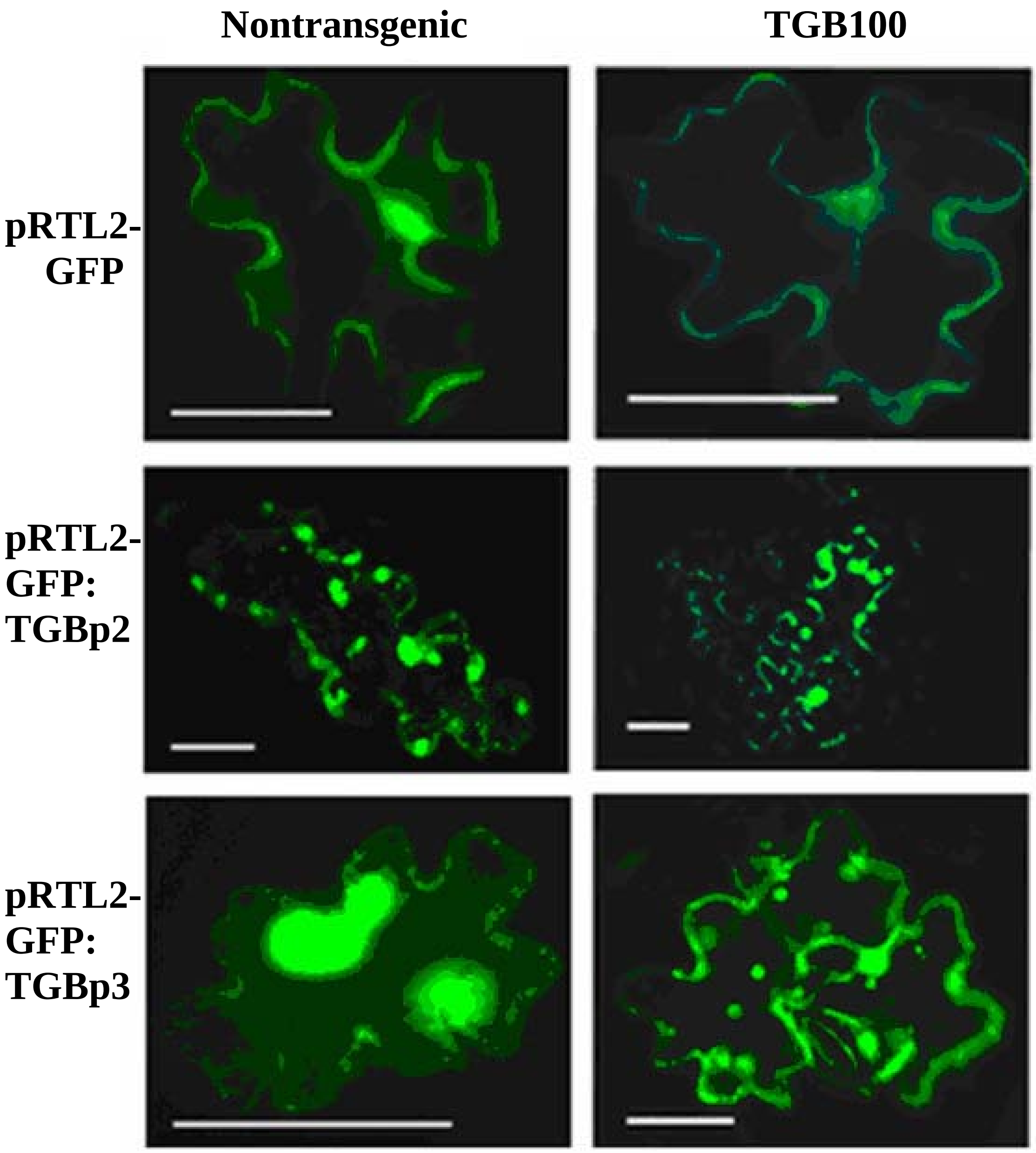

Fig. 2. Images taken 1 dpb from nontransgenic and TGB100 tobacco leaves bombarded with pRTL2-GFP, -GFP:TGBp2, and -GFP:TGBp3. All images were taken using a X40 objective lens, except for GFP:TGBp2 and GFP:TGBp3 in TGB100 leaves, which were taken using a X20 objective lens. The scale bars indicate 100 µm.

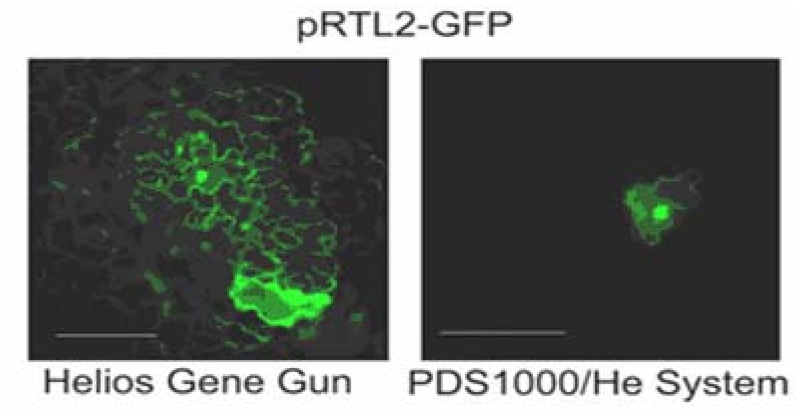

Fig. 3. Images taken 3 dpb of tobacco sink leaves bombarded with pRTL2-GFP using the Helios gene gun and the PDS1000/He delivery systems using a X10 objective lens. The scale bars indicate 100 μm.

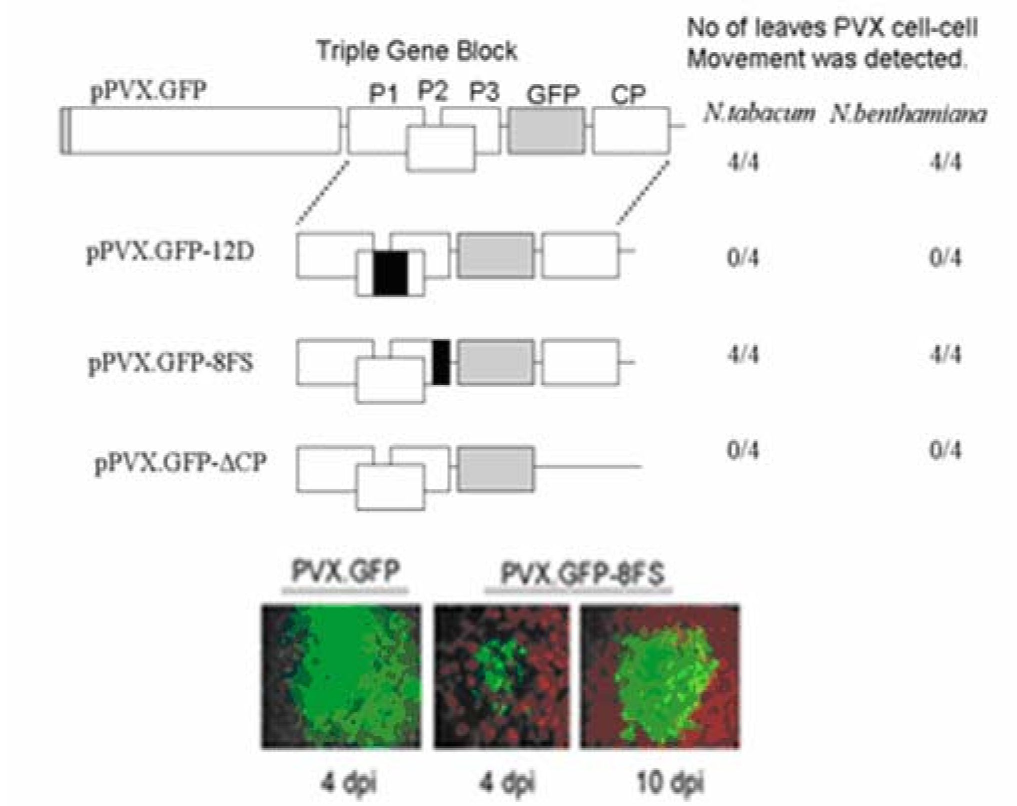

Fig. 4. Cell-to-cell movement of PVX.GFP mutant viruses. (A) Schematic representation of four pPVX.GFP infectious clones. Open boxes indicate the PVX genes. The light gray box at the 5' end of the genome indicates the bacteriophage T7 promoter and the light gray box before the coat protein indicates the GFP gene. The names for the TGB, GFP, and CP genes are indicated at the top. The black box in the pPVX.GFP-12D, pPVX.GFP–8FS, and pPVX.GFP-ΔCP plasmids indicate the region that was deleted by the mutations. The proportion of plants in which viral cell-to-cell movement was observed is indicated on the right. (B) Representative examples of infection foci observed in the transcripts of PVX.GFP and PVX.GFP-TGBp3FS inoculated *N. benthamiana* leaves at 4 and 10 dpi. Images were taken using a X10 objective lens.

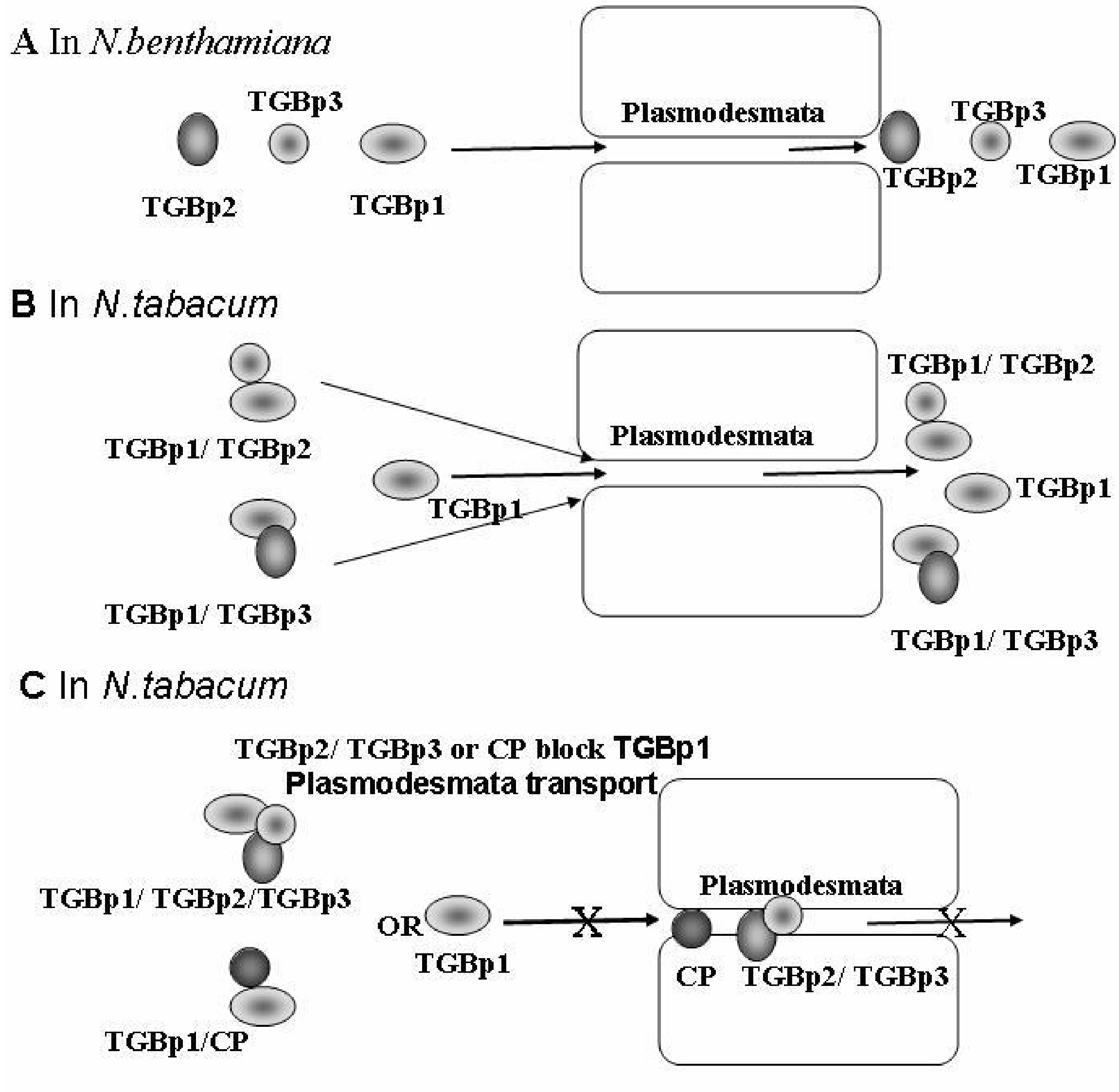

Fig. 5. PVX protein cell-to-cell movement in *N. benthamiana* and *N. tabacum* leaves. (A) PVX TGBp2, and TGBp3 can move independently through PD in *N. benthamiana* leaves. (B) In *N. tabacum* leaves PVX TGBp1 moves cell-to-cell (Yang et al., 2000) and facilitates cell-to-cell movement of PVX TGBp2 or TGBp3.(C) Cell-to-cell movement of PVX TGBp1 is inhibited in transgenic leaves expressing the PVX TGBp2/TGBp3 (Yang et al., 2000).

CHAPTER III

The *Potato virus X* TGBp2 Protein Association With the Endoplasmic Reticulum Plays a Role in But is Not Sufficient for Viral Cell-to-Cell Movement.

ABSTRACT

Potato virus X (PVX) TGBp1, TGBp2, TGBp3, and coat protein are required for virus cell-to-cell movement. Plasmids expressing GFP fused to TGBp2 were bombarded to tobacco leaf epidermal cells to study the subcellular accumulation pattern of the PVX TGBp2 protein. GFP:TGBp2 was detected in a polygonal pattern that resembles the endoplasmic reticulum (ER) network. Amino acid sequence analysis revealed TGBp2 has two putative transmembrane domains. Two mutations separately introduced into the coding sequences encompassing the putative transmembrane domains within TGBp2, disrupted membrane binding of GFP: TGBp2, inhibited GFP:TGBp2 movement in *Nicotiana benthamiana* and TGBp1-expressing *N. tabacum*, and inhibited movement of PVX containing the mutant TGBp2. A third mutation, lying outside the transmembrane domains, had no effect on the ability of GFP:TGBp2 to associate with the ER or to move from cell to cell in *N. benthamiana*, but inhibited GFP:TGBp2 movement in TGBp1-expressing *N. tabacum* and movement of PVX containing the mutant TGBp2 in either *Nicotiana* species. Thus, ER-association of TGBp2 may be required but not be sufficient for virus movement. TGBp2 likely provides an activity for PVX movement beyond ER association.

INTRODUCTION

Potexviruses contain a block of three partially overlapping ORFs termed the triple gene block (TGB) that encode proteins required for virus cell-to-cell movement. In the case of PVX these three proteins are named TGBp1, TGBp2, and TGBp3 and they have molecular masses of 25-kDa, 12-kDa, and 8-kDa, respectively. The PVX CP is also required for virus movement (Forster et al., 1992).

Expression of the PVX TGBp2 and TGBp3 has been difficult to study because available antibodies could not detect these proteins in infected plants (Verchot and Baulcombe, unpublished data). Previous attempts to study TGBp2 or TGBp3 accumulation in plant cells by fusing GFP to the TGBp2 or TGBp3 open reading frames within the PVX infectious clone were also unsuccessful (Verchot and Baulcombe, unpublished data). Protein accumulation following expression from the viral genome may be too low to detect. Thus, transgenic plants expressing TGBp2 or TGBp3, or the combined TGBp2/TGBp3 open reading frames were used tin the past to study expression of these proteins (Verchot et al., 1998; Krishnamurthy et al., 2002). These transgenic plants complemented cell-to-cell movement of viruses containing mutations in TGBp2 or TGBp3 open reading frames and therefore served as a tool to explore protein expression and viral protein-protein interactions (Verchot et al., 1998; Krishnamurthy et al., 2002).

In a related studies, the green fluorescent protein (GFP) gene was fused to each PVX TGB protein coding sequence and cell-to-cell movement of GFP:TGBp1, GFP:TGBp2, and GFP:TGBp3 was studied following biolistic bombardment of plasmids to nontransgenic and transgenic *N. tabacum* expressing each of the PVX TGB or CP ORFs (see Chapter II; Krishnamurthy et al., 2002). GFP:TGBp1 moved between adjacent cells in nontransgenic tobacco leaves, but was restricted to single cells in transgenic tobacco expressing either the PVX CP or the combined TGBp2 and TGBp3 ORFs (Krishnamurthy et al., 2002). GFP:TGBp2 and GFP:TGBp3 moved cell to cell in *N. benthamiana* leaves but not in nontransgenic *N. tabacum* leaves (see Chapter II; Krishnamurthy et al., 2002). GFP:TGBp2 and GFP:TGBp3 moved in source, but not sink, leaves of transgenic *N. tabacum* expressing PVX TGBp1 (see Chapter II; Krishnamurthy et al., 2002). Thus, movement of GFP:TGBp2 and GFP:TGBp3 are host specific. Moreover, GFP:TGBp2 and GFP:TGBp3 movement depends on the presence of TGBp1 as well as on the leaf developmental stage in *N. tabacum*.

Amino acid sequence analyses suggested that TGBp2 and TGBp3 have hydrophobic sequences that may be transmembrane segments (Morozov et al., 1999; Solovyev et al., 2000). TGBp3 has a single transmembrane domain that binds it to the ER (Krishnamurthy et al., 2003). Confocal microscopic analysis revealed GFP:TGBp3 proteins associate with the endoplasmic reticulum (ER) in tobacco leaves (Krishnamurthy et al., 2003). Mutations which disrupted membrane binding of TGBp3 also inhibited PVX cell-to-cell movement suggesting that, ER-association of PVX TGBp3 is important for virus movement (Krishnamurthy et al., 2003).

In this study, we provide evidence that PVX TGBp2, similar to TGBp3, associates with the ER network in both *N. tabacum* and *N. benthamiana* leaves. Targeted mutations were introduced into computer-predicted transmembrane segments to disrupt protein-membrane associations. Effects of these mutations on protein cell-to-cell movement and on PVX movement were studied. While the requirements for protein movement in *N. benthamiana* and *N. tabacum* differ, the requirements for virus movement may be the same in both hosts.

RESULTS

Subcellular accumulation of GFP:TGBp2 in tobacco leaves

Two methods were used to study subcellular accumulation of PVX TGBp2 in tobacco leaves. First, transgenic *N. tabacum* plants were prepared that contain GFP fused with the 5' end of the PVX TGBp2 coding sequence. Second, plasmids containing GFP fused to the 5' end of the PVX TGBp2 coding sequence were biolistically delivered to tobacco leaf epidermal cells. The pattern of fluorescence was analyzed by confocal microscopy and representative examples of images obtained are shown in Figure 1. A fluorescent polygonal network, resembling the ER network, was observed in transgenic and bombarded *N. tabacum* leaves expressing GFP:TGBp2 (Fig. 1).

The pattern of GFP:TGBp2 accumulation was compared with the pattern of mGFP5-ER, GFP:MBD, or GFP:Talin accumulation in *N. tabacum* epidermal cells. mGFP5-ER is a modified GFP containing ER-targeting and retention sequences, and therefore GFP accumulates in the ER lumen (Haseloff et al., 1997). GFP:MBD has the microtubule-binding domain of the *MAP4* gene product fused to the carboxy terminus of GFP (Marc et al., 1998), and GFP:Talin has the F-actin binding domain of the mouse *Talin* gene fused to GFP (Kost et al., 1998). In this study, stable transformants of *N. tabacum* plants expressing mGFP5-ER displayed the same reticulate network (Fig. 1) that has been described in previous studies to represent the ER network (Dunoyer et al., 2002; Ridge et al., 1999;Boevink et al., 1998; Reichel and Beachy, 1998; Haseloff et al., 1997). GFP:TGBp2 and mGFP5-ER accumulated in *N. tabacum* leaves in similar polygonal networks of thin tubules and cisternae (Fig. 1). Confocal images of cells containing GFP:MBD or GFP:Talin show filamentous arrays typical of the microtubule and actin networks, respectively (Fig. 1). The pattern of GFP:TGBp2 accumulation did not resemble the pattern of accumulation in GFP:MBD or GFP:Talin expressing cells.

Chemical inhibitors that disrupt the ER network, alter the pattern of GFP:TGBp2 accumulation

To test whether GFP:TGBp2 is associated with the ER or cytoskeleton, bombarded leaves were treated with brefeldin A (BFA) or latrunculin B. BFA in concentrations exceeding 100 μg/ml severely disrupts the ER and Golgi network. BFA causes the Golgi stacks to fuse with the ER and membranous islands form throughout the cell (Ritzenthaler et al., 2002; Saint-Jore et al., 2002; Henderson et al., 1994). If GFP:TGBp2 is ER associated, there should be islands of fluorescence scattered throughout the cell. Latrunculin B depolymerizes actin filaments (Nebenfuhr et al., 1999). Actin has been implicated in contributing to the shape and movement of the ER in plants (Knebel et al., 1990). In a previous study, chemicals that disrupt actin also changed the distribution of ER within the cell. For example, after treatment of cells with cytochalasin D (which depolymerizes actin cables), blind-ending ER tubules and cisternae were observed (Knebel et al., 1990). Thus, we predict that if GFP:TGBp2 is associated with the microfilaments, then following latrunculin B treatment we should observe blind-ending ER tubules and large cisternae.

Initially, we wanted to determine whether these drugs were generating the desired effects on the endomembrane and cytoskeleton system in *N. tabacum* leaves expressing mGFP5-ER, GFP:MBD, or GFP:Talin. Application of BFA at a concentration of 200 μg/ml for a period of 3- 4 hr was necessary to cause disruption in the pattern of the ER in transgenic leaves expressing mGFP5-ER (data not shown). In contrast to the reticulate pattern consistently observed in untreated mGFP5-ER transgenic leaves, BFA-treated mGFP5-ER-expressing leaves displayed strongly fluorescent islands that were dispersed throughout the cytoplasm (Fig. 2A). In GFP:Talin expressing cells, a 1-2 hr latrunculin B treatment resulted in significantly reduced numbers of filamentous structures, leaving only a few fragmented and thick actin cables in the cell (Fig. 2B). In mGFP5-ER expressing leaves treated with latrunculin B for 1-2 hr we observed blind-ending tubules and cisternae (Fig 2A).

We then examined how these drugs affected the distribution of GFP:TGBp2. As in BFA treated cells expressing mGFP5-ER, BFA caused extensive reorganization of the fluorescent networks in GFP:TGBp2 expressing cells (Fig. 2C). Fluorescence was in islands dispersed throughout the cell (Fig. 2C). Latrunculin B had similar effects on the reticulate network in GFP:TGBp2 expressing cells and in mGFP5-ER expressing cells. As in mGFP5-ER expressing cells, blind-ending tubules and sheets of cisternal ER were often visible in GFP:TGBp2 expressing cells following treatment with latrunculin B (compare Fig. 2A and 2C).

PVX TGBp2 has two predicted transmembrane segments

Since the subcellular localization studies suggest that TGBp2 is associated with cellular membranes, amino acid sequence analyses were conducted to identify putative transmembrane segments of TGBp2 and mutational analysis was used to test the computer predictions. First, the PVX TGBp2 amino acid sequence was aligned with TGBp2 sequences of eight other known potexviruses using ClustalW. The alignment resembles previously published alignments containing stretches of uncharged amino acid residues and a central region of highly conserved amino acid residues (Fig. 3A) (Huisman et al., 1988; Morozov et al., 1987).

TMAP is a method for predicting transmembrane helix segments from multiple aligned sequences (Persson and Argos, 1994), was used to identify putative transmembrane domains of the potexvirus TGBp2 proteins. The prediction is based on the assumption that hydrophobic stretches of approximately 21 amino acids in length are generally required to span a lipid bilayer (Persson and Argos, 1994). The output of TMAP contains the number of predicted transmembrane segments, the predicted start and end of each transmembrane segment, and the predicted length of each transmembrane segment (Persson and Argos, 1994). The potexvirus TGBp2 proteins have two conserved hydrophobic domains that are predicted to be transmembrane segments (Fig. 3B). The predicted transmembrane segments span amino acid position 15 to 38 and 75 to 101, within the PVX TGBp2 protein sequence**.** The output of TMAP predicted the N- and C-terminal regions of TGBp2, and a central domain between the putative transmembrane segments lie outside of the membrane (Fig. 3B).

To test the prediction that the two hydrophobic segments of PVX TGBp2 are transmembrane domains, three mutations (m1, m2, and m3) were introduced into the PVX TGBp2 sequence within the plasmid pRTL2-GFP:TGBp2 (Fig. 4A). The plasmid pRTL2-GFP:TBp2m1 contains a substitution mutation within the region of TGBp2 that encodes the first transmembrane segment. This mutation results in the substitution of Leu-Gly-Leu with Ser-Arg-Pro (Fig. 4A). The plasmid pRTL2-GFP:TGBp2m3 has twelve nts, encoding Ser-Arg-Pro-Thr, inserted into the second putative transmembrane segment. Mutations encoding Ser-Arg-Pro or Ser-Arg-Pro-Thr were specifically designed based on results of a previous report analyzing membrane insertion of the *Tobacco etch virus* (TEV) 6K membrane-spanning protein (Restrepo-Hartwig and Carrington, 1994). Nine nts encoding Ser-Arg-Pro residues were introduced into the TEV 6K gene within the region encoding the transmembrane domain and membrane insertion of TEV 6K was disrupted (Restrepo-Hartwig and Carrington, 1994). The plasmid pRTL2-GFP:TGBp2m2 has 30 nts deleted between the putative transmembrane segments (Fig. 4A). The m2 mutation is not predicted to disrupt membrane insertion of TGBp2 but may alter other TGBp2 activities (Fig 4B). Thus, only the m1 and m3 mutations are predicted to disrupt membrane insertion of GFP:TGBp2 (Fig. 4B).

The pRTL2-GFP:TGBp2m1, -GFP:TGBp2m2, and –GFP:TGBp2m3 plasmids were bombarded to nontransgenic *N. tabacum* and *N. benthamiana* leaves and intracellular protein accumulation was studied 24 hours post bombardment (hpb) using confocal laser scanning microscopy. Fluorescence due to GFP:TGBp2m1 and GFP:TGBp2m3 accumulated primarily in the cytoplasm, suggesting that the m1 and m3 mutations disrupted membrane insertion of these proteins (Fig 4C). The pattern of GFP:TGBp2m2 accumulation resembled the pattern of mGFP5-ER accumulation in Figure 1, suggesting that the m2 mutation did not alter TGBp2 membrane insertion (Fig. 4C).

TGBp2 mutations inhibited virus cell-to-cell movement

The m1, m2, and m3 mutations were each introduced into the PVX genome to determine if membrane association of TGBp2 is essential for viral cell-to-cell movement. The plasmid pPVX204e contains cDNA copies of the PVX genome adjacent to the CaMV 35S promoter. The plasmid contains the GFP gene fused to a duplicated CP subgenomic RNA promoter inserted into the viral genome (Baulcombe et al., 1995). The plasmids pPVX204p2m1, pPVX204p2m2, and pPVX204p2m3 contain the m1, m2, and m3 mutations in the TGBp2 ORF within the PVX genomic cDNA (Fig. 5). These plasmids were biolistically delivered to *N. benthamiana* or nontransgenic *N. tabacum* plants. GFP expression was used to monitor virus cell-to-cell and systemic spread.

PVX204e spread systemically within 10 days post inoculation in *N. benthamiana* or *N. tabacum* leaves. This was evidenced by GFP expression in upper non-inoculated leaves in all plants bombarded with pPVX204e plasmids (Fig. 5). PVX204p2m1, PVX204p2m2, and PVX204p2m3 viruses were restricted to single cells in both *Nicotiana* species (Fig. 5). Thus, two mutations that disrupt membrane association also disrupt virus movement (in both *Nicotiana* spp). The fact that PVX204p2m2 is also defective in movement suggests that ER association is not alone sufficient to support virus movement. TGBp2 likely has additional functions beyond ER association.

TGBp2 mutations alter protein intercellular movement in N. benthamiana and TGB100 leaves

Experiments were conducted to determine if the TGBp2 mutations have an effect on cell-to-cell movement of the protein. In a previous study the pRTL2-GFP:TGBp2 plasmids were biolistically delivered to *N. benthamiana* leaves, *N. tabacum* leaves, and TGBp1-expressing transgenic *N. tabacum* leaves (named TGB100) (see Chapter II; Krishnamurthy et al., 2002). GFP:TGBp2 moved between adjacent cells in *N. benthamiana* leaves and in TGB100 transgenic *N. tabacum* leaves, but did not move cell to cell in *N. tabacum* leaves. Thus, in *N. tabacum* leaves, TGBp1 is essential for TGBp2 cell-to-cell movement (see Chapter II; Krishnamurthy et al., 2002).

The plasmids pRTL2-GFP, -GFP:TGBp2, -GFP:TGBp2m1, -GFP:TGBp2m2, and -GFP:TGBp2m3 were bombarded to *N. benthamiana,* nontransgenic *N. tabacum*, or TGB100 transgenic *N. tabacum* leaves to determine if the mutations altered protein cell-to-cell movement. Cell-to-cell movement of fluorescence was monitored 24 hpb. Representative examples of protein accumulation in one or multiple cells are presented in Fig. 6.

The physiological status of these leaves was determined by CF dye translocation studies (see Chapter II; Oparka et al., 1994; Yang et al., 2000; Krishnamurthy et al., 2002). A young leaf that imported and unloaded CF was designated a sink. A fully expanded leaf that was unable to import CF dye was designated a source leaf (data not shown). Following the CF dye test, leaves were detached from plants that were of a similar age and bombarded with plasmids.

GFP accumulated primarily in single epidermal cells in *N. benthamiana* or nontransgenic *N. tabacum* leaves that were bombarded with pRTL2-GFP plasmids (Table 1). On rare occasions GFP was detected in two adjacent cells. Similar background levels of multiple cell fluorescence were reported in related studies, and might occur on occasions when plasmids were delivered to neighboring cells (see Chapter II; Itaya et al., 1997; Yang et al., 2000; Krishnamurthy et al., 2002).

Previously, we have shown that GFP:TGBp2 accumulates in multiple cell clusters in *N. benthamiana* leaves and in transgenic TGB100 *N. tabacum*, and that it accumulates primarily in single cells in nontransgenic *N. tabacum* leaves (Krishnamurthy et al., 2002). In *N. benthamiana* source leaves in this study, 31.5% of the sites contained GFP:TGBp2 in multiple cell clusters; in nontransgenic *N. tabacum* source or sink leaves, GFP:TGBp2 accumulated primarily in single cells; and in TGB100 source leaves, 25.9% of sites contained GFP:TGBp2 in multiple cell clusters (Table 1). In TGB100 sink leaves GFP:TGBp2 was rarely detected in adjacent cells (Table 1). The proportion of cell clusters containing GFP:TGBp2 in TGB100 source leaves was significantly greater than in nontransgenic leaves ($P<0.05$) and was significantly greater than the proportion of multiple cell clusters containing GFP in TGB100 source leaves ($P<0.05$).

The plasmids pRTL2-GFP:TGBp2m1, m2, and m3 were each bombarded to *N. benthamiana*, nontransgenic *N. tabacum*, or TGB100 leaves to determine if these mutations alter protein cell-to-cell movement. In *N. benthamiana* leaves, the m1 and m3 mutations inhibited GFP:TGBp2 cell-to-cell movement. GFP:TGBp2m1 and GFP:TGBp2m3 were detected primarily in single epidermal cells. Approximately 8.5% and 7% of sites contained GFP:TGBp2m1 and GFP:TGBp2m3, respectively, in adjacent cells (Table 1). Statistical analyses indicate that the proportions of sites containing GFP, GFP:TGBp2m1 and GFP:TGBp2m3 in adjacent cells were not significantly different ($P>0.05$).

The m2 mutation did not affect cell-to-cell movement of GFP:TGBp2 in *N. benthamiana* leaves. GFP:TGBp2m2 accumulated in clusters of adjacent cells, indicating that protein cell-to-cell movement was not severely affected by this mutation (Table 1). Statistical analyses indicate that the proportions of sites containing GFP:TGBp2 and GFP:TGBp2m2 in multiple cell clusters were not significantly different ($P>0.05$).

In nontransgenic and TGB100 source and sink leaves, GFP:TGBp2m1, GFP:TGBp2m2, and GFP:TGBp2m3 were detected primarily in single cells. Thus, each mutation introduced into the TGBp2 ORF inhibited protein movement between cells in

TGB100 source leaves (Table 1). Between 0 and 6% of the sites viewed in TGB100 source leaves bombarded with pRTL2-GFP:TGBp2m1,- GFP:TGBp2m2 or -GFP:TGBp2m3 contained fluorescence in two adjacent cells and these values were not significantly different from the values recorded for GFP in TGB100 leaves ($P>0.05$) (Table 1).

These data suggest that membrane targeting of the TGBp2 protein is important for protein cell-to-cell movement in *N. benthamiana* and *N. tabacum* leaves. While the m2 mutation has no affect on TGBp2 membrane insertion or on protein cell-to-cell movement in *N. benthamiana* leaves, it does alter TGBp2 intercellular movement in TGB100 leaves. The simplest explanation is that the m2 mutation could disrupt interactions between TGBp1 and TGBp2, which are necessary for TGBp2 cell-to-cell movement. Alternatively, TGBp2 may have activities beyond ER-association that contribute to its own plasmodesmata transport.

DISCUSSION

In this study, a GFP fusion with TGBp2 was detected in a polygonal pattern that resembles the ER network seen in cells transiently expressing mGFP5-ER (Fig. 1). To determine if the reticulate network was the ER network, leaf segments bombarded with pRTL2-mGFP5-ER or –GFP:TGBp2 plasmids were treated with BFA. BFA, in concentrations exceeding 100 μg/ml, severely disrupts the ER network (Henderson et al., 1994; Ritzenthaler et al., 2002). In this study, BFA similarly disrupts the fluorescent network in cells containing the mGFP5-ER or GFP:TGBp2 proteins, indicating that GFP:TGBp2 likely accumulates in the ER (Fig. 2).

The ER is a dynamic network and tubules within the peripheral ER require actin to maintain their mobility. The network tubules and cisternae often change in size and position. New tubules may arise from cisternae and may elongate or retract along a trajectory. The effects of latrunculin B on the ER, in mGFP5-ER or GFP:TGBp2 expressing cells, are reminiscent of the effects of cytochalasin D on the ER, as reported previously (Knebel et al., 1990). In onion bulb epidermal cells treated with cytochalasin D the ER network consisted of blind –ending tubules and large cisternae (Knebel et al., 1990). In this study, tobacco leaf epidermal cells were treated with latrunculin B and we observed blind-ending tubules and cisternal ER in mGFP5-ER or GFP:TGBp2 expressing cells (Fig 2A and C).

In a previous report we compared cell-to-cell movement of GFP:TGBp2, GFP:TGBp3, and GFP in *N. tabacum* leaves bombarded with plasmids using the PDS1000/He delivery system and the Helios Gene Gun delivery system (Chapter II; Krishnamurthy et al., 2002). GFP:TGBp2 and GFP:TGBp3 moved cell to cell in TGB100 source leaves but not in TGB100 sink leaves or nontransgenic *N. tabacum* source or sink leaves following plasmid delivery using either system (Chapter II; Krishnamurthy et al., 2002). Protein movement was monitored at 1 and 3 dpb and maximal movement of GFP:TGBp2 or GFP:TGBp3 was seen at 1 dpb. Thus movement of GFP:TGBp2 or GFP:TGBp3 likely depends on intrinsic properties of the viral proteins, and a specific transport mechanism (Chapter II; Krishnamurthy et al., 2002). GFP moved extensively between cells during a 3-day period in *N. tabacum* sink but not source leaves following plasmid delivery using the Helios Gene Gun, but was restricted primarily to single cells in leaves bombarded with the PDS1000/He system (Chapter II;

Krishnamurthy et al., 2002). Thus, movement of GFP in sink leaves may be due in part to the delivery system and in part to the developmental stage of the leaf. Other laboratories have reported occasional nonspecific movement of GFP (Itaya et al., 2000; Crawford and Zambryski, 2000). Having established that nonspecific movement is reduced in studies using the PDS1000/He system this delivery system was used in this study.

Mutations in TGBp2 that disrupt ER association of TGBp2 also inhibit GFP:TGBp2 and virus cell-to-cell movement in both *Nicotiana* species. These data suggest that ER association of the protein might be important for virus and protein movement. The m2 mutation inhibited GFP:TGBp2 cell-to-cell movement only in TGB100 *N. tabacum* leaves, but inhibited PVX cell-to-cell movement in both *Nicotiana* spp. (Table 1 with Fig. 5). The fact that a single mutation, which lies outside of the transmembrane domains, inhibits protein movement in TGB100 leaves and virus movement in *N. benthamiana* and *N. tabacum* leaves suggests that TGBp2 likely has a function beyond ER-membrane binding. One possibility is that TGBp2 interacts with TGBp1 in a manner that is important for virus movement. The m2 mutation might have specifically disrupted a sequence of TGBp2 that interacts with TGBp1 in the TGB100 leaves. Further research is needed to determine other activities of TGBp2 and to determine if TGBp1 and TGBp2 interact.

In the current model for potexvirus cell-to-cell movement, TGBp2 and TGBp3 serve to anchor a complex of TGBp1/viral RNA/ CP to either the ER or cytoskeletal network (Chapter I Fig. 3B; Lough et al., 2000; Lough et al., 1998). The ER or cytoskeleton targets the “movement complex” for plasmodesmata transport. Mutations in TGBp2 and TGBp3 that disrupt membrane binding of the proteins also disrupt virus movement (this study; Krishnamurthy et al., 2003), suggesting that ER-association of TGBp2 and TGBp3 might be important for PVX cell- to-cell movement (Krishnamurthy et al., 2003). There is no evidence yet indicating a role for the cytoskeleton in potexvirus movement.

The results presented in this study and in related studies indicate that TGBp1 provides the motive force for transport of viral proteins and nucleic acids through plasmodesmata (Krishnamurthy et al., 2002; 2003). TGBp1 moves independently through plasmodesmata, and does not require TGBp2 or TGBp3 to induce plasmodesmata gating or mediate its plasmodesmata transport (Yang et al., 2000; Krishnamurthy et al., 2003). TGBp2 and TGBp3 both require TGBp1 to mediate their transport in *N. tabacum* leaves.

MATERIALS AND METHODS

Bacterial Strains and Plasmids

All plasmids were constructed using Escherichia coli strain JM109 (Sambrook et al., 1989). The plasmid pRTL2-GFP was obtained from Dr. B. Ding (Ohio State University, OH) and contains EGFP (Clontech, Palo Alto, CA). The plasmid pRTL2 contains the CaMV 35S promoter and Tobacco etch virus (TEV) translational enhancer element (Carrington and Freed, 1990). The plasmid pBIN-mGFP5-ER plasmid was obtained from Dr. J. Hasselof (MRC Laboratory of Molecular Biology, Cambridge, UK) and contains a modified GFP (mGFP5-ER) fused with sequences that encode endoplasmic reticulum (ER) targeting and retention signals (Siemering et al., 1996; Haseloff et al., 1997). The plasmid pGFP-MBD was a generous gift from Dr. R. Cyr (The

Pennsylvania State University, PA) (Marc et al., 1998). The plasmid contains GFP fused with the 5' end of the microtubule-binding domain (MBD) of MAP4. The plasmid pRTL2-GFP:TGBp2 contains EGFP fused with the 5' end of the PVX TGBp2 coding sequence and was described previously (Krishnamurthy et al., 2002).

All other plasmids were prepared by a two-step PCR procedure (Yang et al., 2000) and sequences were confirmed using the Applied Biosystems ABI Prism Big Dye Terminator Cycle Sequencing Ready Reaction Kit (version 2.0) and an Applied Biosystems 3700 Capillary DNA Sequencer (Applied Biosystems, Foster City, CA). The plasmid pRTL2-GFP:Talin contains EGFP fused with the coding sequence of the F-actin binding domain of mouse *Talin* (Kost et al., 1998; McCann and Craig, 1997). EGFP was amplified using a forward primer containing an X*ho*I site and a reverse primer containing sequences overlapping the 3' end of the *Talin* F-actin binding domain. Similarly, the sequence encoding the F-actin binding domain of *Talin* was amplified using a forward primer complementary to the GFP reverse primer and a reverse primer containing an additional X*ba*I site. These two PCR products were annealed and the EGFP forward primer and the F-actin 3' reverse primer were used to PCR amplify the fused genes. The final PCR product was gel purified. PCR products and pRTL2 plasmids were digested with X*ho*I and X*ba*I, gel purified, and ligated.

Three mutations were separately introduced into pRTL2-GFP:TGBp2 plasmids (Krishnamurthy et al., 2002). pRTL2-GFP:TGBp2m1 has a substitution mutation located between 60 to 68 nucleotides (nts) from the 5' end of the TGBp2 ORF. Nine nts (TTAGGTCTA), which encode Leu-Gly-Leu, were replaced with twelve nts (AGTCGACCAACA), which encode Ser-Arg-Pro-Thr. The plasmid pRTL2-

GFP:TGBp2m2, has 30 nts deleted between 180 and 209 nts from the 5’ end of the PVX TGBp2 coding sequence. pRTL2-GFP:TGBp2m3 contains nine nts (AGTCGACCA) inserted into the TGBp2 sequence adjacent to nt position 167 within the TGBp2 coding sequence. The nine nts encode Ser-Arg-Pro residues.

To prepare the plasmids pRTL2-GFP:TGBp2m1, -GFP:TGBp2m2, and –GFP:TGBp2m3, complementary forward and reverse M1, M2, and M3 primers were used. The M1 primers correspond to the TGBp2 coding sequence surrounding nt positions 60 to 68 and encode a nt substitution mutation. The M2 primers surround nt positions 153 to180 within the TGBp2 coding sequence. The M2 primers contain 14 nts 5’ of the deleted region and 23 nts 3’ of the deleted region. The M3 primers correspond to TGBp2 coding sequences surrounding nt positions 146 to167 plus the nt insertion mutation. A similar PCR strategy was used for preparing each GFP:TGBp2 mutant. In the first PCR step, a EGFP forward primer (which contains an N*co*I site adjacent to the EGFP translation start site) and M1, M2, or M3 reverse primers were used to PCR amplify a fragment of GFP:TGBp2 using pRTL2-GFP:TGBp2 as a template. The TGBp2 M1, M2, or M3 forward primers combined with the TGBp2 3’ reverse primers were used to PCR amplify a fragment of the TGBp2 coding sequence. The 3’ TGBp2 primer contains a sequence adjacent to the TGBp2 translational stop codon that was a B*am*HI restriction site. In the final step, the EGFP and the TGBp2 PCR products were annealed to each other and the EGFP forward primer and the TGB2 3’ reverse primer were used to PCR amplify the GFP:TGBp2 fused genes. The GFP:TGBp2m1, GFP:TGBp2m2, or GFP:TGBp2m3 PCR products and pRTL2 plasmids were each digested with N*co*I and B*am*HI and then ligated.

Four PVX constructs were also prepared using two-step PCR (Verchot et al., 1998). The pPVX204 plasmid was obtained from Dr. D. C. Baulcombe (Sainsbury Laboratory, Colney, UK) and contains the PVX genome and the GFP gene. To prepare pPVX204e the original GFP was replaced with EGFP. First the TGB1 forward primer (extending from nt positions 4938-4964) and a TGB3 reverse primer (containing nts 5651-5671 of the PVX204 genome plus 15 nts of the EGFP sequence) were used to PCR amplify a fragment of the PVX genome. Then the TGB3 forward primer (overlapping nt position 5657-5671 plus 21 nts of the EGFP sequence) and the EGFP reverse primer containing an additional S*al*I site was used to PCR amplify EGFP. The two PCR products were annealed and the TGB1 5' and EGFP 3' primers were used to PCR a large fragment. The pPVX204 plasmid and PCR products were digested with A*pa*I and S*al*I, gel purified, and then ligated.

The pPVX204p2m1, pPVX204p2m2, and pPVX204p2m3 plasmids were also prepared using a two-step PCR procedure (Yang et al., 2000). The TGBp1 5' primer and M1, M2, or M3 reverse primers were used to PCR amplify a fragment of pPVX204e. M1, M2, or M3 forward primers and the EGFP reverse primer were used to PCR amplify a second fragment of PVX204e. These PCR products were annealed. The TGB1 forward primer and EGFP reverse primer were used to PCR amplify a final product containing M1, M2, or M3 mutations. The PCR products and PVX204 were digested with A*pa*I and S*al*I, gel purified, and then ligated.

Plant material

N. benthamiana leaves, nontransgenic and TGB100 transgenic *N. tabacum* (cv. Petit Havana) leaves were used in these experiments. TGB100 transgenic tobacco plants express PVX TGBp1, are susceptible to PVX infection, and can complement cell-to-cell movement of TGBp1-defective PVX viruses, as previously described (Verchot et al., 1995; 1998).

Transgenic *N. tabacum* expressing GFP:TGBp2 was prepared using *Agrobacterium* transformation, as previously described (Verchot et al., 1995). The plasmid pRTL2-GFP:TGBp2 was digested with H*ind*III and the expression cassette, which contains the CaMV 35S promoter, terminator, and the GFP:TGBp2 fused genes, was transferred to the binary vector pGA482 (An et al., 1987). The recombinant plasmid was introduced into *A. tumefaceins* LBA4404 by triparental mating. Transgenic plants were regenerated following the leaf-disk transformation method (Horsch et al., 1985).

Biolistic bombardment

N. benthamiana source leaves, nontransgenic *N. tabacum* source and sink leaves, and TGB100 source and sink leaves were used for these experiments as in Chapter II. Source and sink leaves were identified by applying carboxyfluorescein dye (CF) (Sigma, St. Louis, MO) to the petiole of the most mature leaf of an *N. benthamiana* or *N. tabacum* plant (Krishnamurthy et al., 2003; Yang et al., 2000). Plants were kept in the dark overnight and the next day leaves were detached and observed using an epifluorescence microscope and a 10X objective lens. CF dye was detected uniformly in sink leaves. CF dye was detected only in the veins in source leaves. Following the CF dye experiments, source or sink leaves were detached from plants of similar age and bombarded with plasmids using the PDS 1000/He System (Biorad, Hercules, CA).

Leaves were bombarded with 10 μg plasmids mixed with 1 mg of 1 μm gold particles. 10 μl of a DNA/gold mixture was loaded on a carrier disk and bombarded to detached leaves as described previously (Yang et al., 2000). The leaves were observed 24 hrs post bombardment (hpb) using epifluorescence microscopy to detect GFP expression (Yang et al., 2000).

For plant inoculations, young N. tabacum or N. benthamiana plants were bombarded with wild-type and mutant PVX204e plasmids using the Helios gene gun (Biorad, LaJolla, CA). Gene delivery cartridges were loaded with a mixture of 0.5 mg gold particles and 5μg plasmid using a Tubing Prep Station according to the manufacture's instructions (Biorad, La Jolla, CA). Gold-coated tubing was cut into 0.5 inch pieces to make the gene delivery cartridges and then used for bombardment of leaves at a pressure of 160 kPa.

Chemical inhibitor treatments of leaves

Nontransgenic *N. tabacum* or TGB100 leaves were bombarded with pBIN-mGFP5-ER, pRTL2-GFP:TGBp2, -GFP:TGBp2m1, -GFP:TGBp2m2, or-GFP:TGBp2m3 plasmids and incubated overnight (16 h) on moist filter paper.

Leaves were treated with either BFA, which disrupts the ER and Golgi network, or latrunculin B, which disrupts actin filaments (Henderson et al., *1994*; Nebenfuhr et al., 1999; Ritzenthaler et al., 2002; Saint-Jore et al., 2002). Leaves were cut into segments, analyzed by epifluorescence microscopy to detect GFP expression and then transferred to either a solution of 200 μg/ml BFA (Molecular Probes, Eugene, OR) or 1 μm latrunculin B (A.G. Scientific, Inc., San Diego, CA). Each chemical inhibitor was dissolved in 0.1% DMSO (w/v) solution. Leaf segments were incubated in each chemical inhibitor solution for 2- 4 hrs and then analyzed by confocal laser scanning microscopy. As a control, leaf segments were incubated in sterile water or 0.1% DMSO (w/v) for 4 hrs and then analyzed by confocal laser scanning microscopy.

Microscopy

GFP cell-to-cell movement in tobacco leaves was studied using a Nikon E600 (Nikon Inc., Dallas, TX) epifluorescence microscope with a Nikon B2A filter cube (containing a 470-490 nm excitation filter, a DM505 dichroic mirror, and a BA520 barrier filter). Images were captured using the Optronics Magnafire camera (Intelligent Imaging Innovations, Inc., Denver, CO) attached to the Nikon E600 microscope. A Leica TCS SP2 (Leica Microsystems, Bannockburn, IL, USA) or a BioRad 1024ES (BioRad, Hercules, CA) confocal imaging system was used to study subcellular localization of GFP fusion proteins in tobacco epidermal cells. The Leica TCS SP2 system was attached to a Leica DMRE microscope. The BioRad 1024ES system was attached to a Zeiss Axioskop microscope (Carl Zeiss, Thornwood, NY). Both microscopes were equipped with epifluorescence and water immersion objectives. The 488 nm excitation wavelength produced by Krypton/Argon lasers was used to examine GFP expression. Fifteen to thirty optical sections were taken of each cell at 0.3 to 2 μm intervals. All images were processed using Adobe Photoshop version 4.0 software (Adobe Systems Inc., San Jose, CA).

Statistical analyses

All data analysis was conducted using procedures from SAS (Cary, NC), and a significance level of 0.05 was used for all mean comparisons. Statistical analysis in Table 1, comparing the effects of plasmid and leaves, were assessed by chi-square tests using PROC FREQ. Each factor's simple effects were analyzed by fixing the other factors.

Sequence alignments and prediction of transmembrane domains.

The TGBp2 sequences of nine potexviruses were obtained by searching the National Center for Biotechnology Information (NCBI) database using Entrez-Protein. The TGBp2 amino acid sequences of *Potato virus M* (PVM) (gi/9626092/ref/NP_056769.1), *Narcissus mosaic virus* (NMV) (gi/9626478/ref/NP_040780.1), *Bamboo mosaic virus* (BaMV) (gi/2407621/gb/AAB70564.1), *Papaya mosaic virus* (PMV) (gi/9629170/ref/NP_044332.1), *Cymbidium mosaic virus* (CyMV) (gi/2460067/gb/AAB71855.1) *Garlic virus C* (GVC) (gi/2826159/dbj/BAA61820.1), *Cactus virus X* (CVX) (gi/14602402/ref/NP_148782.1) and *White clover mosaic virus M* (WClMVM) (gi/141129/sp/P09500/VMEM) and PVX (gi|222445|dbj|BAA00251.1) were aligned using ClustalW (SDSC Biology Workbench, San Diego, CA). The default matrix settings (gonnet) and gap penalty (10) were maintained for this alignment. The multiple sequence alignment was imported into the TMAP version 3.2 (SDSC Biology Workbench). TMAP utilizes an algorithm to identify transmembrane segments of aligned sequences (Persson and Argos, 1994).

Table 1

Intercellular movement of GFP, GFP:TGB2, GFP: TGB2m1, GFP: TGB2m2, and GFP: TGB2m3 in tobacco.

Proportion of sites containing GFP activity in multiple cells[a] .

	pRTL2-GFP	pRTL2-GFP:TGBp2	pRTL2-GFP: TGBp2m1	pRTL2-GFP: TGBp2m2	pRTL2-GFP: TGBp2m3
N. benthamiana					
<u>Source</u>					
	3.2%(2/62)a	**31.5%(29/92)b**	**8.5%(5/59)a**	**23.5%(20/85)b**	**7.0%(5/71)a**
N. tabacum					
<u>Source</u>					
Nontransgenic	**3.8%(15/396)a**	2.3%(5/218)**a**	0%(0/100)**a**	**4.5%(9/200)a**	**4%(5/126)a**
TGB100	**6.9 (27/389)a**	**25.9 (33/206)b**	**5.0 (6/119)a**	**6.0 (7/115)a**	**6.0 (4/67)a**
<u>Sink</u>					
Nontransgenic	**5.2 (10/191)a**	**5.5 (36/660)a**	**5.6 (22/394)a**	**4.0 (11/274)a**	**0 (0/75)a**
TGB100	2.4 (20/826)a	2.7 (2/75)a	5.2 (4/77)a	5.4 (35/652)a	3.0(5/166) a

[a] Percentages of fluorescent cell clusters observed 24 hpb in source and sink leaves is indicated. The total numbers of cell clusters relative to the total number of sites containing GFP are in parentheses. Two to eight source or sink leaves of each *N. benthamiana*, *N. tabacum* nontransgenic, or *N. tabacum* TGB100 tobacco line were bombarded with each plasmid to obtain the numbers indicated. Multiple comparisons were performed for each plasmid in *N. benthamiana*, *N. tabacum* nontransgenic source, *N. tabacum* nontransgenic sink, TGB100 source, or TGB100 sink leaves. Values followed by the same letter within each row are not significantly different using PROC FREQ of SAS at P>0.05.

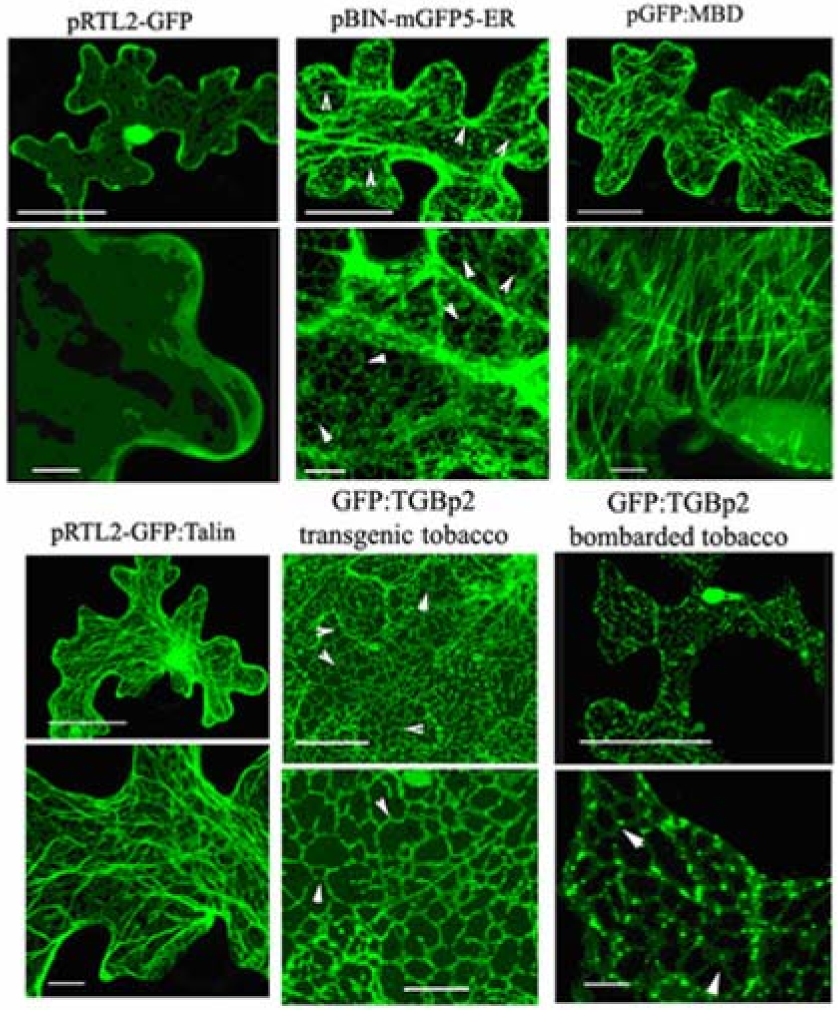

Fig. 1. Images of tobacco epidermal cells expressing GFP, mGFP5-ER, GFP:MBD, GFP:Talin, and GFP:TGBp2. Plasmids are indicated above each pair of images. Images are paired in columns of low and high power images. Bars in the upper panels represent 40 μm and in the lower panels represent 8 μm. Free GFP displays diffuse cytoplasmic fluorescence. GFP:Talin and GFP:MBD display the filamentous labeling pattern typical of the cytoskeletal network. Images showing fluorescence in mGFP5-ER and GFP:TGBp2-expressing cells have similar polygonal networks (white arrowheads). Images of GFP:TGBp2 were taken from plants transgenically expressing the fusion protein and from tobacco leaves bombarded with pRTL2-GFP:TGBp2 plasmids.

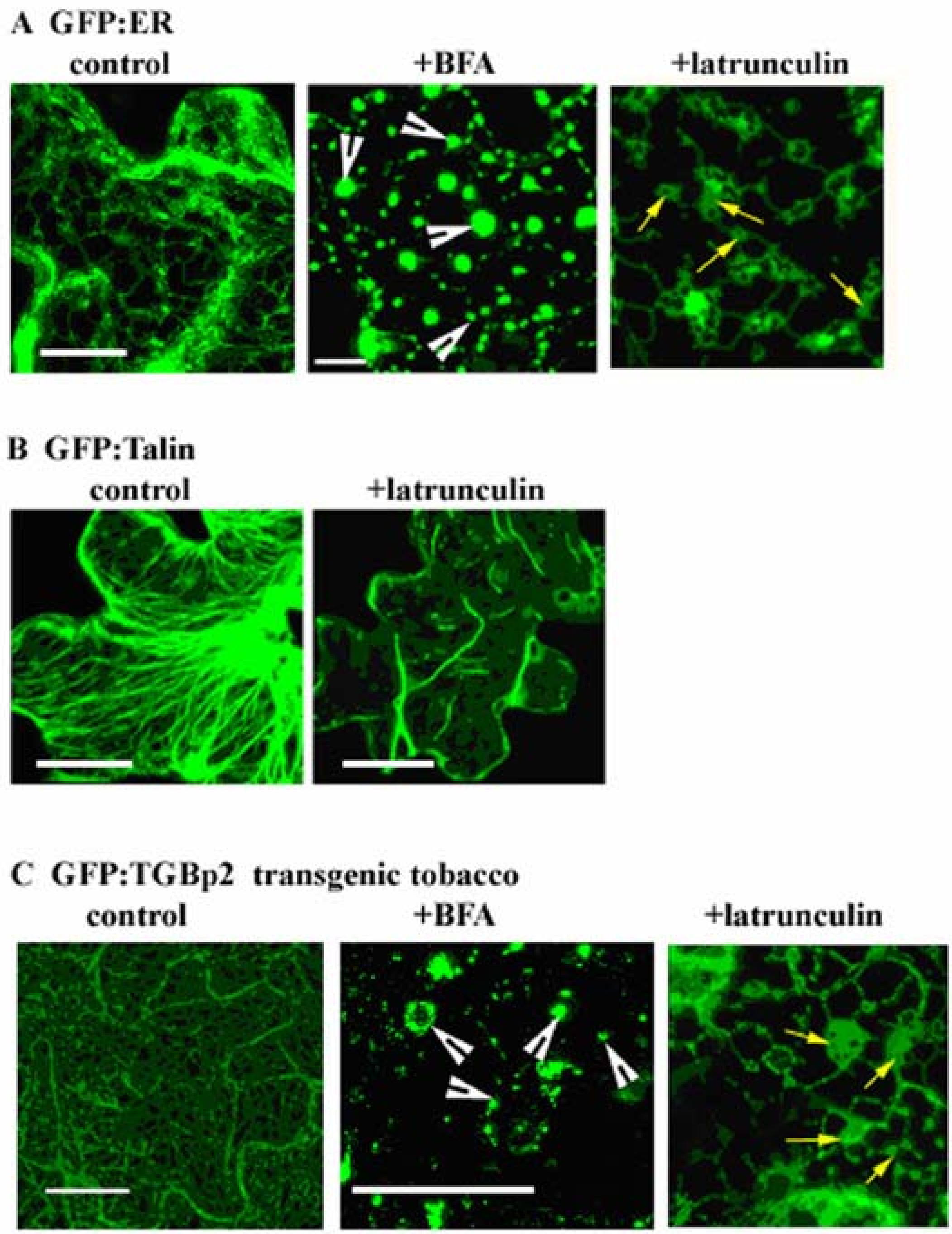

Fig. 2. Transgenic or bombarded *N. tabacum* leaves expressing various GFP fusion proteins that were treated with chemical inhibitors. Bars represent 40 μm. (A) Transgenic *N. tabacum* leaves expressing mGFP5-ER were treated with BFA or latrunculin B. Control image (untreated cell) show the polygonal ER network. In cells treated with BFA, fluorescent aggregates (white arrowheads) that are variable in size become dispersed throughout the cell. Cisternal ER (yellow arrows) and blind-ending tubules are in latrunculin B treated cells. (B) In leaves bombarded with pGFP:Talin, cells expressing GFP:Talin show abundant parallel actin filaments. Images show less

filaments in cells treated with latrunculin B than in untreated cells. (C) Transgenic leaves expressing GFP:TGBp2 were treated with BFA, or latrunculin B. Fluorescent aggregates appeared BFA-treated cells (white arrowheads). Cisternal ER (yellow arrows) and blind ending tubules are in latrunculin B treated cells.

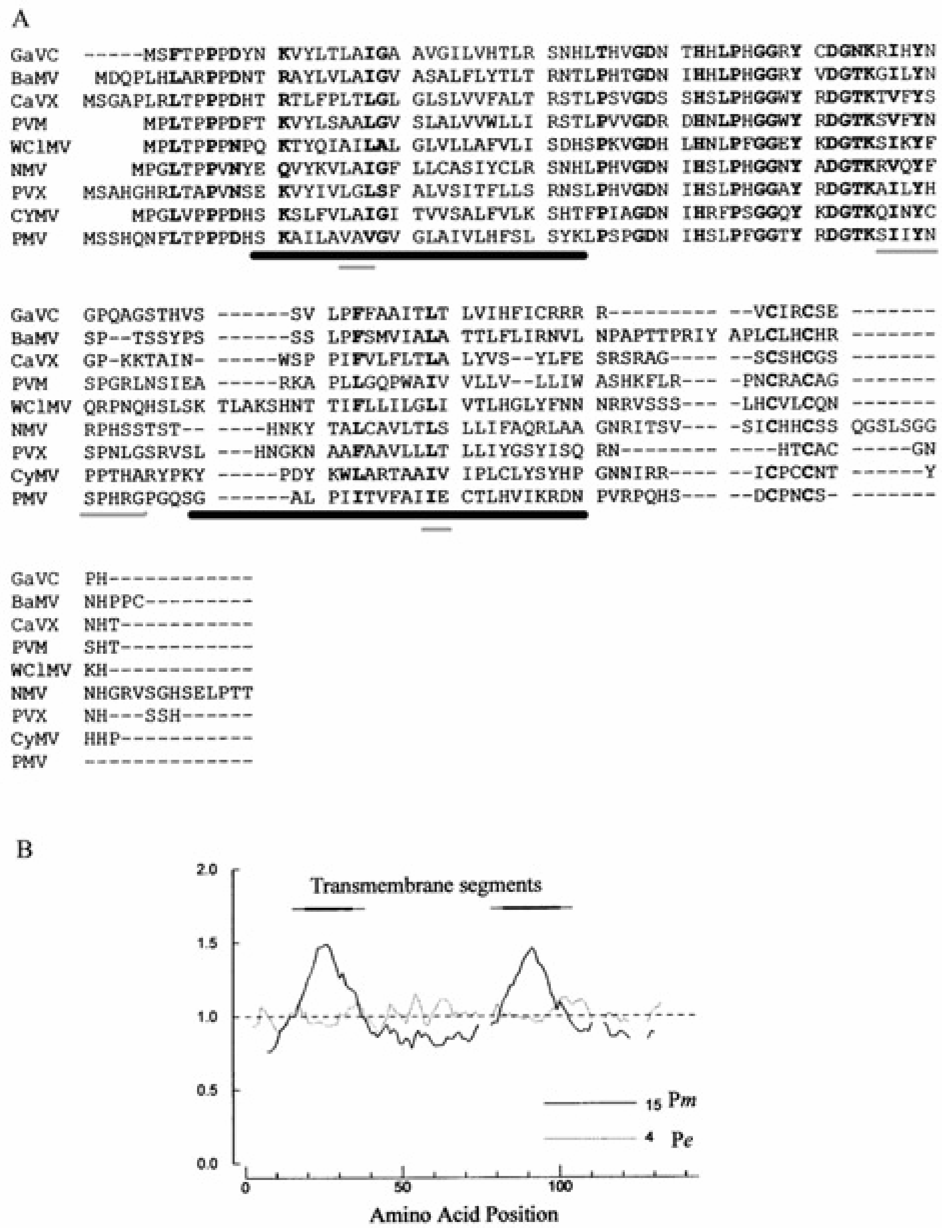

Fig. 3. Amino acid sequence analysis of potexvirus TGBp2 proteins.
Amino acid sequence alignment was conducted using CLUSTALW and shows domains conserved among potexvirus TGBp2 proteins. Thick black bars indicate putative transmembrane domains. Grey bars indicate sites where mutations were inserted. (B) The aligned sequences were imported into TMAP program and this graphic depiction of putative transmembrane domains was obtained. The bars at the top indicate the two putative transmembrane segments. Two transmembrane domains were identified which span amino acid position 15 to 38 and 75 to 101. The X-axis indicates the position of each residue in the TGBp2 sequence. The Y-axis is the propensity value associated with each position. The black line corresponds to *P*m values and values above 1.0 indicate a propensity for membrane association. TMAP uses two propensity values to predict the middle portions of the transmembrane segments (P_m) and the terminal regions of the

transmembrane segments (P_e) that are based on the average scores calculated for each position in an alignment. Values above 1.0 indicate a preference to be lipid associated**.** Eight or more consecutive P_m values greater than 1.18 and peak values greater than 1.23 determine membrane spanning segments. P_e values above 1.08 but less than 1.17 determine termini of the membrane spanning regions and the peak P_e values were required to be 20 to 33 positions apart. Where the gray line for *P*e values is above 1.0 and overlaps the black line for *P*m values identifies likely ends of the transmembrane segments.

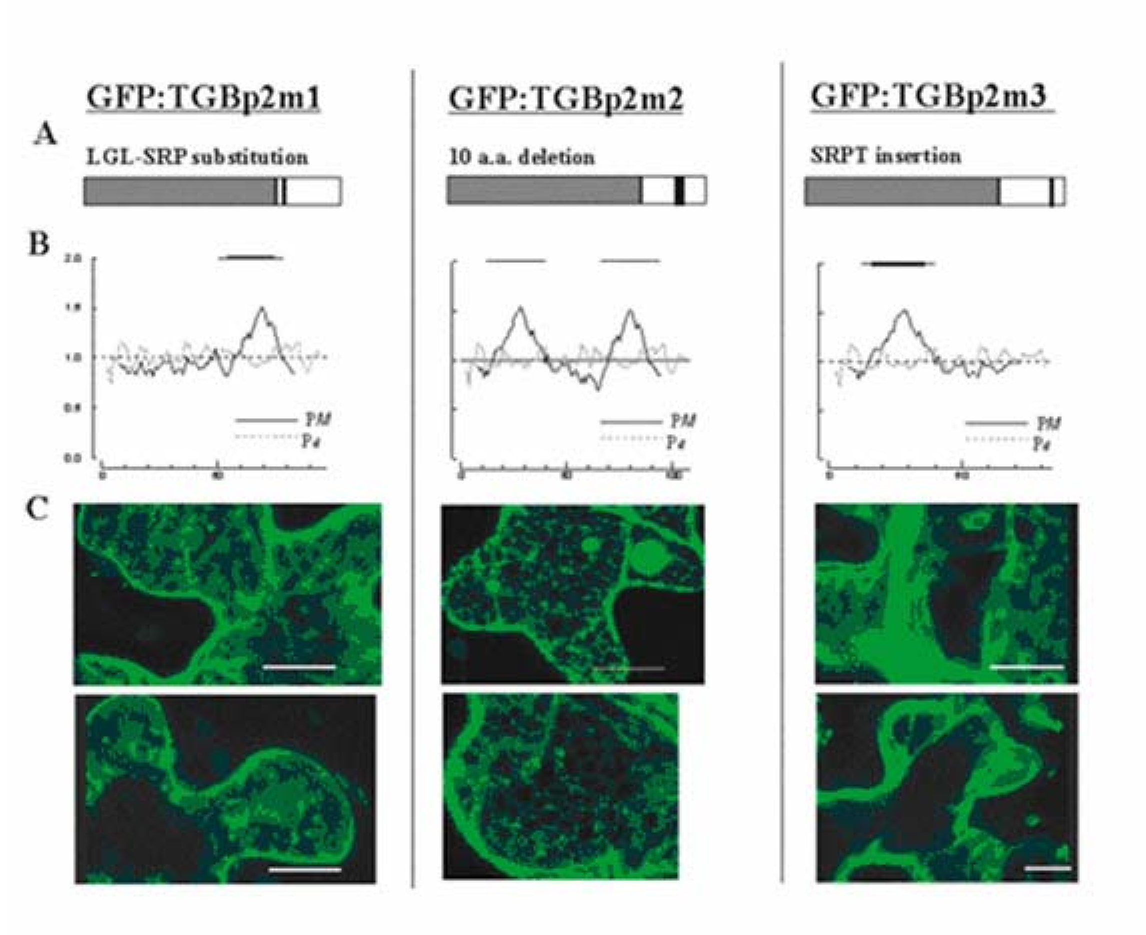

Fig. 4. Mutant pRTL2-GFP:TGBp2 plasmids bombarded to tobacco leaves.
Diagrammatic representation of the GFP coding sequence (grey box) fused to mutant PVX TGBp2 (open box) sequences. Thick black lines in the TGBp2 ORF indicate the mutations m1, m2, and m3. Changes in the TGBp2 amino acid sequence due to each mutation are indicated. (B) TGBp2 mutant sequences were imported into TMAP to determine whether the mutations should affect the predicted transmembrane domains. The graph on the left is for TGBp2m1, the middle is TGBp2m2 and the right is TGBp2m3. Bars at the top of the graphs indicate each transmembrane domain. The m1 mutation eliminates the first transmembrane domain, the m2 mutation has no effect on the transmembrane domains, and the m3 mutation eliminates the C-terminal transmembrane domain. (C) Images showing fluorescence due to GFP:TGBp2m1, GFP:TGBp2m2, or GFP:TGBp2m3 in *N. tabacum* (top panel) and *N. benthamiana* (bottom panel) leaves. GFP:TGBp2m1 and GFP:TGBp2m3 were dispersed throughout the cells in *N. tabacum* and *N. benthamiana* leaves. GFP:TGBp2m2 was in a reticulated network in *N. tabacum* and *N. benthamiana* leaves. Bars represent 40µm.

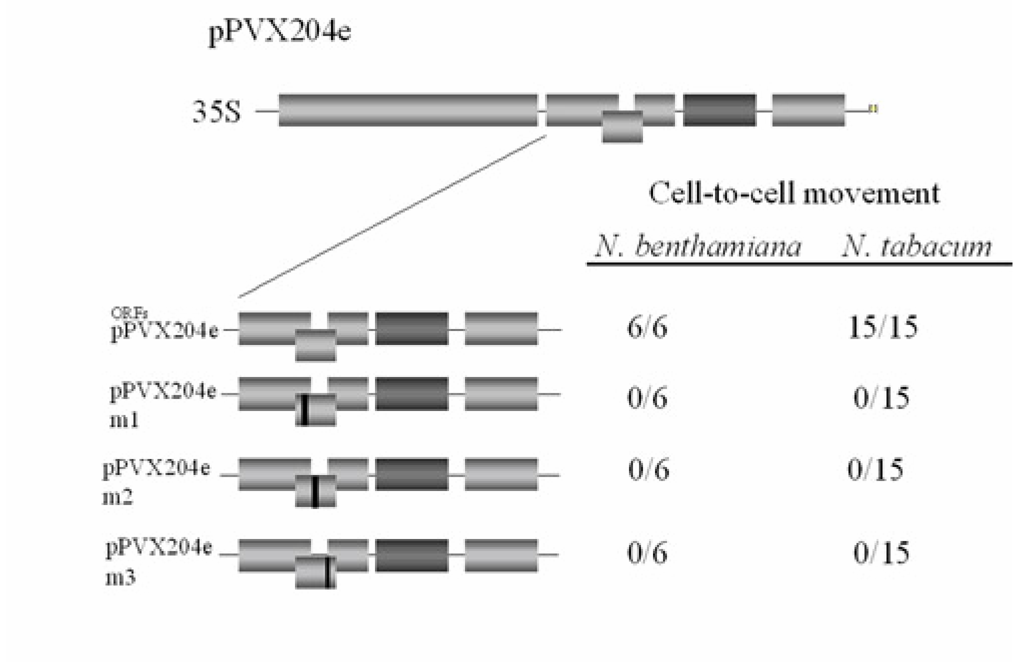

Fig. 5. The abilities of PVX204e, PVX204p2m1, PVX204p2m2, and PVX204p2m3 mutations to move cell-to-cell and systemically were compared. Diagrammatic representations of wild type and mutant PVX204e viruses are indicated on the left. Viruses were inoculated to *N. tabacum* and *N. benthamiana* plants. Total numbers of plants in which virus cell-to-cell movement relative to the total number of plants inoculated is presented. PVX204e moved cell to cell and systemically. None of the mutant viruses moved between adjacent cells or systemically in either *Nicotiana* species.

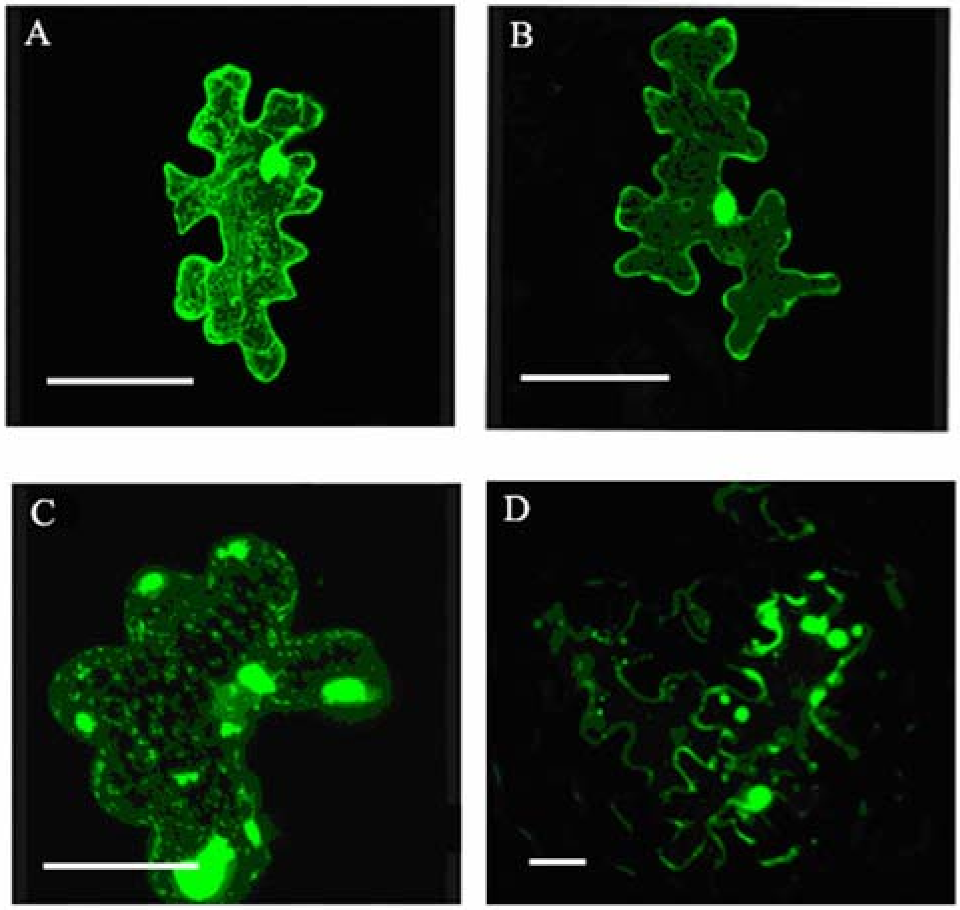

Fig. 6. Representative examples of GFP:TGBp2 accumulation in nontransgenic and TGB100 *N. tabacum* leaves following biolistic bombardment of pRTL2-GFP:TGBp2 plasmids. Bars represent 100 μm. (A) Single epidermal cell of a nontransgenic *N. tabacum* leaf expressing GFP. (B) A single epidermal cell of TGB100 leaf expressing GFP. (C) Single epidermal cell of nontransgenic *N. tabacum* leaf expressing GFP:TGBp2. (D) Multiple adjacent epidermal cells of TGB100 leaf expressing GFP:TGBp2.

CHAPTER IV

Potato virus X TGBp2 Causes Reorganization of the ER Network

ABSTRACT

The *Potato virus X* (PVX) TGBp2 and TGBp3 were reported to associate with the endoplasmic reticulum (ER). Upon further investigation TGBp2 was also found to be associated with vesicles that are ER derived. These vesicles were associated with actin filaments. In tobacco leaves expressing GFP:TGBp2 that were treated with brefeldin A (BFA) or latrunculin B, fluorescent vesicles were seen in discrete clusters within the cell. In control experiments tobacco leaves expressing GFP:TGBp3 or mGFP5-ER were treated with brefeldin A (BFA) and latrunculin B. Since both of these proteins accumulate mainly in the ER, the effects of BFA and latrunculin B on these samples were different. The reticulated network expressing GFP:TGBp3 and mGFP5-ER appeared to be dissolved in BFA treated cells, but not in latrunculin B treated cells. The cyan fluorecent protein (CFP) was fused to the 5'end of the TGBp2 ORF. When CFP:TGBp2 was coexpressed using biolistic bombardment with either GFP:TGBp3 or mGFP5-ER, the ER targeting was completely disrupted and fluorescence was detected in vesicles. Therefore the TGBp2 may be responsible for the vesiculation of the ER and driving TGBp3 into vesicles.

INTRODUCTION

Plant viruses encode movement proteins (MPs) that promote virus cell-to-cell and vascular transport in the plant hosts. In several studies, viral genes encoding MPs have been interchanged between viral genomes to yield chimeric viruses that are infectious (Solovyev, et al., 1999; Giesman-Cookmeyer, et al., 1995; Agranovsky, et al., 1998; Solovyev, et al., 1999; Solovyev, et al., 1996). Other tests conducted using co-infecting plant viruses have shown that the MP of one virus alleviates cell type or host restrictions for another virus (Mise et al., 1993; Morozov et al., 1997; Palukaitis 2003; Syller et al., 2002; Ryabov et al., 1999). Because of the interchangeability of the viral MPs, researchers have proposed general models to describe the transport mechanisms for a wide range of plant viruses.

In one of the first general models that were proposed to explain virus cell-to-cell movement, viral MPs bind to the viral genomic nucleic acid and carry it across PD (PD) into adjacent cells (Kalinina et al., 2001; Giesman-Cookmeyer et al., 1993; Noueiry et al., 1994; Alzhanova et al., 2001). This model was based on evidence from microinjection and biolistic bombardment studies indicating that plant viral MPs often increase plasmodesmal permeability to promote virus cell-to-cell movement. The MPs of *Tobacco mosaic virus* (TMV), *Red clover necrotic mosaic virus* (RCNMV), *Bean dwarf mosaic virus* (BDMV), *Tobacco rattle virus* (TRV), and *Cucumber mosaic virus* (CMV), and *White clover mosaic virus* (WClMV) were shown in microinjection studies to increase plasmodesmal permeability in tobacco leaves (Wolf et al., 1991; Derrick et al., 1992; Fujiwara et al., 1993; Noueiry et al., 1994). In other experiments plasmids expressing GFP fused to the MP genes of TMV, CMV, or PVX were biolistically delivered to single leaf epidermal cells and protein movement was observed directly (Itaya et al., 1998; Crawford et al., 2001).

There are two models proposed for viruses whose virions move from cell to cell. In the first model, the MPs belonging to como-, nepo-, badna-, and tospoviruses form hollow tubules that extend between cells and serve as conduits for transport of virions (Storms et al., 2002; Cheng et al., 1998) (Chapter I, Fig. 3B). The second model was proposed for closteroviruses, whose MP is an Hsp70 homolog (called Hsp70h) (Alzhanova et al., 2001). In this model the major CP forms the virion while the minor capsid protein and Hsp70h form a tail assembly that propels the virion particle into the plasmodesmata (PD). The Hsp70h has ATPase, activity which is necessary for tail assembly and cell-to-cell movement. Hsp70h associates with the PD and provides the driving force for translocation of the virion through the pore. PD association of Hsp70h triggers tail disassembly which subsequently destabilizes the virion, exposing viral RNA for translation as it moves into the adjacent cell (Alzhanova et al., 2001).

Most recently it was shown that TMV VRCs (viral replication complexes) move from cell to cell via PD (Kawakami et al., 2004). Early in TMV infection, the viral MP, replicase and RNA are detected in membrane associated VRCs. These membranous vesicles are transported by the viral MP across the PD. Once the VRC has moved through the PD, replicating viral RNA is released into the adjacent cell (Kawakami et al., 2004).

PVX is a positive strand RNA virus and is the type species of the *Potexvirus* genus (Huisman et al., 1988). The PVX genome contains five overlapping ORFs encoding the viral replicase, the TGB, and the CP. The TGB encodes three MPs designated TGBp1, TGBp2, and TGBp3 (Beck et al., 1991; Verchot et al., 1998). The viral CP is required for genome encapsidation and virus cell-to-cell movement (Fedorkin et al., 2001; Forster et al., 1992).

The TGB is highly conserved among members of the potex-, hordei-, beny-, pomo-, and pecluvirus genera. TGBp1 is a multifunctional protein that increases plasmodesmal permeability for virus cell-to-cell movement, has RNA helicase activity, and promotes translation of virion RNAs. Several studies have shown that the TGBp2 and TGBp3 associate with the ER (Krishnamurthy et al., 2003; Mitra et al., 2003 Zamyatnin et al., 2002, 2004; Heinlein et al., 2004). Mutations disrupting the ER association of either TGBp2 or TGBp3 disrupt virus movement, suggesting that ER association of these two proteins is important (Krishnamurthy et al., 2003; Mitra et al., 2003). The hordeivirus TGBp2 and TGBp3 proteins co-localize to 'peripheral bodies' that accumulate near the PD. Some have suggested these 'peripheral bodies' are membrane vesicles (Morozov et al., 2003; Solovyev et al., 2000; Zamyatnin et al., 2004; Heinlein et al., 2004).

Here, we examine the subcellular distribution of GFP or cyan fluorescent protein (CFP) tagged TGBp2 and TGBp3 proteins in tobacco leaves. When the fused proteins were co-expressed from a 35S promoter, GFP:TGBp2 or CFP:TGBp2 associated with membranous vesicles while GFP:TGBp3 associated with the ER. The TGBp2 induced vesicles were ER-derived and associated with actin filaments. When CFP:TGBp2 was co-expressed with either GFP:TGBp3 or mGFP5-ER in plant cells, both fusion proteins localized to vesicles. These data suggest that TGBp2 directs TGBp3 to the ER-derived vesicles and also causes the vesiculation of the ER

RESULTS

GFP:TGBp2 and GFP:TGBp3 accumulate in ER and in ER-derived vesicles.

Plasmids containing GFP fused to TGBp2 or TGBp3 (Fig.1) were biolistically bombarded to tobacco leaves and the pattern of protein subcellular accumulation was studied using confocal microscopy (Fig. 2). As in previous studies, (Mitra et al., 2003; Krishnamurthy et al., 2003) the GFP:TGBp2, GFP:TGBp3 proteins accumulated in a network that resembled the polygonal ER network (Fig. 2 B, and C). For comparison, plasmids expressing a modified GFP with ER targeting and retention signals (mGFP5-ER), causing GFP to accumulate in the ER lumen, were bombarded to tobacco leaves (Haseloff et al., 1997; Mitra et al., 2003; Krishnamurthy et al., 2003). The pattern of fluorescence due to mGFP5-ER was a typical polygonal ER network (Fig. 2A). Additional controls included plasmids expressing GFP:MBD, which contains the microtubule binding domain of MAP4 (Marc et al., 1998), and GFP:Talin, which contains the actin binding domain of mouse talin gene fused to GFP (Kost et al., 1999) (Fig. 2 H, and L). Cells expressing GFP:MBD show thin microtubule filaments extending from various orientations across the cell (Fig.2 H). Cells expressing GFP:Talin show actin filaments that look like parallel fibers extending across the cell (Fig. 2L)

The network pattern of GFP:TGBp2 and GFP:TGBp3 resembled the pattern of mGFP5-ER (Fig. 2A). In addition, cells expressing GFP:TGBp2 had abundant spherical fluorescent bodies imposed on the network (Fig. 2C). In some transient expression assays, the fluorescent bodies were more obvious than the ER network. Plasmids were also prepared containing CFP fused to TGBp2 and, following biolistic bombardment, fluorescent bodies expressing the CFP-tagged proteins were evident (Fig. 2D).

Segments of leaves expressing mGFP5-ER, GFP:TGBp2, or GFP:TGBp3 were treated with brefeldin A (BFA) or latrunculin B to disrupt the ER or microfilament networks. In a previous study we demonstrated that samples treated with 200 μg/ml BFA for a period of 3-4 h was sufficient to disrupt the ER network (Mitra et al., 2003, Krishnamurthy et al., 2003). In mGFP5-ER, GFP:TGBp2, or GFP:TGBp3 expressing cells treated with BFA, the ER network is reorganized into large and small patches of fluorescence scattered throughout the cell (Fig. 2E, F, and G). These data support the hypothesis that GFP:TGBp2 and GFP:TGBp3 associate with ER membranes.

Actin has been implicated in contributing to the shape and movement of the ER in plants (Knebel, et al., 1990). Latrunculin B causes actin depolymerization (Nebenfuhr, et al., 1999) and has minor effects on the shape of the ER. Samples were treated for 1-2 h with latrunculin B. The ER network shows blind-ending tubules and cisternae in mGFP5-ER and GFP:TGBp3 expressing cells (Fig. 2I and J). In GFP:TGBp2 cells treated with latrunculin B, there are numerous clusters of fluorescent bodies. While latrunculin B had minor effects on the ER network, the GFP:TGBp2 containing fluorescent bodies reorganized into clusters within the cell (Fig. 2K).

If GFP:TGBp2 fluorescent bodies were anchored along actin filaments, then treatment with latrunculin B would disrupt the distribution of these bodies within the cell. Leaves were co-bombarded with plasmids expressing GFP:TGBp2 and DsRed:Talin, the latter of which contains DsRed fused to the actin-binding domain of the mouse talin gene (Kost et al., 1999). GFP:TGBp2 was detected in numerous vesicles along the actin filaments (Fig.

2M and N). Leaves were also co-bombarded with plasmids expressing GFP:TGBp2 and GFP:Talin and GFP fluorescence was associated with fluorescent vesicles and actin filaments (Fig. 2 O and P).

Since GFP:TGBp2 accumulates in the ER and fluorescent bodies, experiments were conducted to determine if the fluorescent bodies were ER-derived vesicles. Plasmids expressing CFP:TGBp2 and mGFP5-ER were cobombarded to tobacco leaves and the subcellular distribution of the fluorescent proteins was analyzed. mGFP5-ER and CFP:TGBp2 accumulated predominantly in vesicles throughout the cell. The ER network was not visible (Fig. 2 T, U, and V). It is possible that CFP:TGBp2 induced reorganization of the ER causing both fluorescent proteins to co-localize in membrane vesicles. Leaves were co-bombarded with plasmids expressing CFP:TGBp2 and GFP:TGBp3. Both proteins colocalized to fluorescent bodies. The ER network in cells expressing both CFP:TGBp2 and GFP:TGBp3 was faint (Fig. 2 Q, R, and S).

Electron microscopic analysis of the subcellular accumulation of GFP:TGBp2 and GFP:TGBp3

Since antibodies to PVX TGBp2 and TGBp3 are unavailable, immunogold labeling and electron microscopic analysis were conducted using anti-GFP serum and transgenic tobacco expressing GFP:TGBp2, GFP:TGBp3, or mGFP5-ER. Nontransgenic samples were included in the study as controls. The distribution of gold particles in the cell wall, plasma membrane, ER, vesicles, and Golgi apparatus was assessed based on the calculated average number of gold particles found in 1 μm^2 fields (Tables 1 and 2).
Membrane vesicles were abundant in GFP:TGBp2 expressing tissues (Figs. 3C, D, E, G, and H). Vesicles were located primarily in the cortical region of the cell and ranged from

150 nm to 300 nm in diameter. These vesicles were not detected in mGFP5-ER, GFP:TGBp3, or nontransgenic samples (Figs. 4 and 5). When immunogold labeling using anti-GFP serum (Clontech monoclonal A.V. antiserum) was conducted and gold particles were detected in vesicles in GFP:TGBp2 expressing cells (Fig. 3G and H; Table 2). In mGFP5-ER and GFP:TGBp3 expressing cells, gold particles were detected along ER strands (Fig.. 4B; Fig.. 5C; Table 1). Nontransgenic samples were also treated with anti-GFP serum and minimal labeling was detected (Fig. 5F; Tables 1 and 2). All samples were treated with buffer and secondary antiserum and minimal labeling was detected (Fig. 3B, Fig. 4E, and Fig. 5B; Table 1). We conducted statistical analyses to compare the concentration of the gold particles in the cell wall (CW), plasma membrane (PM), ER, and vesicles for each transgenic and the non transgenic samples. The average number of gold particles in mGFP5-ER, GFP:TGBp3, and GFP:TGBp2 samples were greater in the ER than in the CW or PM (Table 1). These data indicate that the GFP:TGBp2 and GFP:TGBp3 proteins, similar to the mGFP5-ER protein, associate primarily with ER membranes. Statistical analysis failed to reveal any significant differences in all the three fields when probed with no primary antiserum (Table 1).

Dual labeling experiments were conducted using anti-GFP and anti-BiP sera. BiP is an ER resident chaperone protein is present only in the lumen of the ER and is not in other areas of the endomembrane system (Fontes, et al., 1991). In GFP:TGBp2 transgenic cells, anti-GFP and anti-BiP sera labeled vesicles and ER strands (Fig. 3C, D, and E; Tables 1 and 2). In GFP:TGBp3 and mGFP5-ER, anti-GFP and anti-BiP sera primarily labeled ER strands (Fig. 4C and D; Fig. 5A and D) and the same was revealed through statistical analysis. However in case of GFP:TGBp2 transgene, the gold labeled the ER, vesicles, as well as the PM.

As controls, nontransgenic and mGFP5-ER transgenic samples were treated with anti-BiP serum alone. Statistical analysis revealed that the gold particles were detected primarily in the ER (Fig. 5E and G). However in case of GFP:TGBp2 transgene, the gold labeled the ER as well as the PM and the two fields were significantly similar. In addition, GFP:TGBp2 and GFP:TGBp3 samples were treated with anti-GFP and anti-TMV sera. Gold label due to anti-GFP serum was detected while no gold label was present due to anti-TMV serum (Table 1).

Tables 1 and 2 show the distribution of gold particles in the cell wall, plasma membrane, ER, vesicles, and Golgi apparatus. GFP:TGBp2 and GFP:TGBp3 were detected primarily in the ER. Some gold label was detected in the plasma membrane and cell wall. In the mGFP5-ER samples, gold particles were detected primarily in the ER (Table 1). In co-labeling studies using GFP and BiP antisera, both antisera primarily labeled ER membranes. BiP was not detected in the cell wall or plasma membrane (Table 1). In nontransgenic cells, BiP label was detected primarily in the ER, while there was minimal labeling due to GFP (Table 1). Neither GFP or BiP antiserum labeled Golgi stacks, although both labeled GFP:TGBp2 vesicles. This was statistically significant also (Table2)

These data suggest the GFP:TGBp2 vesicles are ER derived and not Golgi related. GFP:TGBp3 accumulates primarily in ER strands. Evidence in confocal microscopy studies showing colocalization of TGBp2 and TGBp3 to vesicles is likely due to vesiculation of the ER by TGBp2. If TGBp3 is already associated with the ER then it might get packaged into vesicles along with TGBp2.

The same results were obtained when the transgene expressing leaf tissues were probed with both the antiserum simultaneously. There was no labeling of the CW, PM, or ER when the tissues were probed with no primary antiserum or with TMV antiserum.

DISCUSSION

In this study we used confocal microscopy, GFP fusions, chemical inhibitors, and immunogold labeling to understand the mechanism of PVX TGBp2 and TGBp3 interaction with the cellular membranes for viral cell-to-cell movement. Our results indicate that the PVX TGBp3 is associated with the ER network and TGBp2 is associated with the ER as well as vesicles. In the previous chapters (chapter II, III) and also published work from our lab showed that membrane association is important for both protein and viral cell-to-cell movement (Krishnamurthy *et al*, 2003; Mitra *et al*, 2003).

In the present and previous chapter (chapter III) we tested the effects of BFA and latrunculin B on leaves expressing GFP:TGBp3, GFP:TGBp2, and mGFP5-ER . As expected we found the disruption of the ER in GFP:TGBp3 and mGFP5-ER expressing leaves but fluorescence was in scattered aggregates of fluorescent bodies distributed throughout the cell in case of GFP:TGBp2 expressing leaves. We used latrunculin B, which is a chemical that causes depolymerization of the actin filament (Nebenfuhr et al., 1999). Actin contributes to the shape and movement of the ER in plants (Knebel et al., 1990). The GFP:TGBp2 bombarded leaves were treated with latrunculin B and fluorescence was scattered in aggregate of fluorescent bodies. . The TGBp2 fluorescent bodies also seemed to decorate the actin filament, when co-expressed with DsRed:Talin.

Therefore the fluorescent bodies produced by PVX TGBp2 were found along the actin filament.

In order to determine if the fluorescent bodies are ER derived vesicles, we used cryo-electron microscopy to study the nature of these vesicles. We made tobacco plants expressing the GFP:TGBp2, GFP:TGBp3 and mGFP5-ER transgenes and probed them with GFP and BiP antiserum. We found large vesicles associated with TGBp2, which often were labeled with both antisera. These vesicles were mostly found along the cell wall, close to the cortical ER. The Golgi stacks were well preserved and were not labeled with either antiserum. Therefore the fluorescent bodies under the confocal microscope were indeed ER-derived vesicles.

Previous studies with *Poa Semilatent Virus* (PSLV, genus *Hordeivirus*) showed punctate bodies produced during transient expression of PLSV TGBp3 along the plasma membrane (Zamyatnin *et al*, 2002; Gorshkova et al., 2003). The hordeivirus movement proteins are also organized as the triple gene block, which is a conserved module in *Hordei, Carla, Beny, Furo* and *Potex* viruses.

The hordeivirus TGBp3 has two transmembrane domains while the PVX TGBp3 has a single transmembrane domain (Morozov et al., 2003) It has been shown in previous studies that PSLV TGBp2 associates with the ER while PSLV TGBp3 associates with membrane bodies located at the cell periphery. In cells expressing both the hordeivirus TGBp2 and the TGBp3, fluorescence was associated only with peripheral bodies and it was suggested that TGBp3 drives the TGBp2 from the ER to the peripheral bodies (Soloyev et al., 2000; Zamyatnin et al., 2002). However the questions whether these cortical bodies are vesicles, or caused due to protein over expression remained unanswered. Our studies showed that the PVX:TGBp2 is associated with the ER and ER derived vesicles and the TGBp3 is targeted mostly to the ER. On co-expression using CFP:TGBp2 and GFP:TGBp3, we found fluorescence in vesicles only. Thus in case of PVX, the TGBp2 protein redirects the TGBp3 protein from the ER into vesicles. PVX TGBp2 also causes vesiculation and the change in the targeting pattern of mGFP5-ER when co-expressed transiently by biolistic bombardment. Thus it can be suggested that PVX TGBp2 causes vesiculation of the ER.

A model of *Potex* cell-to-cell movement was suggested by studies based on *White Clover Mosaic Virus* (WClMV) (Lough et al., 1998, 2000). They suggested that the TGBp2 and TGBp3 serve as ER anchors for the viral ribonucleoprotein complex as it moves through the PD using the ER tract. Studies in our laboratory, were focused on testing the Lough model in the PVX context. The Lough model has no evidence of vesicle association of the TGBp2. Besides it is also possible that there is a role of TGBp2 and TGBp3 during virus infection that goes beyond membrane binding.

MATERIALS AND METHODS

Plant Material

N. benthamiana and *N. tabacum* plants were used for studying subcellular accumulation of GFP:TGBp2 and GFP:TGBp3. Transgenic *N. tabacum* plants expressing mGFP5-ER, GFP:TGBp2 or GFP:TGBp3 were prepared previously using *Agrobacterium* transformation, as previously described (Chapter II) (Mitra et al., 2003: Krishnamurthy et al.,2003).

Bacterial Strains and Plasmids

All plasmids were constructed using *Escherichia coli* strain JM109 (Sambrook, 1989). The plasmids pRTL2-GFP:TGBp2 and –GFP:TGBp3 were prepared previously (Fig. 1A) (Mitra et al., 2003; Krishnamurthy et al., 2003). The plasmid pRTL2-GFP was obtained from Dr. B. Ding (Ohio State University, OH) and contains the EGFP gene (Living Colors™, Clontech, Palo Alto, CA), pBIN-mGFP5-ER plasmid was obtained from Dr. J. Hasselof (MRC Laboratory of Molecular Biology, Cambridge, UK)(Siemering et al., 1996), pGFP-MBD was a generous gift from Dr. R. Cyr (Penn. State University, PA)(Marc et al., 1998), pRTL2-GFP**:**Talin and –DsRed:Talin, which contain either EGFP or DsRed (Living Colors™, Clontech, Palo Alto, CA) fused with the coding sequence of the F-actin binding domain of mouse *Talin* (Kost, et al., 1998; McCann, et al., 1997)(Fig. 1A). All plasmids, except DsRed:Talin, were described in the materials and methods section of Chapter II and III.

A two-step PCR procedure was used to prepare pRTL2-CFP:TGBp2 (Fig. 1A) (Yang et al., 2000). The plasmid pUC18-ECFP was obtained from Elison Blancaflor (Noble Foundation, OK) and contains the Living Colors™ ECFP gene (Clontech, Palo Alto, CA). CFP was amplified using a forward primer (CCG GCC G<u>CC ATG G</u>TG AGC AAG GGC GAG GAG CTG TTC) containing an *NcoI* restriction site (underlined) and a reverse primer containing sequences overlapping the 5' end of the PVX TGBp2 ORF (CAT ACC CGG GGG CTT GTA CAG CTC GTC CAT GCC GAG). Similarly, the sequence encoding the PVX TGBp2 gene was amplified using a forward primer overlapping the 3' end of CFP (GTA CAA GCC CCC GGG TAT GTC CGC GCA GGG CCA TAG GCT GAC) and a reverse primer containing an additional *BamH*I site (GCG

GGA TCC CGC TAA TGA CTG CTA TGA TTG TT). These two PCR products were annealed and the CFP forward primer and PVX TGBp2 reverse primer were used to PCR amplify the fused genes. The final PCR product was gel purified and ligated to pGEM-T (Promega, Madison, WI). Presence of the CFP:TGBp2 fusion in the plasmid pGEMT-CFP:TGBp2 was confirmed by sequencing using the Applied Biosystems ABI Prism Big Dye Terminator Cycle Sequencing Ready Reaction Kit (version 2.0) and an Applied Biosystems 3700 Capillary DNA Sequencer (Applied Biosystems, Foster City, CA). The pGEMT-CFP:TGBp2 and pRTL2 plasmids were digested with *Nco*I and *BamH*I. The CFP:TGBp2 and pRTL2 fragments were gel purified, and ligated.

Biolistic Bombardment

N. benthamiana and nontransgenic *N. tabacum* source leaves were bombarded with pRTL2-GFP, -GFP:TGBp2, -GFP:TGBp3, -CFP:TGBp2, -GFP:Talin, -DsRed:Talin, pGFP:MBD, and pBIN-mGFP5-ER to study subcellular accumulation of the fusion proteins. Source leaves were identified by applying carboxyfluorescein dye (CF) (Sigma, St. Louis, MO) to the petiole of the most mature leaf of an *N. benthamiana* or *N. tabacum* plant (Krishnamurthy et al., 2003; Yang et al., 2000). Plants were kept in the dark overnight and the next day leaves were detached and observed using an epifluorescence microscope and a 10X objective lens. CF dye was detected uniformly in sink leaves. CF dye was detected only in the veins in source leaves. Following the CF dye experiments, source or sink leaves were detached from plants of similar age and bombarded with plasmids using the PDS 1000/He System (Biorad, Hercules, CA).

Leaves were bombarded with 10 μg plasmids mixed with 1 mg of 1 μm gold particles. 10 μl of a DNA/gold mixture was loaded on a carrier disk and bombarded to detached leaves as described previously (Yang et al., 2000). The leaves were observed 24 h post bombardment (hpb) using confocal microscopy.

Chemical inhibitor treatments of leaves

Bombarded leaves were incubated overnight (16 h) on moist filter paper. Leaves were treated with either BFA, which disrupts the ER and Golgi network, or latrunculin B, which disrupts actin filaments (Henderson et al., 1994; Nebenfuhr et al., 1999; Ritzenthaler et al., 2002; Saint-Jore et al., 2002). Leaves were cut into segments, analyzed by epifluorescence microscopy to detect GFP expression and then transferred to either a solution of 200 ug/ml BFA (Molecular Probes, Eugene, OR) or 1 um latrunculin B (A.G. Scientific Inc., San Diego, CA). Each chemical inhibitor was dissolved in 0.1% DMSO (w/v) solution. Leaf segments were incubated in each chemical inhibitor solution for 2-4 h at room temperature, and then analyzed by confocal laser scanning microscopy. As a control, leaf segments were incubated in sterile water or 0.1% DMSO (w/v) for 4 h and then analyzed by confocal laser scanning microscopy.

Fixation, LR-White embedding, and immunolabelling of plant material

For the electron microscopy studies, nontransgenic, mGFP5-ER, GFP:TGBp2, and GFP:TGBp3 transgenic *N. tabacum* leaf segments were fixed using the Balzer HPM010 high pressure freezer machine (Manchester, NH) located at the Oklahoma Medical Research Center according to the protocol of Kiss *et al*. (1990). Leaf pieces were excised, washed with ddH_2O water, and fitted into 0.4 mm freezer hats (Ted Pella Inc., Reading, CA) filled with lecithin solution (100 mg/ml in chloroform). A drop of 15% (w/v) aqueous dextran (MW 38,800) was added to each freezer hat. Freezer hats were then loaded onto a holder and inserted into the cryo-chamber at -80^{o}C. Immediately after freezing, the freezer hats were transferred into Nalgene™ cryogenic vials (Rochester, NY) containing supercooled 100% acetone located in the liquid nitrogen bath.

Freeze substitution was carried out by transferring samples in the freezer hats to a solution of 1% OsO_4 and acetone. Samples were maintained in a dry ice/acetone bath for 2.5 days at -78.6°C. Samples were transferred from the freezer hats to vials of acetone and incubated in a freezer at –20 °C for two h, then in a refrigerator at 0 °C for two h, and then on the lab bench (23 °C) for two h. Samples in vials were then rinsed three times in acetone for 20 min, three times in 100% ethanol for 20 min and then embedded in LR-White resin (London Resin Co, UK).

Ultrathin sections (60 nm) were cut using a diamond knife on a Sorvall MT 6000 ultramicrotome and mounted on formvar coated nickel grids (Electron Microscopy Science Inc., Hatfield, PA). Immunogold labeling of LR-White embedded tissues (Huang and Russell, 1994) was conducted using full length mouse monoclonal A.V. antiserum (BD Living Colors™, Clontech) to detect EGFP and rabbit polyclonal anti-BiP sera obtained from Dr. R. Boston (North Carolina State University). Grids were incubated in blocking solution consisting of phosphate buffered saline pH 7.5 (PBS; 130 mM NaCl, 7.0 mM Na_2HPO_4, 3.0 mM NaH_2PO_4) plus 2% bovine sera albumin (BSA; w/v) for 15 min, and then incubated in 2% normal goat serum in PBS plus 2% BSA for 15 min. Then samples were incubated with either anti- EGFP serum diluted 1:500 in PBS plus 2% BSA (w/v), or anti-BiP sera diluted 1:10 in PBS plus 0.1 % Tween (v/v) for 2 h. The grids were then washed five times for five min with PBS and then with PBS plus 2% fish gelatin (v/v) for 15 min. The grids were then incubated for 1 h with either 10 nm or 25 nm gold-conjugated anti-rabbit sera (EY Labs Inc. San Mateo, CA) diluted 1:10 in PBS plus 2% fish gelatin. Grids were washed three times for 5 min with ddH_2O, and stained with a solution of 2.5% uranyl acetate and 70% methanol for 30 min, and then with a solution of 2% Reynold's lead citrate pH 12.0 for 20 min. Samples were washed with lukewarm ddH_2O three times for 5 min and then blot dried. Control samples were incubated with either blocking solutions or 10 nm gold-conjugated anti rabbit sera.

For dual labeling to detect both BiP and EGFP simultaneously, a longer procedure was followed. Samples were first incubated with anti-BiP serum diluted 1:10 in PBS plus 0.1 % Tween (v/v) for 2 h and then with the 25 nm gold-conjugated anti-rabbit serum diluted 1:10 in PBS plus 2% fish gelatin for 2 h as described above. Samples were washed twice for 10 min with PBS, and then incubated for 30 min with full length mouse monoclonal A.V. antiserum diluted 1:500 in PBS. Samples were washed five times for 5 min each with PBS, then for 15 min with PBS with 2% fish gelatin, and then incubated with for 30 min with 10-nm gold-conjugated secondary antibody (EY Labs Inc., San Mateo, CA) diluted to 1:10 in PBS plus 2% fish gelatin. Grids were washed twice for 10 min each with PBS, and then three times for 5 min each with ddH_2O. Samples were stained with uranyl acetate and Reynold's lead citrate as described above. Control samples were treated with BiP and rabbit anti-TMV serum diluted 1:50.

Epifluorescence, confocal and electron microscopy

Cell-to-cell movement of PVX.GFP viruses was monitored in tobacco leaves using a Nikon E600 (Nikon Inc., Dallas, TX) epifluorescence microscope with a Nikon B2A filter cube (containing a 470-490 nm excitation filter, a DM505 dichroic mirror, and a BA520 barrier filter). Images were captured using the Optronics Magnafire camera

(Intelligent Imaging Innovations, Inc., Denver, CO) attached to the Nikon E600 microscope.

A Leica TCS SP2 (Leica Microsystems, Bannockburn, IL, USA) or a BioRad 1024ES (Bio-Rad Laboratories, Hercules, CA) confocal imaging system was used to study subcellular localization of GFP fusion proteins in tobacco epidermal cells that were bombarded with plasmids. The Leica TCS SP2 system was attached to a Leica DMRE microscope. The BioRad 1024ES system was attached to a Zeiss Axioskop microscope (Carl Zeiss, Thornwood, NY). Both microscopes were equipped with epifluorescence and water immersion objectives. For confocal microscopy a Krypton/Argon laser was used to examine all fluorescent proteins. A 488 nm excitation wavelength was used to examine GFP expression, a 458 nm excitation wavelength for CFP expression, and a 514 nm excitation wavelength for DsRed expression. In general, fifteen to thirty optical sections were taken of each cell at 0.3 to 2 μm intervals. In leaves co-expressing CFP:TGBp2 and GFP:TGBp3, or CFP:TGBp2 and mGFP5-ER, the two fluorescent proteins were imaged using the sequential scanning option of the Leica TCS SP2 software. Images were merged using Leica TCS SP2 software. DsRed:Talin and GFP:TGBp2 images were taken by Elison Blancaflor at the Noble Foundation, Ardmore, OK, using the BioRad 1024ES confocal laser scanning microscope.

Electron microscopic analysis of samples was carried out using a JEOL JEM 100 CXII scanning transmission electron microscope. Photographs were taken and developed in a dark room and then scanned using an HP scan jet 4570c. All images obtained by epifluorescence, confocal, or electron microscopy were processed using Adobe Photoshop CS version 8.0 software (Adobe Systems Inc., San Jose, CA).

Statistical analysis of Table 1

Analysis of variance procedures with PC SAS Version 8.2 (SAS Institute, Cary, NC) and PROC GLM were used to evaluate differences in location in the number of gold particles observed. The analysis was performed for each combination of transgene and antiserum. Due to problems in homogeneity of variance and distributional assumptions, a square root transformation was used prior to the conduct of the analyses of variance. When the ANOVA was significant, pairwise comparisons of the locations were made with a PDIFF option in an LSMEANS statement. A significance level of 0.05 was used for all comparisons.

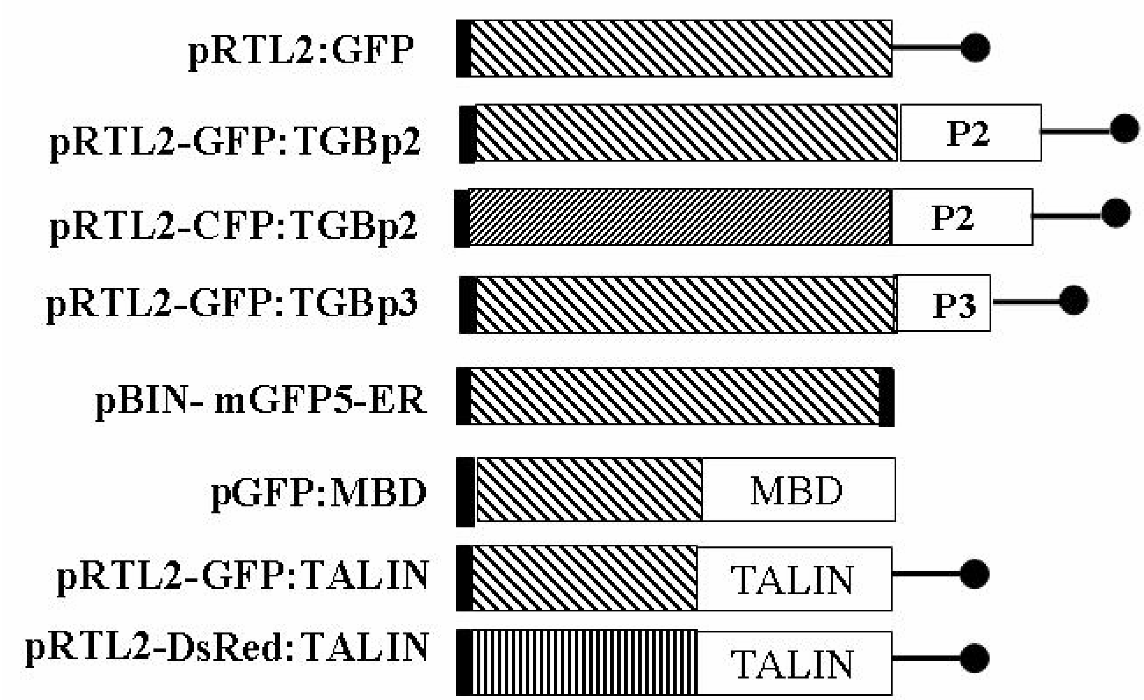

Fig.1. Schematic representation of plasmids used in this study. Four pRTL2 plasmids expressing GFP alone (hatch box), GFP or CFP (dense hatched box) fused to the 5' end of the PVX TGBp2 or TGBp3 genes (open boxes). Four control plasmids were used: pBIN-mGFP5-ER, GFP:Talin, DsRed:Talin, and pGFP:MBD. The DsRed is represented by a vertical hatched box. All plasmids contain a CaMV 35S promoter (black box) and a nos terminator (black circle) (Kost, et al., 1998; McCann, et al., 1997). All plasmids, except DsRed:Talin, were described in the materials and methods section of Chapter II and III. The gray box at the 3' end of the mGFP5-ER represents the ER targeting signal.

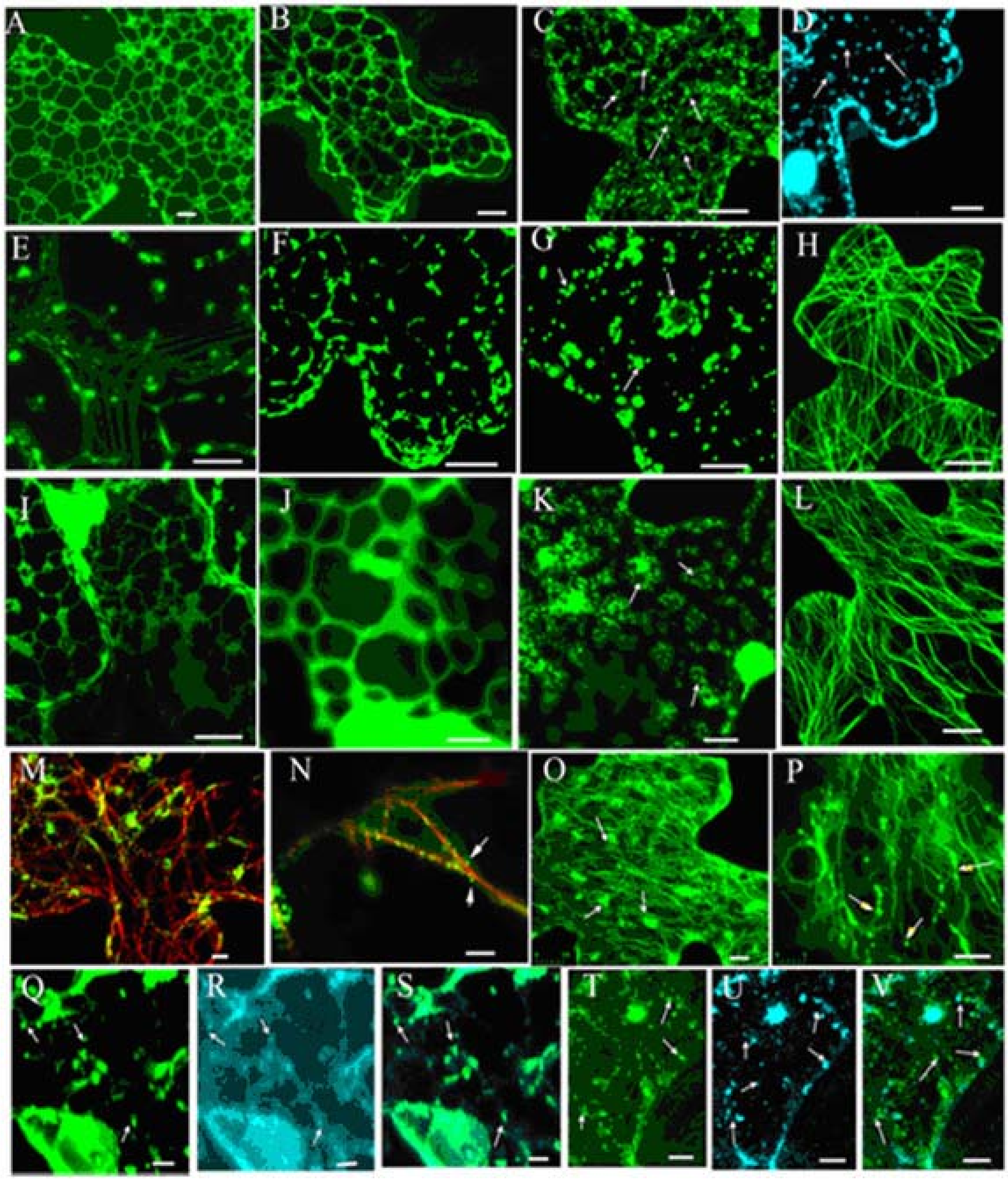

Fig. 2. Subcellular accumulation of fluorescent proteins analyzed by confocal microscopy. All images are of tobacco leaves bombarded with plasmids expressing (A) mGFP5-ER, (B) GFP:TGBp3, (C) GFP:TGBp2, and (D) CFP:TGBp2. The following samples were treated with brefeldin A: (E) mGFP5-ER, (F) GFP:TGBp3, and (G) GFP:TGBp2, and (H) shows GFP:MBD. The following samples were treated with latrunculin B: (I) mGFP5-ER, (J) GFP:TGBp3, (K) GFP:TGBp2, and (L) GFP:Talin. High power images of tobacco leaves bombarded with two plasmids expressing: (M and N) both DsRed:Talin

and GFP:TGBp2; (O and P) both GFP:Talin and GFP:TGBp2; (Q, R and S) high power images of GFP:TGBp3 and CFP:TGBp2; (T, U and V) mGFP5-ER and CFP:TGBp2 at high power. Q, R, T, U show high power images of GFP or CFP fused genes only while S and V show the merged images. Arrows in each panel point to GFP:TGBp2-containing vesicles. Bars equal 8μm.

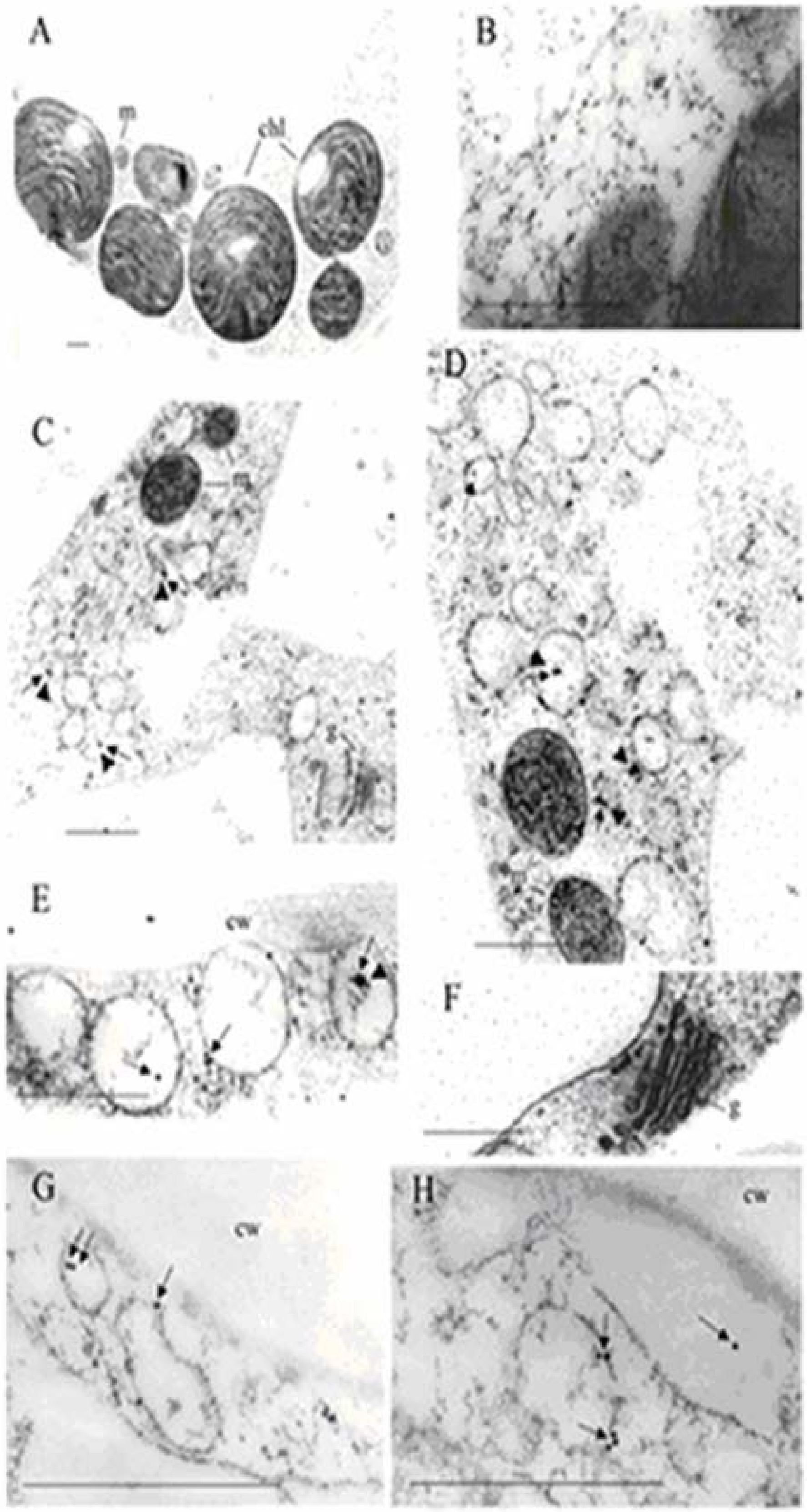
A
B
C
D
E
F
G
H
m
chl
g
cw

Fig.3. Electron micrographs of freeze-substituted transgenic *N.tabacum* leaves expressing GFP:TGBp2, probed with antisera against GFP (10nm gold) and BiP (20nm gold).(A) Low power image shows intact cell wall and organelles.(B) Samples treated with buffer and secondary antiserum. (C, D & E) Samples treated with antisera against GFP and BiP. The GFP:TGBp2 immunolabelled with BiP (bold black arrowheads and 20nm gold label), and GFP (long black arrows and 10nm gold label) show co-localization in the vesicles and ER. Mitochondria, Golgi stacks are represented by m and g respectively. (F) An intact unlabeled Golgi stack. (G and H) Single labeling with GFP antisera. Bar, 0.5 μm.

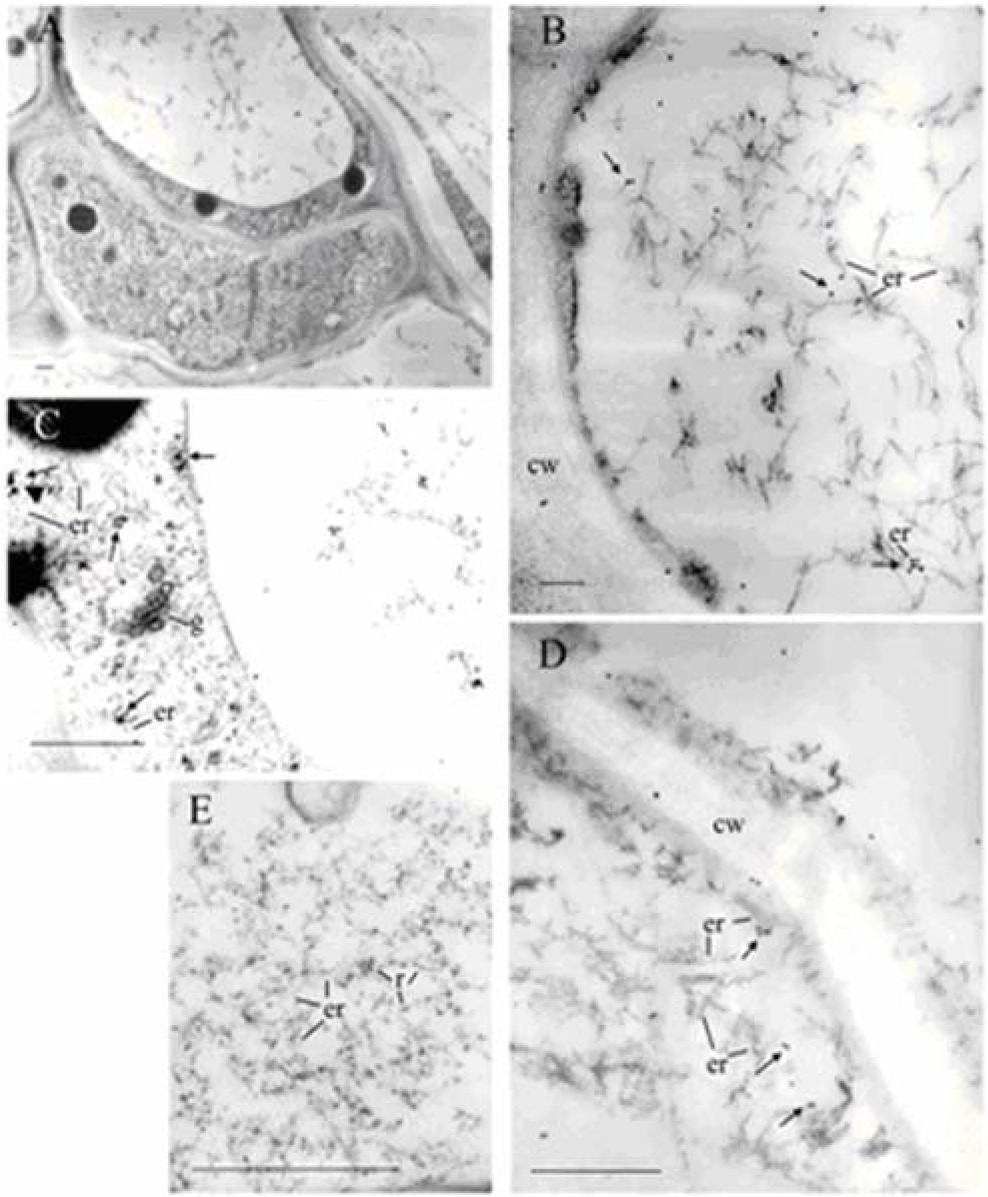

Fig..4. Ultrastructure of freeze-substituted transgenic *N. tabacum* leaves expressing GFP:TGBp3 protein, probed with GFP (10nm gold) and BiP (20nm gold) antiserum. (A) Low power image of the tissue showing intact cell wall and organelles. (B and D) Single labeling in the ER with GFP antibody. Cell wall is represented by CW. (C) GFP:TGBp3 immunolabelled with BiP (bold black arrowheads) and GFP (long arrows) show co-localization to the ER . Golgi stacks are represented by g. (E) Control; no primary antibody was used. No labeling was visible in ER. Ribosomes are depicted by 'r'. Bar, 0.5 µm.

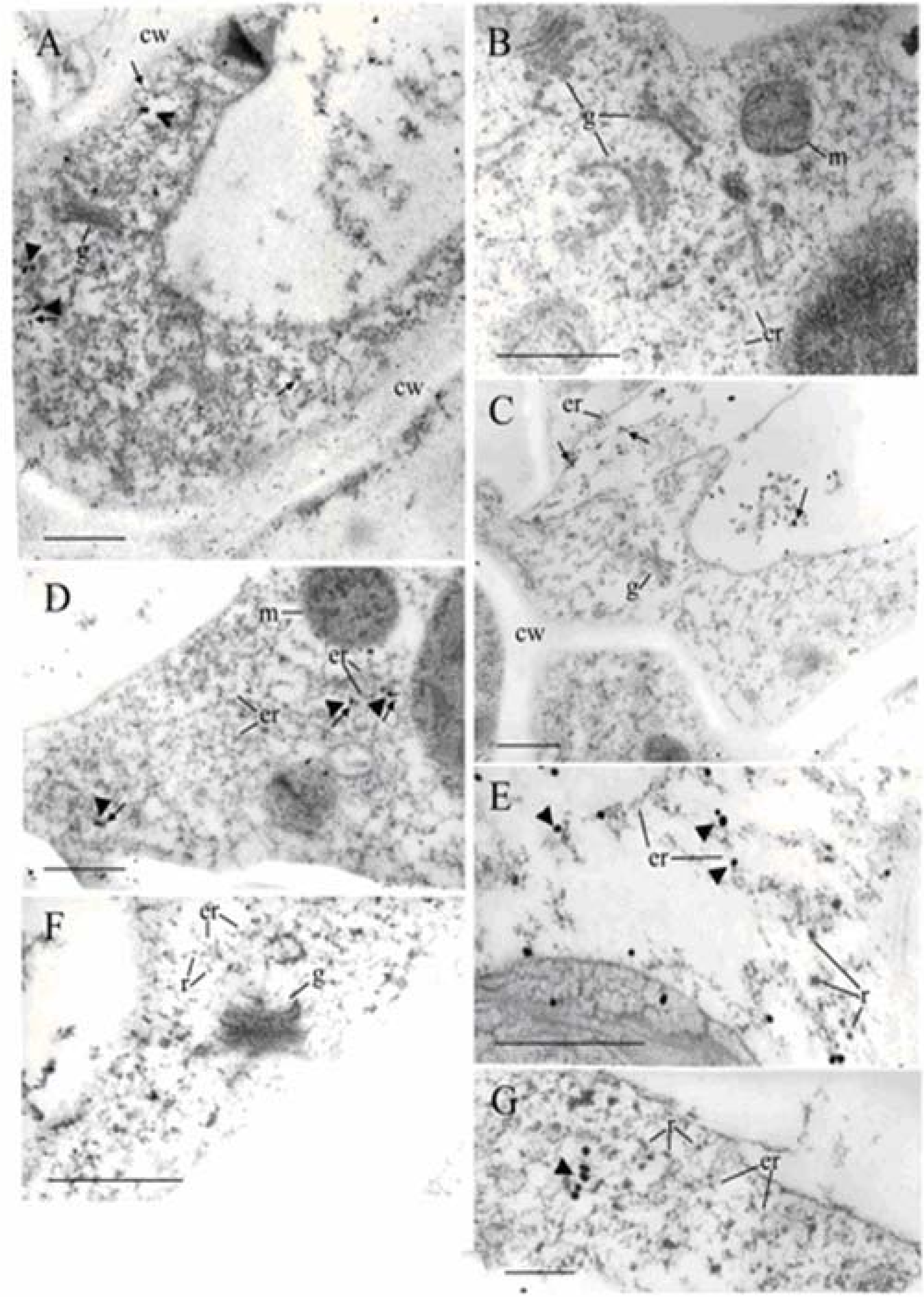

Fig.5. Ultrastructure of freeze-substituted nontransgenic and transgenic *N.tabacum* leaves expressing mGFP5-ER, probed with GFP (10nm gold) and BiP (20nm gold) antiserum. (A and D) mGFP5-ER transgenic tobacco leaves dual-labeled with BiP and GFP antiserum. The long black arrows and the black arrow-heads point to GFP and BiP labeled ultrastructures respectively. Golgi apparatus is represented by g and the cell wall

by CW. (B) Control. No primary antibody was used, and no labeling was visible in ER. Mitochondria (m) and the Golgi stacks (g) are evident. (C) Tissue probed with GFP antibody. Black arrows represent the GFP antibodies on the ER. Golgi stacks, mitochondria and the cell wall are represented by letters g, m, and CW, respectively. (E) mGFP5-ER expressing tobacco leaf ultrathin sections probed with BiP antibody and the labeling is seen on the ribosome (r) studded ER. (F and G) Ultrastructure of nontransgenic tobacco leaves. (F) Control. Tissue probed with GFP antibody. No labeling is visible. (G) Non transgenic tobacco leaves labeled with BiP antibody depicted by the black arrowhead. Bars, 0.5 μm.

Table 1

Distribution of immuno gold labeling of ER, CW, and PM, mean ± std. error

Transgene[a]	Antisera[b]	Total Fields[c]	Mean ±std. err. of number of gold particles in:[d] CW	PM	ER
Experiments using single antisera:					
GFP:TGBp2	GFP	30	1.0±0.3b	1.4±0.6b	4.2±1.9a
GFP:TGBp3	GFP	21	1.0±0.7b	1.4±0.5b	5.5±1.2a
mGFP5-ER	GFP	37	0.4±0.2b	0.1±0.1b	2.4±0.4a
Nontransgenic	GFP	36	0.3±0.1a	0.2±0.1a	0.3±0.1a
GFP:TGBp2	BiP	8	0.3±0.3b	1.4±0.5a	1.6±0.5a
GFP:TGBp3	BiP	12	0±0b	0.3±0.2b	2.5±0.3a
mGFP5-ER	BiP	12	0±0b	0.1±0.1b	1.5±0.3a
Nontransgenic	BiP	15	0.1±0.1b	0.4±0.2b	2.3±0.4a
GFP:TGBp2	No	22	0±0a	0±0a	0±0a
GFP:TGBp3	No	20	0±0a	0±0a	0.1±0.1a
mGFP5-ER	No	13	0±0b	0±0b	0.6±0.2a
Nontransgenic	No	10	0±0a	0±0a	0±0a
Experiments using two antisera:					
GFP:TGBp2	GFP	20	0.8±0.3b	2.3±0.6a	3.7±0.8a
	BiP	20	0±0b	0.1±0.1b	0.9±0.3a
GFP:TGBp3	GFP	24	1.7±0.5b	0.8±0.6b	5.8±0.9a
	BiP	24	0.1±0.1b	0±0b	1.2±0.3a
mGFP5-ER	GFP	29	2.0±0.6b	1.3±0.4b	9.1±0.7a
	BiP	29	0±0b	0.1±0.1b	1.5±0.3a
GFP:TGBp2	GFP	16	0.1±0.1b	0±0a	4.6±1.1a
	TMV	16	0±0a	0±0a	0±0a
GFP:TGBp3	GFP	17	1.2±0.6b	0.5±0.3b	5.8±1.0a
	TMV	17	0±0a	0±0a	0±0a
mGFP5-ER	GFP	13	0±0b	0±0b	0.6±0.2a
	TMV	13	0±0a	0±0a	0±0a

[a] Transgenic *N. tabacum* leaf samples were embedded in LR-White, sectioned, and analyzed by immunoglod labeling and electron microscopy to assess the subcellular patterns of GFP:TGBp2 and GFP:TGBp3. Control samples included nontransgenic leaves and transgenic leaves expressing GFP targeted to the ER (mGFP5-ER). Since we lack antisera to PVX TGBp2 and TGBp3, transgenic plants expressing GFP fused genes were used. Immunogold labeling was then conducted using commercially available anti-GFP serum.

[b] In the top half of the table, samples of transgenic or nontransgenic tobacco leaves were treated with either full length mouse monoclonal A.V. antiserum (BD Living Colors[TM], Clontech) to detect GFP, BiP antiserum obtained from Dr. R. Boston (North Carolina State University), or no primary antiserum. All samples were treated with 10nm gold-conjugated anti-mouse or anti-rabbit sera. In the bottom half of the table, samples were dual-labeled using antiserum to detect GFP and BiP. As a control, some samples were treated with antiserum to detect GFP and TMV. These samples were treated with 10nm and 25 nm gold-conjugated anti-mouse and anti-rabbit serum.

[c] Fields are defined as areas of 1μm^2 (using an ultrastructure size calculator) which contain gold particles. Gold particles in each field were counted manually. The total numbers of fields analyzed for each transgenic plant sample are indicated.

[d] The numbers of gold particles detected in the cell wall (CW), plasma membrane (PM) and endoplasmic reticulum (ER) were determined for all fields treated with each antiserum. Means within the same row with the same letter are not significantly different using Fisher's Protected Least Significant Different procedure at a 0.05 significance level on square root transformed data. Zeros indicate samples that had the CW, PM, or ER but no labeling.

Table2

Distribution and immunogold labeling of golgi stacks, mean ± std. error

			Average (total) number vesicles or Golgi stacks containing gold particles			
Transgene[a]	Sera[b]	Fields[c]	No. vesicles[d]	Gold in vesicles	No. Golgi stacks[c]	Gold in Golgi
Experiments using single antibodies:						
GFP: TGBp2	GFP	13	1.8±0.5	3.3±0.9	1.0±0.0	0.0±0.0 *
GFP: TGBp3	GFP	14	NO	NO	1.0±0.0	0.0±0.0
mGFP5-ER	GFP	30	NO	NO	1.1±0.0	0.1±0.0
Nontransgenic	GFP	11	NO	NO	1.0±0.0	0.0±0.0
Experiments using two antibodies:						
GFP: TGBp2	GFP	44	2.1±0.3	1.9±0.3	1.0±0.0	0.0±0.0 *
	BiP	44	2.1±0.3	0.5±0.2	1.0±0.0	0.0±0.0 *
GFP: TGBp3	GFP	14	NO	NO	1.0±0.0	0.0±0.0
	BiP	14	NO	NO	1.0±0.0	0.0±0.0
mGFP5-ER	GFP	10	NO	NO	1.1±0.1	0.3±0.2
	BiP	10	NO	NO	1.1±0.1	0.0±0.0

[a] Transgenic *N. tabacum* leaf samples were embedded in LR-White, sectioned, and analyzed by immunogold labeling and electron microscopy to assess the subcellular accumulation patterns of GFP:TGBp2 and GFP:TGBp3. Control samples included nontransgenic leaves and transgenic leaves expressing GFP targeted to the ER (mGFP5-ER).

[b]In the top half of the table, samples of transgenic or nontransgenic tobacco leaves were treated with either full length mouse monoclonal A.V. antiserum (BD Living Colors™, Clontech) to detect GFP, BiP antiserum obtained from Dr. R. Boston (North Carolina State University), or no primary antiserum. All samples were treated with 10 nm gold-conjugated anti-mouse or anti-rabbit sera. In the bottom half of the table samples were dual-labeled using antiserum to detect GFP and BiP. As a control, some samples were treated with antiserum to detect GFP and TMV. These samples were treated with 10 nm and 25 nm gold-conjugated anti-mouse and anti-rabbit serum.

[c]Fields are defined as areas of 1 μm^2 (using an ultrastructure size calculator) which contain gold particles in vesicles or Golgi stacks only. Gold particles in each field were counted manually. The total numbers of fields analyzed for each transgenic plant sample are indicated.

[d]The numbers of gold particles detected in the vesicles or Golgi stacks were determined for all fields treated with each antiserum. Asterisks (*) next to means of Golgi gold values represent statistical significance (at a 0.05 level) when compared to mean gold in vesicles. Zeros indicate samples that had the CW, PM, or ER but no labeling. NO means "none observed". NO was used to designate the lack of vesicles in GFP:TGBp3, mGFP5-ER, and nontransgenic samples.

REFERENCES

Alzhanova, D. V., Napuli, A. J., Creamer, R., and Dolja,V.V. (2001). Cell-to-cell movement and assembly of a plant closterovirus: roles for the capsid proteins and Hsp70 homolog. *EMBO* **20**(24)**,** 6997-7007.

Asurmendi, S., Berg, R.H., Koo,J.C., and Beachy, R.N. (2004). Coat protein regulates formation of replication complexes during tobacco mosaic virus infection. *Proc. Natl. Acad. Sci*. **101**, 1415-1420.

Atabekov, J.G., Rodionova, N.P., Karpova, O.V., Kozlovsky, S.V., Poljakov, V.Y. (2000). The movement protein-triggered *in situ* conversion of *Potato virus X* virion RNA from a nontranslatable to translatable form. *Virology* **271**, 259-263.

Atabekov, J.G., Rodionova, N.P., Karpova, O.V., Kozlovsky, S.V., Nonikov, V.K., and Arkhipenko, M.V. (2001). Translational activation of encapsidated Potato virus X by coat protein phosphorylation. *Virology* **286**, 466-474.

Atsushi, T., and Meshi, T. (2001). Tobamoviral movement protein transiently expressed in a single epidermal cell functions beyond multiple plasmodesmata and spreads multicellularly in an infection-coupled manner. *Molec. Plant-Microbe Interact.* **14,** 126-134.

Baulcombe, D. C., Chapman, S., and Santa Cruz, S. (1995). Jellyfish green fluorescent protein as a reporter for virus infections . *Plant J.* **7,** 1045-1053.

Beachy, R. N., and Heinlein, M. (2000). Role of P30 in replication and spread of TMV. *Traffic* **1,** 540-544.

Beck, D. L., Guilford, P. J., Voot, D. M., Andersen, M. T., and Forster, R. L. S. (1991). Triple gene block proteins of *White clover mosaic potexvirus* are required for transport. *Virology* **183,** 695-702.

Blackman,L.M., and Overall,R.L.1998. Immunolocalization of the cytoskeleton to plasmodesmata of Chara corallina. *Plant J.* **14**,733-741.

Boevink, P., Oparka, K., Santa Cruz, S., Martin, B., Betteridge, A., and Hawes, C. (1998). Stacks on tracks: The plant Golgi apparatus traffics on an actin/ER network. *Plant J.* **15**, 441-447.

Canto, T., Prior, D.A.,Hellwald, K.H.,Oparka,K.J.,Palulaitis,P. (1997). Characterization of cucumber mosaic virus.IV.Movement protein and coat protein are both essential for cell-to-cell movement of cucumber mosaic virus. *Virology* **237**(2), 237-48.

Cheng, C.-P., Tzafrir, I., Lockart, B.E.L., and Olszewski, N.E. (1998).Tubules containing virions are present in plant tissues infected with *Commelina* yellow mottle badnavirus. *J. Gen. Virol* **79,** 925-929.

Citovsky, V., and Zambryski, P. (1991). How do plant virus nucleic acids move through intercellular connections? *BioEssays* **13,** 373-379.

Crawford, K.M. and Zambryski, P.C. 2001. Non-targeted and targeted protein movement through plasmodesmata in leaves in different developmental and physiological states. *Plant Physiol*. 125: 1802-1812.

Derrick, P. M., Barker,H., and Oparka, K.J. (1992). Increase in plasmodesmatal permeability during cell-to-cell spread of *Tobacco rattle virus* from individually inoculated cells. *Plant Cell* **4**, 1405-1412.

Ding, B. (1998). Intercellular protein trafficking through plasmodesmata. *Plant Molecular Biology* **38**, 279-310.

Ding, B., Haudenshield, J. S., Hull, R. J., Wolf, S., Beachy, R. N., and Lucas, W. J. (1992a). Secondary plasmodesmata are specific sites of localization of the *Tobacco mosaic virus* movement protein in transgenic tobacco plants. *Plant Cell* **4,** 915-928.

Donald, R. G. K., Lawrence, D. M., and Jackson, A. O. (1997). The *Barley stripe mosaic virus* 58-Kilodalton Bb protein is a multifunctional RNA binding protein. *J. Virol.* **71,** 1538-1546.

Dunoyer, P., Ritzenthaler, C., Hemmer, O., Michler, P., and Fritsch, C. (2002). Intracellular localization of the Peanut clump virus replication complex in tobacco BY-2 protoplasts containing green fluorescent protein-labeled endoplasmic reticulum or Golgi apparatus. *J. Virol.* **76**, 865-874.

Fedorkin, O. N., Soloyev, A.G., Yelena, N.E. (2001). Cell-to-cell movement of Potato virus X involves distinct functions of the coat protein. *J. Gen. Virol* **82,** 449-458.

Fontes EB, Shank BB, Wrobel RL, Moose SP, OBrian GR, Wurtzel ET, Boston RS.(1991). Characterization of an immunoglobulin binding protein homolog in the maize floury-2 endosperm mutant. Plant Cell.**3**(5),483-96.

Forster, R. L. S., Beck, D. L., Guilford, P. J., Voot, D. M., Van Dolleweerd, C. J., and Andersen M. T. (1992). The coat protein of White clover mosaic potexvirus has a role in facilitating cell-to-cell transport in plants. *Virology_* **191**, 480-484.

Fujiwara, T., Giesman-Cookmeyer, D., Ding, B., Lommel, S., and Lucas, W.J. (1993). Cell-to-cell trafficking of macromolecules through plasmodesmata potentiated by the *Red clover necrotic mosaic virus* movement protein. *Plant Cell* **5,** 1783-1794.

Giesmancookmeyer, and Lommel, S.A..(1993).Alanine scanning mutagenesis of a plant virus movement protein identifies 3 functional domains. *Plant Cell* **5,** 973-982.

Giesmancookmeyer, D., Silver, S., Vaewhongs, A.A. Lommel, S.A.. and Deom, C.M.(1995). Tobamovirus and dianthovirus movement proteins are functionally homologous. *Virology* _ **213**, 38-45.

Hake, S. (1992). Unraveling the knots in plant development. *Trends in Genetics* **8**(3)**,** 109-114.

Haseloff, J., Simering, K. R., Porasher, D. C., and Hodge, S. (1997). Removal of a cryptic intron and subcellular localizaiton of green fluroescent protein are required to mark transgenic *Arabidopsis* plants brightly. Proc. Natl. Acad. Sci. USA. **94**, 2122-2127.

Heinlein, M., Padgett, H. S., Gens, J. S., Pickard, B. G., Casper, S. J., Epel, B. L., Beachy, R. N. (1998). Changing patterns of localization of the *Tobacco mosaic virus* movement protein and replicase to the endoplasmic reticulum and microtubules during infection. *Plant Cell* **10,** 1107-1120.

Heinlein M, Epel BL.(2004). Macromolecular transport and signaling through plasmodesmata. *Int Rev Cytol*. **235**, 93-164.

Henderson, J., Satiat-Jeunemaitre, B., Napier, R., Hawes, C. (1994). Brefeldin A-induced disassembly of the Golgi apparatus is followed by disruption of the endoplasmic reticulum in plant cells. *J. Exp. Bot.* **45,** 1347-1351.

Howard, A.R., Heppler, M.L., Ju, H.-J., Krishanmuthy, K., Payton, M.E., and Verchot-Lubicz, J. Potato virus X TGBp1 induces plasmodesmata getting and move between cells in several host species whereas CP moves only in *N. benthaminana* leaves. *Virology* **328**, 185-197.

Huang, B.-Q., Russell, S. D. (1994). Fertilization in Nicotiana tabacum: Cytoskeletal modifications in the embryo sac during synergid degeneration. *Planta* **194,** 200-214.

Huisman , M. J., Linthorst, H. J. M., Bol, J. F., Cornelissen, B. J. C. (1998). The complete nucleotide sequence of *Potato virus X* and its homologies at the amino acid level with various plus-stranded RNA viruses. *J. Gen. Virol* **69,** 1789-1798.

Imlau, A., Truernit,E., and Sauer,N. (1999). "Cell-to-cell and long distance trafficking of the green fluorescent protein in the phloem and symplastic unloading of the protein into sink tissues." *Plant Cell* **11**, 309-322.

Itaya, A., Hickman, H., Bao, Y., Nelson, R., and Ding, B. (1997). Cell-to-cell trafficking of Cucumber mosaic virus movement protein: Green fluorescent protein fusion produced by biolistic gene bombardment in tobacco. *Plant J.* **12,** 1223-1230.

Itaya, A., Woo, Y.-M., Masuta, C., Bao, Y., Nelson, R.S.,and Ding, B. 1998. Development regulation of intercellular protein trafficking through plasmodesmata in tobacco leaf epidermis. Plant Physiol. **118**, 373-385.

Itaya, A., Liang, G., Woo, Y.-M., Nelson, R. S., Ding, B. (2000). Nonspecific intercellular protein trafficking probed by green-fluorescent protein in plants. *Protoplasma* **213,** 165-175.

Jorgensen, R. A., Atkinson, R. G., Forster, R. L. S., Lucas, W. J. (1998). An RNA-based information superhighway in plants. *Science* **279,** 1486-1487.

Kalinina, N. O., Fegorkin, O.N., Samuilova, O.V., Korpela, T., and Morozov, S. Y. 1996. Expression and biochemical analysis of the recombinant potato virus X 25K movement protein. *FEBS Lett.* **397**,75-78.

Kasteel, D. T. J., Wellink, J., Goldbach, R.W., van Lent, J. W. M. (1997). Isolation and characterization of tubular structures of *Cowpea mosaic virus*. *J. Gen. Virol.* **78,** 3167-3170.

Kawakami, S., Watanabe, Y., and Beachy. 2004. Tobacco mosaic virus infection spreads cell to cell as intact replication complexes. *Proc. Nat. Acad. Sci*., **101**, 6291-6296.

Kim, J. Y., Yuan, Z., Cilia, M., Khalfan-Jagani, Z., Jackson, D. (2002). Intercellular trafficking of a KNOTTED1 green fluorescent protein fusion in the leaf and shoot meristem of Arabidopsis. *Proc. Natl. Acad. Sci. USA* **99,** 4103-4108.

Kiss, J. Z., Giddings Jr., T. J., Staehelin, L.A., and Sack, F. D. (1990). Comparison of the ultrastructure of conventionally fixed and high pressure frozen/freeze substituted root tips of *Nicotiana* and Arabidopsis. *Protoplasma* **157,** 64-74.

Krishnamurthy, K., Mitra, R., Payton, M. E., and Verchot-Lubicz, J. (2002) Cell -to-cell movement of the *Potato virus X* 12K, 8K,or coat proteins may depend on the host ,leaf developmental stage, and the PVX 25K protein. *Virology* **200**, 269-281.

Krisnamurthy, K., Heppler, M., Mitra, R., Blancaflor, E., Payton, M., Nelson, R.S., and Verchot-Lubicz, J. (2003). The potato virus X TGBp3 protein associates with the ER network for virus cell-to-cell movement. *Virology* **309**, 135-151.

Knebel, W., Quader, H., Schnepf,E. (1990). Mobile and immobile endoplasmic reticulum in onion bulb epidermis cells:short- and long- term observations with a confocal laser scanning microscope. *European Journal of Cell Biology*. **52**, 328-340.

Kost, B., Spielhofer, P., Chua, N.-H. (1998). A GFP-mouse talin fusion protein labels plant actin filaments in vivo and visualizes the actin cytoskeleton in growing pollen tubes. *Plant J.* **16,** 393-401.

Lazarowitz, S. and Beachy R.N. 1999. Viral movement proteins as probes for intracellular and intercellular trafficking in plant. *Plant Cell* **11**, 535-548.

Lough, T. J., Netzler, N.E., Emerson, S.J., Sutherland, P., Carr, F., Beck, D.L., Lucas, W.J., and Foster, L.S. 2000. Cell-to-cell movement of potexvirus: Evidence for ribonucleoprotein complex involveing the coat protein and first triple gene block protein. Mol. Plant-Microbe Interact. **13**, 962-974.

Lough , T. J., Shash, K., Xoconostle-Cazares, B., Hofstra, K. R .,Beck, D. L., Balmori, E., Forster, R. L. S., Lucas, W. J. (1998). Molecular dissection of the mechanism by which Potexvirus triple gene block proteins mediate cell-to- cell transport of the infectious RNA. *Mol. Plant-Microbe Interact.* **11,** 801-814.

Lucas, W. J. (1995). Plasmodesmata:Intercellular channels for macromolecular transport in plants. *Current opinions in Cell Biology*. **7**, 673-680.

Lucas, W. J. and Gilbertson., R.L. (1994). Plasmodesmata in relation to viral movement with leaf tissue. *Annual Review of Phytopathology* **32**, 387-411.

Marc, J., Granger, C. L., Brincat, J., Fisher, D. D., Kao, T.-H., McCubbin, A. G., Cyr, R. J. (1998). A GFP-MAP4 reporter gene for visualizing cortical microtubule rearrangements in living epidermal cells. *Plant Cell* **10,** 1927-1939.

Mas, P., and Beachy, R. N. (2000). Role of microtubules in the intracellular distribution of tobacco mosaic virus movement protein. *Proc. Natl. Acad. Sci. USA* **97,** 12345-12349.

McLean, B. G., Zupan, J., and Zambryski, P. C. (1995). Tobacco mosaic virus movement protein associates with the cytoskeleton in tobacco cells. *Plant Cell* **7,** 2101-2114.

Melcher, U. (2000). The '30K' superfamily of viral movement proteins. *J. Gen. Virol.* **81,** 257-266.

Memelink, J., van der Vlugt, C. I. M., Linthorst, H. J. M., Derk, A. F. L. M., Asjes, C. J., and Bol, J. F. (1990). Homologies between the genomes of a carlavirus (*Lily symptomless virus*) and a potexvirus (*Lily virus X*) from lily plants. *J. Gen. Virol.* **71,** 917-924.

Mise, K., Allison, R.F.., Janda, M., and Ahlquist, P. (1993). Bromovirus movement protein genes play a crucial role in host specificity. *J. Virol* .**67**,2815-2823.

Mitra, R, Krisnamurthy, K., Blancaflor, E., Payton, M., Nelson, R.S., and Verchot-Lubicz, J. 2003. The potato virus X TGBp2 protein association with the endoplasmic reticulum plays a role in but is not sufficient for viral cell-to-cell movement. *Virology* **312**, 35-48.

Morozov, S. Y., Lukasheva, L. I., Chernov, B.K., Skryabin, K.G., and Atabekov, J.G. (1987). Nucleotide sequence of the open reading frames adjacent to the coat protein cistron in *Potato virus X* genome. *FEBS Letters* **213,** 438-442.

Morozov, S. Y., Fedorkin, O. N.,Juttner, G., Schiemann, J., Baulcombe, D. C. and Atabekov.(1997) Complementation of *Potato virus X* mutant mediated by bombardment of plant tissues with cloned viral movement protein genes. *J. Gen. Virol.* **78**,2077-2083.

Morozov, S. Y., Solovyev, A.G., Kalinina, N. O., Fedorkin, O. N., Samuilova, O. V., Schiemann, J., and Atabekov, J.G. (1999). Evidence for two nonoverlapping functional domains in the *Potato virus X* 25K movement protein. *Virology* **260,** 55-63.

Morzov, S.Y. and Solovyev, A.G. 2003. Triple gene block: modular design of a mulfunctional machine for plant virus movement. *J. Gen. Virol*. **84**, 1351-1366.

Nebenfuhr, A., Gallagher, L. A., Dunahay, T. G., Frohlick, J. A., Mazurkiewicz, A. M., Meehl, J. B., Staehelin, L. A. (1999). Stop-and-go movements of plant Golgi stacks are mediated by the acto-myosin system. *Plant Physiology*. **121,** 1127-1141.

Noueiry, A.O., Lucas, W.L., and Gilbertson, R.L. 1994. Two proteins of plant DNA virus coordinate nuclear and plasmodesmata. *Cell* **76**, 925-932.

Oparka , K. J., Roberts, A.G.,Boevink,P., Santa Cruz, S,Roberts,I.M., Pradel, K.S., Imlau,A.,Kotlizky,G.,Sauer,N.,and Epel,B. (1999). Simple, but not branched, plasmodesmata allow the nonspecific trafficking of proteins in developing tobacco leaves *Cell* **97**, 743-754.

Oparka, K. J., Prior, D. A. M., Santa Cruz, S., Padgett, H. S., and Beachy, R. N. (1997). Gating of epidermal plasmodesmata is restricted to the leading edge of expanding infection sites of *Tobacco mosaic virus* (TMV). *Plant J.* **12,** 781-789.

Oparka , K. J., Roberts, A.G., Roberts,I.M., Prior, D.A.M., and Santa Cruz, S. (1996). Viral coat protein is targeted to ,but does not gate plasmodesmata during cell-to-cell movement of Potato virus X . *Plant J*. **10**(5), 805-813.

Oparka , K. J., Duckette,C.M., Prior, D.A.M., and Fisher,D.B. (1994). Real-time imaging of phloem unloading in the root tip of *Arabidopsis*. *Plant Journal* **6**, 759-766.

Palukaitis P, Garcia-Arenal F.(2003). Cucumoviruses. *Adv Virus Res*.**62**,241-323.

Persson, B., and Argos, P. (1994). Prediction of transmembrane segments in proteins utilizing multiple sequence alignments. *J. Mol. Biol.* **237,** 182-192.

Quadt, R., and Jaspars, E. M. J. (1990). Purification and characterization of *Brome mosaic virus* RNA-dependent RNA polymerase. *Virology*. **178,** 189-194.

Restrepo-Hartwig, M. A., and Carrington, J. C. (1994). The *Tobacco etch potyvirus* 6-kilodalton protein is membrane associated and involved in viral replication. *J. Virol.* **68,** 2388-2397.

Reichel, C., and Beachy, R. N. (1998). Tobacco mosaic virus infection induces severe morphological changes of endoplasmic reticulum. *Proc. Natl. Acad. Sci.,* USA **95**, 11169-11174.

Restrepo-Hartwig, M. A., and Carrington, J. C. (1994). The Tobacco etch potyvirus 6-kilodalton protein is membrane associated and involved in viral replication. *J. Virol*. **68**, 2388-2397.

Ridge, R., Uozumi, Y., Plazinski, J., Hurley, U. A., and Williamson, R. E. (1999). Developmental transitions and dynamics of the cortical ER of Arabidopsis cells seen with green fluorescent protein. *Plant Cell Physiol.* **40**, 1253-1261.

Ritzenthaler, C., Nebenfuhr, A., Movafeghi, A., Stussi-Garaud, C., Behnia, L., Pimpi, P., Staehelin, L. A., and Robinson, D. G. . (2002). Reevaluation of the effects of brefeldin A on plant cells using tobacco bright yellow 2 cells expressing Golgi-targeted green fluorescent protein and copi antisera. *Plant Cell* **14,** 237-261.

Robards, A. W., and Lucas, W. J. (1990). Plasmodesmata. *Ann. Rev. Plant Physiol. and Plant Molec. Biol.* **41,** 369-419.

Roberts, A. G., Santa Cruz, S., Roberts,I.M., Prior, D.A.M.,Turgeon,R.,and Oparka ,K.J. (1997). Phloem unloading in sink leaves of Nicotiana benthamiana :Comparison of a fluorescent solute with a fluorescent virus. *The Plant Cell* **9**, 1381-1396.

Rouleau, M., Smith, R. J., Bancroft, J. B., and Mackie, G. A. (1994). Purification, properties, and subcellular localization of *Foxtail mosaic potexvirus* 26-kDa protein. *Virology* **204,** 254-265.

Ryabov, E.V.,Robinson, D.J. and Taliansky, M.E.(1999). A plant virus encoded protein facilitates long distance movementof heterologous viral RNA. *Proc. Nat. Acad. Sci*., **96**, 1212-1217.

Saint-Jore, C. M., Evins, J., Batoko, H., Brandizzi, F., Moore, I., and Hawes, C. (2002). Redistribution of membrane proteins between the Golgi apparatus and endoplasmic reticulum in plants is reversible and not dependent on cytoskeletal networks. *Plant J.* . **29,** 661-678.

Sambrook, J., Fritsch, E. F., and Maniatis, T. (1989). Molecular Cloning: A Laboratory Manual. (Cold Spring Harbor, NY: Cold Spring Harbor Laboratory).

Schaad, M. C., Jensen, P.E., and Carrington, J.C. (1997). Formation of plant RNA virus replication complexes on membranes: Role of an endoplasmic reticulum-targeted viral protein. *EMBO* **16,** 4049-4059.

Shalla TA, Shepard JF.(1972). The structure and antigenic analysis of amorphous inclusion bodies induced by potato virus X. *Virology*. **49**(3),654-67.

Skryabin, K. G., Morozov, S. Y., Kraev, A. S., Rozanov, M. N., Chernov, B. K., Lukasheva, L. I. and Atabekov, J.G. (1988). Conserved and variable elements in RNA genomes of potexviruses. *FEBS Letters* **240,** 33-40.

Solovyev, A. G., Stroganova, T. A., Zamyantnin, A. A. Jr., Fedorkin, O. N., Schiemann, J., and Morozov, S.Y. (2000). Subcellular sorting of small membrane-associated triple gene block proteins: TGBp3-assistaed targeting of TGBp2. *Virology* **269,** 113-127.

Sonenberg , N., Shatkin, A. J., Ricciardi, R. P., Rubin, M. and Goodman, R.M.C (1978). *Nucleic Acids Res.* **5,** 2501-2512.

Spillane, C., Verchot,J.,Kavanagh,T.A., and Baulcombe,D.C. (1997). Concurrent suppression of virus replication and rescue of movement-defective virus in transgenic plantsexpressing the coat protein of *Potato Virus X. Virology* **236**, 76-84.

Storms MM, Nagata T, Kormelink R, Goldbach RW, van Lent JW.(2002). Expression of the movement protein of Tomato spotted wilt virus in its insect vector Frankliniella occidentalis**.** *Arch Virol*. **147**(4), 825-31.

Syller J.(2000). Umbraviruses--the unique plant viruses that do not encode a capsid protein. *Acta Microbiol Pol***.** **51**(2), 99-113.

van Lent, J., Storms, M., van der Meer, F., Wellink, J., and Goldbach, R. (1991). Tubular structures involved in movement of *Cowpea mosaic virus* are also formed in infected cowpea protoplasts. *J. Gen. Virol.* **72,** 2615-2623.

Verchot, J., Angell, S. M., and Baulcombe, D. C. (1998). In vivo translation of the triple gene block of Potato virus X (PVX) requires two mRNAs. *J. Virology* **72**, 8316-8320.

Verchot, J., and Carrington, J. C. (1995). Evidence that the Potyvirus P1 proteinase functions in trans as an accessory factor for genome amplification. *J. Virol.* **69**, 3668-3674.

Voinnet, O., Lederer, C. and Baulcombe, D.C. (2000). A viral movement protein prevents spread of the gene silencing signal in *Nicotiana benthamiana*. *Cell* **103,** 157-167.

Waigmann, E., Lucas, W. J., Citovsky, V., and Zambryski, P. (1994). Direct functional assay for *Tobacco mosaic virus* cell-to-cell movement protein and identification of a domain involved in increasing plasmodesma permeability. *Proc. Natl. Acad. Sci. USA* **91,** 1433- 1437.

Waterhouse, P. M., Smith, N. A., and Wang, M.-B. (1999). Virus resistance and gene silencing: killing the messenger. *Trends in Plant Science* **4,** 452-457.

Wellink, J., van Lent, J. W. M., Verver, J., Sijen, T., Goldbach, R.W., and van Kammen, A. (1993). The *Cowpea mosaic virus* M RNA-encoded 48-kDa protein is responsible for induction of tubular structures in protoplasts. *J. Virol.* **67,** 3660-3664.

Wellink, J., van Lent, J. W. M., Verver, J., Sijen, T., Goldbach, R.W., and van Kammen, A. (1993). The Cowpea mosaic virus M RNA-encoded 48-kDa protein is responsible for induction of tubular structures in protoplasts. *J. Virology*. **67**, 3660-3664.

Wieczorek, A., and Sanfacon, H. (1993). Characterization and subcellular localization of *Tomato ringspot nepovirus* putative movement protein. *Virology* . **194,** 734-742.

Wolf, S. D., Beachy, R. N. and Lucas, W. J. (1989). Movement protein of *Tobacco mosaic virus* modifies plasmodesmatal size exclusion limit. *Science* **246,** 377-339.

Wolf, S. Deom, C. M., Beachy, R.N., and Lucas, W.J. 1991. Plasmodesmatal function is probed using transgenic tobacco plants that express a virus movement protein. *Plant Cell* **3**, 593-604.

Yang, Y., Ding, B., Baulcombe, D. C., and Verchot, J. (2000). Cell-to-cell movement of the 25k protein of *Potato virus X* is regulated by three other viral proteins. *Molec. Plant-Microbe Interact.* **14,** 1158-1167.

Zamyatnin Jr., A.A., Solovyev, A.G., Sablina, A.A., Agranovsky, A.A., Katul, L., Vetten, H.J., Schiemann, J., Hinkkanen, A.E., and Morozov, S.Y. 2002. Dual-color imageing of membrane protein targeting directed by poasemilatent virus movement protein TGBp3 in plant and mammalian cells. *J. Gen. Virol*. **83**, 651-662.

Zamyatnin AA Jr, Solovyev AG, Savenkov EI, Germundsson A, Sandgren M, Valkonen JP, Morozov SY.(2004). Transient coexpression of individual genes encoded by the triple gene block of potato mop-top virus reveals requirements for TGBp1 trafficking. *Mol Plant Microbe Interact*. 2004, **17**(8),921-30.

VITA

RUCHIRA MITRA

Candidate for the Degree of

Doctor of Philosophy

Thesis: SUBCELLULAR LOCALIZATION AND ROLE OF *POTATO VIRUS X* (PVX) TGBp2 IN VIRUS CELL-TO-CELL MOVEMENT.

Major Field: Plant Pathology

Biographical:

Education: Graduated from Bidhan Chandra Krishi Viswavidhyalaya, 1997. Completed the Requirements for the Doctor of Science degree in Plant Pathology at Oklahoma State University in May, 2005.

Professional Memberships: American Society for Virology